CHALMERS
UNIVERSITY OF TECHNOLOGY

Non-heating Floquet systems

Analysis of energy absorption in (1+1)D CFTs with a square wave drive, using a sine-k-square deformation

Master's thesis in Physics and Astronomy

MICHAEL HÖGBERG

Department of Physics
CHALMERS UNIVERSITY OF TECHNOLOGY
Gothenburg, Sweden 2020

Master's thesis 2020

Non-heating Floquet systems

Analysis of energy absorption in (1+1)D CFTs with a square wave drive, using a sine-k-square deformation

MICHAEL HÖGBERG

CHALMERS
UNIVERSITY OF TECHNOLOGY

Department of Physics
Division of Condensed Matter Physics
Chalmers University of Technology
Gothenburg, Sweden 2020

Non-heating Floquet systems
Analysis of energy absorption in (1+1)D CFTs with a square wave drive, using a sine-k-square deformation
MICHAEL HÖGBERG

Supervisor: Henrik Johannesson, Department of Physics
Examiner: Ulf Gran, Department of Physics

Master's Thesis 2020
Department of Physics
Division of Condensed Matter Physics
Chalmers University of Technology
SE-412 96 Gothenburg
Telephone +46 31 772 1000

Typeset in LaTeX
Printed by Chalmers Reproservice
Gothenburg, Sweden 2020

Non-heating Floquet systems
Analysis of energy absorption in (1+1)D CFTs with a square wave drive, using a sine-k-square deformation
MICHAEL HÖGBERG
Department of Physics
Chalmers University of Technology

Abstract

In the last decade there has been immense progress in experimentally realizing periodically driven, so-called Floquet systems, that exhibit topological features. However, there is an expectation that most Floquet systems heat up with time, absorbing energy from the drive, and thus evolve towards a featureless state in which all local correlations are fully random. In this thesis it is shown that it is theoretically possible to have a Floquet system which do not heat up, giving that any existing local correlations could be infinitely long lived. In other words, this shows that interesting physical phenomenon, such as a non-trivial topological phase, could in principal be present in a Floquet system for infinitely long times. The Floquet model which exhibits this non-heating phase is that of a square-wave drive where the Hamiltonian of the system jumps between an arbitrarily chosen CFT and a sine-square deformation of the same CFT. This model was first proposed in 2018 by Wen and Wu in Ref. [1]. We present in this thesis a generalization of the Floquet system proposed by Wen and Wu – we still use the same square wave drive but now with what we call a sine-k-square deformation, hence a deformation of higher harmonics. With this generalization we also find the interesting property of a non-heating phase for certain values of the driving parameters. Furthermore, we find that the value of k in the sine-k-squared deformation that we propose has some rather important implications for which driving parameter values we can have in a non-heating phase: The region of the driving parameter values which gives the non-heating phase shrinks with growing k.

Keywords: CFT, Floquet theory, Floquet heating problem, sine-square deformation, sine-k-square deformation.

Acknowledgements

First and foremost, I would like to express my greatest gratitude to my supervisor Prof. Henrik Johannesson who has been most patient and encouraging throughout the project. The long meetings, ending first after we have turned every stone of the problem at hand for that week, have been essential for the progress of this project.

In these extraordinary times would I also like to attribute a sincere thanks to my flatmates who have had to fill the void of my thesis colleges with much needed coffee breaks enjoying the sun and discussions of some unrelated philosophical topic at the balcony.

Lastly, I would like to direct a great thanks to you who are about to read my thesis. After this many days, weeks and months of work it is really nice if someone finds it interesting and even nicer if you find it useful for your own projects. I hope you will forgive me for the numerous shortcomings in how to make a pedagogical presentation of the material.

Michael Högberg, Gothenburg, 2020

Contents

1

Introduction

We review and clarify the analysis of a newly proposed Floquet system described with conformal field theory (CFT), discussed by Fan et al. in Ref. [2], building on previous work by Wen and Wu in [1, 3]. The system is defined by a square-wave drive between an arbitrary CFT and a sine-square deformation of the same CFT, allowing for a detailed study of the time evolution of the energy density. Furthermore, we generalize the work done by Fan et al. by using a more general deformation which we call a sine-k-square deformation. Before we start with all technicalities we here give a motivation and a brief review of the status of the field of Floquet systems, continuing with an introduction to elementary Floquet theory, and then finishing the introduction with an outline of the thesis.

1.1 Motivation

Periodically driven systems (Floquet systems), e.g. a solid exposed to periodic laser pulses, are interesting for a number of reasons, not least the fact that they may show non-trivial topological phases. Moreover, these phases are in non-equilibrium, since the system is exposed to a driving field. The study of topological phases, mostly then on systems in equilibrium, has gotten much attention in recent years as evident by the 2016 Nobel prize to Thouless, Kosterlitz and Haldane for their groundbreaking theoretical discoveries in topological phases and phase transitions. Floquet systems which exhibit non-trivial topological phases also exhibit an ”on demand” property: By changing the frequency of the driving field we can get the system to change its topological phase. Furthermore, systems with topological phases are seen as prominent candidates for new technologies exploiting quantum physics for future applications. One of the hopes for these systems is that they can serve as components in quantum computers, since it has been shown that systems with non-trivial topological phases can exhibit robust an localized quantum states. Since Floquet systems can exhibit both topological phases and have an ”on demand” property we can understand their potential for future technologies [4].

One unfortunate drawback with Floquet systems is that they are generally believed to ”heat up”. The basic argument is that the system absorbs energy from the field that exhibits the periodic drive, thus the local entropy increases implying that the system will tend towards a featureless state at large times in which any local

correlations will be fully random (as in an "infinite temperature" state) [5, 6]. Several solutions have been proposed, and some experiments have been successful in creating Floquet systems with non-trivial topological phases which don't heat, at least not at intermediate time scales [7–11]. However, the analytical examination of systems to understand when heating or non-heating occur is a hard problem, and a very new area of research, in particular when looking at the quantum engineering of Floquet systems as components in new technologies.

During the last two years there have been some developments in how we can analytically understand when a Floquet system may heats or not. A system relevant to this thesis, discussed in two recently published papers, Refs. [1, 2], has been shown to absorb or not absorb energy depending on with which frequency the system is driven with. The theoretical framework used was based on two-dimensional CFT, with the analysis using a newly developed theory about the so called sine-squared deformation, studied in [1–3, 12–28]. This deformation is interesting in its own right, especially with its connection to numerical calculations when seeking bulk properties in the thermodynamical limit. It has been theoretically shown for several systems that using the sine-squared deformation with open boundary conditions and the more conventional periodic boundary conditions are in very good agreement thus giving the sine-square deformation to be prominent for numerical calculations [12]. But here we will, instead of further investigations of the sine-square deformation's reliability to be a good choice when making numerical calculations, take advantage of the theoretical frame work develop about the sine-square deformation.

In this thesis we will make a careful analysis of the Floquet system proposed in Refs. [1, 2] to analytically describe the energy absorption (or non-absorption) properties, and their dependence on the driving frequency. Furthermore, we will present an analysis of a generalization of this system where we can also find the same intriguing phase as in the system proposed in Refs. [1, 2] – where the driven system does not absorb energy. We hope this work can contribute to future findings of Floquet systems which not only exhibit non-trivial topological phases, but are also built not to absorb energy by the drive. This would hold promise for future long-lived topological "on demand" quantum states.

1.2 Floquet theory

Most of the theory needed in this work is that of CFT, however to not lose track of the background of the modeling of the system we here present some basic Floquet theory. Since this will be a very brief introduction to a vast and important field, the interested reader could benefit from reading one of two excellent review articles which have been the author's own introduction to the subject. First, we have one by Bukov et al., Ref. [29], which gives a very nice overview of the theoretical and technical aspects of working with quantum Floquet systems. The second article by Rudner and Lindner, Ref. [4], gives a neat review of the experimental developments from the first quantum Floquet system in 2015 to the latest experiment in 2019.

Floquet theory is named after the French mathematician Gaston Floquet, 1847 - 1920, and deals with periodically linear differential equations. One of the most famous classical physics phenomenon described by Floquet theory is the Kapitza pendulum. For a rigid pendulum we have two equilibrium points – a stable one right below the suspension point and one unstable right above the suspension point. By vertically vibrating the suspension point with high enough frequency one finds that the equilibrium point above the suspension point also becomes stable. This kind of features, allowing unstable equilibrium points to become stable and finding new equilibrium points in the driven system, is what makes Floquet physics so interesting. This picture of how we can induce new stable states in a system by applying a drive is also applicable for quantum Floquet systems. We will now review the most important aspects of Floquet theory in a quantum mechanical setting.

The characteristics of a Floquet system is that it is described by a periodic Hamiltonian, H:

$$H(t) = H(t+T), \tag{1.1}$$

where T is the period. Given the Schrödinger equation

$$i\partial_t \left|\psi(t)\right\rangle = H(t) \left|\psi(t)\right\rangle, \tag{1.2}$$

with $\hbar = 1$, its formal solution implies the time evolution operator, $U(t)$:

$$U(t) = TOOe^{-i\int_0^t H(t')\mathrm{d}t'}. \tag{1.3}$$

Here TOO is the time-ordering operator. We note that it is the time dependence in the Hamiltonian that make this expression especially hard to handle. That is, to find all eigenstates or at all prove that there exists a complete set of eigenstates to this unitary time-evolution operator, which is what we need in order to successfully describe time evolution of the system, or equivalently, explicitly solve the time-dependent Schrödinger equation. From that the Hamiltonian $H(t)$ is periodic and piecewice continuous, and the Schrödinger equation, eq. (1.2), is a linear first-order differential equation, we have that the system fulfils the requirements in Floquet theory. The theory states that we have a complete set of eigenstates to the unitary time-evolution operator, eq. (1.3), [30]. These eigenstates can be written to show the time-periodic structure of the eigenstates:

$$\left|\psi(t)\right\rangle = e^{-i\epsilon t}\left|\phi(t)\right\rangle, \quad \left|\phi(t)\right\rangle = \left|\phi(t+T)\right\rangle. \tag{1.4}$$

Here ϵ is called quasi energy and plays an analogous role to energy but with the important difference that it is only defined mod $2\pi/T$, where T is the period of the drive. We have that ϵ is real and that $e^{-i\epsilon t}$ being the eigenvalue to the time-evolution operator which manifests its similarities with energy in a equilibrium system.

In this work we will not need to be explicit about the eigenstates to the unitary time-evolution operator. Instead we will work with a model where we actually can write the time-evolution operator on closed form since the Hamiltonian we work with admits easy integration and hence gives the usually quite difficult Floquet theory work for free. However, for other Floquet systems where one cannot find the unitary time-evolution operator on closed form but only as a formal expression as in eq. (1.3), one frequently rely on results from Floquet theory to approximate the Hamiltonian so as to make it amenable to analysis.

1.3 Outline

We will start the next chapter by introducing CFT, a vast subject for which we we will focus our attention on the stress-energy tensor and its relation to the so called Virasoro algebra in two-dimensional theories. Another important aspect of the conformal symmetry in this thesis is that of the special class of conformal transformations that goes under the name of Möbius transformations. In particular, we shall derive in detail certain properties following from successive applications by the same Möbius transformation. Continuing with chapter 3 we make a careful review of the work by Fan et al. in [2] and expand and deepen the analysis to make it more transparent. That is, we will discuss in detail how a setup with a square-wave drive can exhibit both a heating and a non-heating phase governed by the driving parameters. Here the square-wave drive is such that the Hamiltonian which controls the system jumps between an arbitrary CFT and its sine-square deformation. In chapter 4 we continue with a generalization of the work done by Fan et al. in Ref. [2] which we discussed in chapter 3. The generalization applies to the deformation in Ref. [2], from a sine-square to a sine-k-square deformation, hence a deformation of higher harmonics. One may see this as a step towards understanding what would happen for an arbitrary deformation that admits a Fourier expansion. We will again find that we have both a heating and non-heating phase depending on the driving parameters, but the interesting parameter values that give the non-heating phase now depends on the k used in the sine-k-squared deformation.

2

Conformal field theory

In this chapter will we give a short introduction to the vast subject of Conformal Field Theory (CFT). We will assume some background knowledge of Quantum Field Theory (QFT), with CFT being a special type of QFT where one takes advantage of the presence of conformal symmetry. Said differently, a CFT is a QFT that is invariant under local scale transformations which preserves angles. The focus will be towards two-dimensional theories where CFT is exceptionally powerful. For readers for which this is their first acquaintance with CFT and would like a more thorough text the standard reference in the subject (often referred to as the "Yellow Book") is the one written by Fransesco et al. [31]. Much of the material in this chapter is borrowed from the Yellow Book.

We start this chapter by defining a conformal transformation. By analysing this definition we identify a conformal algebra, something we will first do for dimension $d \geq 3$. We follow up with a discussion of what happens for fields during conformal transformations, where we have already assumed that the fields form irreducible representations of the Lorentz group. In other words, we here work within the framework of QFT.

After these two more introductory sections, sections 2.1 and 2.2, we turn to the more exciting subject of what happens for conformal transformations in two dimensions. We here make a connection to holomorphic functions which indicates that the conformal algebra in two dimensions is infinite-dimensional. This is the very reason for the powerfulness of conformal theories in two dimensions. We conclude section 2.3 by giving the transformation rule for a so-called primary operator, which we use as a pedagogical example to connect conformal transformations of operators to specific coordinate changes.

We continue in section 2.4 with a discussion about the stress-energy tensor, especially how it transforms under conformal coordinate changes. Here we introduce another way to express how to generate conformal transformations of fields, in this way uncovering some more structure of the theory. We investigate this structure in the next section, 2.5, where we find the Virasoro algebra that generates 2d conformal transformations. We can then connect how a transformation of an operator relates to a coordinate change in a neat way.

This theory chapter is concluded by a section about Möbius theory, section 2.6. Möbius transformations form an important class of conformal transformations. After

a brief reminder of some basic mathematical facts, we then derive an expression for successive applications of a Möbius transformation. As we shall see in chapter 3, this is a key result, to be exploited in the application of CFT to Floquet theory.

2.1 Introduction to conformal transformations

In this first section of the theory chapter we will begin by introducing the general definition of a conformal coordinate transformation. From this definition we will then find the group structure of all conformal coordinate transformations, finding the conformal algebra by studying infinitesimal transformations.

A conformal coordinate transformation $x \mapsto x'$ is defined by that the metric is only locally scaled

$$g'_{\mu\nu}(x') = \Lambda(x) g_{\mu\nu}(x), \tag{2.1}$$

where $\Lambda(x)$ is a scalar function, $g_{\mu\nu}$ the metric in the "old" coordinates x and $g'_{\mu\nu}$ the metric in the "new" coordinates x'. We can write this defining equation, eq. (2.1), on infinitesimal form and in this way attain some insights about conformal transformations which will lead us to find the conformal algebraic structure. By the general rule for coordinate transformations of the metric tensor, an infinitesimal transformation $x^\mu \to x'^\mu = x^\mu + \epsilon^\mu(x)$ to first order in ϵ takes the form

$$\begin{aligned} g_{\mu\nu} \to g'_{\mu\nu} &= \frac{\partial x^\alpha}{\partial x'^\mu} \frac{\partial x^\beta}{\partial x'^\nu} g_{\alpha\beta} \\ &= (\delta^\alpha_\mu - \partial_\mu \epsilon^\alpha)(\delta^\beta_\nu - \partial_\nu \epsilon^\beta) g_{\alpha\beta} \\ &= g_{\mu\nu} - (\partial_\mu \epsilon_\nu + \partial_\nu \epsilon_\mu). \end{aligned} \tag{2.2}$$

If we then require that this should be a conformal transformation we have to combine eqs. (2.1) and (2.2), thus obtaining

$$g_{\mu\nu}(x) - (\partial_\mu \epsilon_\nu(x) + \partial_\nu \epsilon_\mu(x)) = g_{\mu\nu}(x) - f(x) g_{\mu\nu}(x), \tag{2.3}$$

where $\Lambda(x) = 1 - f(x)$ and where Λ is expanded in a neighborhood around x, defining f as its first-order expansion. From eq. (2.3) follows the first important equation in deriving the conformal algebra,

$$\partial_\mu \epsilon_\nu + \partial_\nu \epsilon_\mu = f(x) g_{\mu\nu}. \tag{2.4}$$

Taking the trace on both sides of eq. (2.4) gives

$$f = \frac{2}{d} \partial_\mu \epsilon^\mu, \tag{2.5}$$

where d is the space-time dimension. On the other hand, if we would have taken the derivative ∂_ρ on eq. (2.4) with some permutations on the indices we obtain

$$\begin{aligned} &\partial_\rho \partial_\mu \epsilon_\nu + \partial_\rho \partial_\nu \epsilon_\mu = \eta_{\mu\nu} \partial_\rho f \\ &\partial_\mu \partial_\rho \epsilon_\nu + \partial_\mu \partial_\nu \epsilon_\rho = \eta_{\rho\nu} \partial_\mu f \\ &\partial_\nu \partial_\mu \epsilon_\rho + \partial_\nu \partial_\rho \epsilon_\mu = \eta_{\mu\rho} \partial_\nu f \\ \Rightarrow \quad &2\partial_\mu \partial_\nu \epsilon_\rho = \eta_{\mu\rho} \partial_\nu f + \eta_{\nu\rho} \partial_\mu f - \eta_{\mu\nu} \partial_\rho f, \end{aligned} \tag{2.6}$$

where we have added the two last lines and subtracted the first. We have here assumed that the metric is constant, for simplicity that $g_{\mu\nu} = \eta_{\mu\nu} = \text{diag}(1, 1, ..., 1)$ when using a Euclidean metric. Contracting eq. (2.6) with $\eta^{\mu\nu}$ gives

$$2\partial^2\epsilon_\rho = (2-d)\partial_\rho f. \tag{2.7}$$

If we rename the indices, $\rho \to \mu$, in eq. (2.7) and then apply ∂_ν to the resulting expression, we have

$$2\partial^2\partial_\nu\epsilon_\mu = (2-d)\partial_\mu\partial_\nu f. \tag{2.8}$$

Going back to eq. (2.4) and applying ∂^2, one obtains

$$2\partial^2\partial_\nu\epsilon_\mu = \eta_{\mu\nu}\partial^2 f. \tag{2.9}$$

Combining eq. (2.8) and eq. (2.9) we can immediately conclude

$$(2-d)\partial_\nu\partial_\mu f = \eta_{\mu\nu}\partial^2 f. \tag{2.10}$$

A final contraction with $\eta^{\mu\nu}$ on eq. (2.10) yields

$$(d-1)\partial^2 f(x) = 0. \tag{2.11}$$

From eqs. (2.4) - (2.7), (2.10) and (2.11) we can derive the explicit form of conformal transformations. First a note about the dimensions $d = 1$ and $d = 2$ which we can see are special, as they take away restrictions on f from the equations. First, $d = 1$ gives that these equations imply no restriction on f, that is, any continuous f works as an infinitesimal conformal transformation. This is however not too surprising since the notion of angle doesn't exist in one dimension. Thus, the higher-dimensional requirement that f must preserve angles is not applicable here. In section 2.3 we will see that conformal transformations in two dimensions do have restrictions, but fewer than in $d > 2$, implying that CFT becomes particularly powerful in two dimensions.

For now, let us briefly discuss how conformal transformations look like and how they act, with focus on $d \geq 3$ so as to develop some intuition about the formalism.

For $d \geq 2$ we have that eq. (2.11) implies that $\partial^2 f = 0$. Inserting this in eq. (2.10) gives $\partial_\mu\partial_\nu f = 0$, for $d \geq 3$, that is, f can only be linear in the coordinate x:

$$f(x) = A + B_\mu x^\mu, \tag{2.12}$$

where A and B_μ are constants. If we use this form of f in eq. (2.7) then we have that $\partial_\mu\partial_\nu\epsilon_\rho$ is constant since one more applied derivative gives that the right-hand side is zero (since a second derivative of f is zero). From that $\partial_\mu\partial_\nu\epsilon_\rho$ is constant follows that ϵ_μ is second order in x,

$$\epsilon_\mu = a_\mu + b_{\mu\nu}x^\nu + c_{\mu\nu\rho}x^\nu x^\rho, \quad c_{\mu\nu\rho} = c_{\mu\rho\nu}, \tag{2.13}$$

where a_μ, $b_{\mu\nu}$ and $c_{\mu\nu\rho}$ are infinitesimal constants. We can investigate these three coefficients one by one since all equations giving restrictions on ϵ, eqs. (2.4) - (2.6), are valid for all x, i.e. we can choose x such that the other two terms vanish.

First let us consider $\epsilon_\mu = a_\mu$. We then have no restrictions, since in all equations there is a derivative of ϵ and f is equal to a derivative of ϵ as well; see eq. (2.5). It follows that $\epsilon_\mu = a_\mu$ constitutes a translation,

$$x^\mu \to x'^\mu = x^\mu + a^\mu. \tag{2.14}$$

Then if we look at $\epsilon_\mu = b_{\mu\nu}x^\nu$ and substitute this into eq. (2.4), using the expression for f from eq. (2.5), we get

$$b_{\mu\nu} + b_{\nu\mu} = \frac{2}{d} b^\rho{}_\rho \eta_{\mu\nu}. \tag{2.15}$$

On the right hand side we have an expression proportional to the trace of b giving that

$$b_{\mu\nu} = \alpha\eta_{\mu\nu} + m_{\mu\nu}, \quad \alpha = b^\rho{}_\rho \quad m_{\mu\nu} = -m_{\nu\mu}, \tag{2.16}$$

where α corresponds to scaling and m to rotations. Thus, we have the transformations

$$x'^\mu = x^\mu + \epsilon^\mu = x^\mu + \alpha x^\mu, \tag{2.17}$$

and

$$x'^\mu = x^\mu + \epsilon^\mu = x^\mu + m_{\mu\nu}x^\nu, \tag{2.18}$$

for $\epsilon_\mu = \alpha\eta_{\mu\nu}x^\nu$ and $\epsilon_\mu = m_{\mu\nu}x^\nu$ respectively.

Lastly we have $\epsilon_\mu = c_{\mu\nu\rho}x^\nu x^\rho$ which we can substitute into eq. (2.6), again with f as in eq. (2.5), giving

$$\begin{aligned} 2\partial_\nu\partial_\rho c_{\mu\nu\rho}x^\nu x^\rho &= \frac{2}{d}\eta_{\rho\mu}c^\lambda{}_{\nu\rho}\partial_\nu\partial_\lambda x^\nu x^\rho + \frac{2}{d}\eta_{\nu\mu}c^\lambda{}_{\nu\rho}\partial_\rho\partial_\lambda x^\nu x^\rho - \frac{2}{d}\eta_{\nu\rho}c^\lambda{}_{\nu\rho}\partial_\mu\partial_\lambda x^\nu x^\rho \\ &= \frac{2}{d}\eta_{\rho\mu}c^\lambda{}_{\nu\lambda} + \frac{2}{d}\eta_{\nu\mu}c^\lambda{}_{\lambda\rho} - \frac{2}{d}\eta_{\nu\rho}c^\lambda{}_{\lambda\mu} \\ \Rightarrow c_{\mu\nu\rho} &= \eta_{\mu\rho}b_\nu + \eta_{\mu\nu}b_\rho - \eta_{\nu\rho}b_\mu, \quad b_\mu = \frac{1}{d}c^\lambda{}_{\lambda\mu}, \end{aligned} \tag{2.19}$$

where the only relation used is $\partial_\mu x^\nu = \delta^\nu_\mu$ together with some flipping of symmetric indices for cosmetic reasons. Thus we have the infinitesimal transformation

$$x'^\mu = x_\mu + \epsilon_\mu = x_\mu + 2(x\cdot b)x_\mu - b_\mu x^2, \tag{2.20}$$

which is called special conformal transformation (SCT).

For completeness we will finish this introduction to conformal coordinate transformations by writing out the conformal algebra for the conformal generators in $d \geq 3$, generators which as we shortly will see can be found in eqs. (2.14), (2.17), (2.18) and (2.20). We remember the definition of a generator – as usually given in the context of Noether's theorem – as the difference between the fields after an infinitesimal transformation. This gives the general expression for the generators T_a as

$$iT_a\Phi(x) = \frac{\delta x^\mu}{\delta\omega_a}\partial_\mu\Phi(x) - \frac{\delta\mathcal{F}}{\delta\omega_a}, \tag{2.21}$$

with $\mathcal{F}$ describing how the fields transform (for now we set $\mathcal{F}(\Phi) = \Phi$) and where ω_a are some infinitesimal parameters. When working with conformal symmetries, as we do, we have $\frac{1}{2}(d+2)(d+1)$ infinitesimal parameters and we have above already named them to sort into four groups to: a_μ, α, $m_{\mu\nu}$ and $c_{\mu\nu\rho}$. From eqs. (2.14), (2.17), (2.18) and (2.20) we have the equations for δ^x for all conformal transformations and by identifying ω_a to the specified names for the infinitesimal parameters, a_μ, α, $m_{\mu\nu}$ and $c_{\mu\nu\rho}$, in these equations we can use eq. (2.21) to find the generators and then by exponentiation their finite transformations [31]:

$$\begin{aligned}
&\text{(translation)} && P_\mu = -i\partial_\mu, && x'^\mu = x^\mu + a^\mu, && (2.22)\\
&\text{(dilation)} && D = -ix^\mu\partial_\mu, && x'^\mu = \alpha x^\mu, && (2.23)\\
&\text{(rigid rotation)} && L_{\mu\nu} = i(x_\mu\partial_\nu - x_\nu\partial_\mu), && x'^\mu = M^\mu{}_\nu x^\nu, && (2.24)\\
&\text{(SCT)} && K_\mu = -i(2x_\mu x^\nu\partial_\nu - x^2\partial_\mu), && x'^\mu = \frac{x^\mu - b^\nu x^2}{1 - 2b\cdot x + b^2x^2}. && (2.25)
\end{aligned}$$

By computing the commutators between the generators in eqs. (2.22) - (2.25), thinking of them as acting on a coordinate, we finally obtain the conformal Lie algebra in $d \geq 3$:

$$\begin{aligned}
[D, P_\mu] &= iP_\mu,\\
[D, K_\mu] &= -iK_\mu,\\
[K_\mu, P_\mu] &= 2i(\eta_{\mu\nu}D - L_{\mu\nu}),\\
[K_\rho, L_{\mu\nu}] &= i(\eta_{\rho\mu}K_\nu - \eta_{\rho\nu}K_\mu),\\
[P_\rho, L_{\mu\nu}] &= i(\eta_{\rho\mu}P_\nu - \eta_{\rho\nu}P_\mu),\\
[L_{\mu\nu}, L_{\rho\sigma}] &= i(\eta_{\nu\rho}L_{\mu\sigma} + \eta_{\mu\sigma}L_{\nu\rho} - \eta_{\mu\rho}L_{\nu\sigma} - \eta_{\nu\sigma}L_{\mu\rho}),\\
[D, L_{\mu\nu}] &= [K_\mu, K_\nu] = [P_\mu, P_\nu] = 0.
\end{aligned} \qquad (2.26)$$

2.2 Conformal transformations of fields

In this section we will investigate how to conformally transform a field. We start by reminding ourselves about the general transformation for a field $\Phi(x)$, at an algebraic level where we can make an infinitesimal transformation as

$$\begin{aligned}
x \mapsto x' &= (1 - i\omega^a T_a)x,\\
\Phi(x) \mapsto \Phi'(x') &= (1 - i\omega^a \pi(T_a))\Phi(x),
\end{aligned} \qquad (2.27)$$

where T_a are the generators of the transformation and $\pi(T_a)$ are the matrices acting on the fields, obeying $[\pi(T_a), \pi(T_b)] = \pi([T_a, T_b])$, and where ω_a are infinitesimal parameters.

We now want to understand how to write $\pi(T_a)$ for the different generators given in eqs. (2.22) - (2.25). This is a question of finding the irreducible representations for the conformal algebra, eq. (2.26). However, we will assume that we start with a QFT, that is, we have irreducible representations of the Lorentz group, which

is a subalgebra to the conformal algebra, as seen from the fact that the $L_{\mu\nu}$ only transform to other Lorentz transformations under the Lie-bracket in eq. (2.26).

We start with the dilation transformation $\pi(D)$. We shall work with irreducible representations of the Lorentz algebra, that is we assume that the fields take their values at the origin, and then by translation we deduce their action on the full group,

$$\pi(T_a)\Phi(x) = e^{ix^\mu P_\mu}\pi_0(T_a)e^{-ix^\mu P_\mu}\Phi(x). \tag{2.28}$$

In eq. (2.26) we can see that $[D, L_{\mu\nu}] = 0$ and from Schur's first lemma with the assumption of that we work with an irreducible representation of the Lorentz algebra, we conclude that

$$\pi_0(D) \propto I. \tag{2.29}$$

From $\pi_0(D) \propto I$ follows that all commutators with $\pi_0(D)$ must be zero, especially this affects the SCT generators,

$$[\pi_0(D), \pi_0(K_\mu)] = -i\pi_0(K_\mu) = 0. \tag{2.30}$$

From this relation we conclude that the special conformal transformation does not affect the fields when working with an irreducible representation of the Lorentz group: when translating the zero matrix by eq. (2.28) we still get the zero matrix. Then the finite transformation obtained from exponentiation implies that the transformation rule is implemented by the identity matrix.

Using that $\pi_0(D)$ is proportional to the identity matrix, eq. (2.29), together with the translation of the field, eq. (2.28), the CBH formula allows us to find the representation of the dilation generator

$$\begin{aligned}\pi(D)\Phi(x) &= e^{ix^\mu P_\mu}\pi_0(D)e^{-ix^\mu P_\mu}\Phi(x)\\ &= (\pi_0(D) + [\pi_0(D), -ix^\mu\pi(P_\mu)])\Phi(x)\\ &= (\pi_0(D) + x^\mu P_\mu)\Phi(x)\\ &= (\pi_0(D) - ix^\mu\partial_\mu)\Phi(x),\end{aligned} \tag{2.31}$$

where, in the third line, we have used that the CBH formula terminates when we obtain an expression that commutes with the exponent, such as the exponent itself. We can now rewrite $\pi_0(D)$ as it is usually given, with only one real parameter, Δ,

$$\pi_0(D) = -i\Delta. \tag{2.32}$$

Here the identity matrix on the right-hand side is implicit.

The general procedure to go from infinitesimal transformations generated by the T_a (algebraic level) to finite transformations, call them g (group level), is by using the exponential map

$$g = \exp\{\xi^a T_a\}, \tag{2.33}$$

with an implicit sum for $a = 1, ..., \dim(\mathfrak{g})$, where $\mathfrak{g}$ is the Lie-algebra, T_a the generators of the algebra and ξ^a some parameters [32]. It may be worth pointing out that eq. (2.33) is locally true for any finite-dimensional Lie algebra, such as ours.

In principal we are now ready to write down any finite conformal transformation, by using: (i) The exponential map given in eq. (2.33), (ii) the representation of the Poincaré algebra familiar from QFT, (iii) the action of dilation given in eq. (2.31), and (iv) observing the non-action of special conformal transformations seen in eq. (2.30). We will however only write the result for a spinless field whose 2-dimensional counterpart is the only transformation of a special field that we will have use for – and that more in a pedagogical sense. Letting $\phi(x)$ be a scalar field, we thus obtain for a finite conformal transformation:

$$\phi(x) \mapsto \phi'(x') = \left|\frac{\partial x'}{\partial x}\right|^{-\Delta/d} \phi(x), \quad \left|\frac{\partial x'}{\partial x}\right| = \Lambda(x)^{d/2}, \tag{2.34}$$

where Λ is the scalar function defining the conformal transformation in eq. (2.1), d the space-time, and Δ is defined via eq. (2.32) [31].

With this we can now look at what restrictions this impose on a classical (quantum) theory from demanding the action (all correlation functions) to be invariant under a conformal transformation. However, in this work we are more concerned about how we can use this knowledge in order to find how the stress-energy tensor transforms under conformal transformations in a conformal theory. We shall take on this problem in section 2.4 but before that will we need to say something about two-dimensional CFT's. These are the CFT's that we will work with and where we can also say the most about the transformation properties of the stress-energy tensor.

2.3 Two-dimensional CFT

In this project on a CFT approach to Floquet theory we are only considering two-dimensional theories where, as we have already mentioned, CFT is at its most powerful. That two dimensions is exceptional transpires from section 2.1 where eq. (2.7) indicates fewer restrictions on the infinitesimal transformation ϵ_μ. In fact, ϵ_μ can be given by a power series in two dimensions, thus implying an infinite parameter space instead of the $\frac{1}{2}(d+1)(d+2)$ dimensional parameter space seen by the transformation relations given by eqs. (2.14), (2.17), (2.18) and (2.20). The power series for ϵ_μ comes from the connection between conformal coordinate transformations and analytic complex functions. We show this connection between conformal transformations and analytic functions by analysing the conformal coordinate transformations given in eq. (2.1) for flat, Euclidean, space with metric $g^{\mu\nu} = \delta^{\mu\nu} = \text{diag}\{1, 1\}$. That we use a Euclidean metric is not a restriction for quantum field theories which are played out in Minkowski space: we can always use Wick rotations, that is, using imaginary time instead of real time, taking us back to Euclidean metric.

We start with a general coordinate transformation, say $(\omega^0, \omega^1) \mapsto (z^0, z^1)$, for the metric:

$$g'^{\mu\nu}(z) = \frac{\partial z^\mu}{\partial \omega^\alpha} \frac{\partial z^\nu}{\partial \omega^\beta} g^{\alpha\beta}(\omega), \tag{2.35}$$

Using the proportionality condition that we have for conformal transformations, eq. (2.1), and writing out the three equations from eq. (2.35), which is a $2 \times$

2 matrix equation but since the metric is symmetric we only have three independent equations. That is, by explicitly writing out all equations implied by $\frac{\partial z^\mu}{\partial \omega^\alpha}\frac{\partial z^\nu}{\partial \omega^\beta}\delta^{\alpha\beta}(\omega) = \Lambda(\omega)\delta^{\mu\nu}$, we find the 00- and 11-component to be equal and the 01- (10)-component to be zero. We thus have

$$\left(\frac{\partial z^0}{\partial \omega^0}\right)^2 + \left(\frac{\partial z^0}{\partial \omega^1}\right)^2 = \left(\frac{\partial z^1}{\partial \omega^0}\right)^2 + \left(\frac{\partial z^1}{\partial \omega^1}\right)^2, \tag{2.36}$$

and

$$\frac{\partial z^0}{\partial \omega^0}\frac{\partial z^1}{\partial \omega^0} + \frac{\partial z^0}{\partial \omega^1}\frac{\partial z^1}{\partial \omega^1} = 0. \tag{2.37}$$

This is equivalent to

$$\frac{\partial z^1}{\partial \omega^0} = \frac{\partial z^0}{\partial \omega^1} \quad \text{and} \quad \frac{\partial z^0}{\partial \omega^0} = -\frac{\partial z^1}{\partial \omega^1}, \tag{2.38}$$

or

$$\frac{\partial z^1}{\partial \omega^0} = -\frac{\partial z^0}{\partial \omega^1} \quad \text{and} \quad \frac{\partial z^0}{\partial \omega^0} = \frac{\partial z^1}{\partial \omega^1}. \tag{2.39}$$

We recognize the set of equations in eq. (2.38) as the Cauchy-Riemann equations which we know from complex analysis. From ordinary complex analysis we remember that complex functions who fulfill the Cauchy-Riemann equations, with it's real and imaginary part as the two functions, z^0 and z^1 in eq. (2.38), are complex differentiable. Such functions are called holomorphic functions. Furthermore, we know that complex functions that are differentiable once are also infinitely differentiable. Thus holomorphic functions are analytic, that is, we can write all of them as power series – a very powerful tool. The other equation, eq. (2.39), is analogous, but referred to as anti-holomorphic since if a function $f(z)$ is holomorphic then its complex conjugate, $\bar{f}(\bar{z})$, fulfills eq. (2.39) [33].

To be able to exploit complex analysis as a tool in CFT, we make a coordinate change to complex coordinates:

$$\omega = \omega^0 + i\omega^1, \qquad \overline{\omega} = \omega^0 - i\omega^1. \tag{2.40}$$

As it is written, ω and $\overline{\omega}$ depend on each other, but by making an analytic continuation to $\mathbb{C}^2$, with four instead of two independent variables, ω and $\overline{\omega}$ become two independent complex variables. At the end of a calculation we then go back to the physical plane where the bar really means complex conjugation, $\bar{\omega} = \omega^*$. In order to trust the results as unique even though we may have a choice when doing the analytic continuation we can rely on the complex analysis theorem often refereed to as the identity theorem. This theorem states that if two functions, f and g defined on $\mathbb{C}$, are equal on an open subset, U, then they are equal on the whole complex-plane [33].

Now when we have established how to make conformal coordinate transformations in two dimensions, simply using holomorphic and antiholomorphic functions (functions satisfying eqs. (2.38) and (2.39) respectively), we would like to find the generators of these transformations, as we did for the transformations in eqs. (2.22) - (2.25),

defining the smaller set of conformal transformations valid in any dimension. From the conclusion that a conformal coordinate change is given by complex analytic functions we can understand the generic form of an infinitesimal transformation, $\epsilon, \bar{\epsilon}$. Note that in two dimensions the space-time index is not needed since the distinction is made by whether or not we have a bar. Furthermore, we will only discuss ϵ since everything is analogous for $\bar{\epsilon}$. In dimensions $d \geq 3$, we had that ϵ_μ must be of second order, eq. (2.13), which followed from certain constraints that are not at play for $d = 2$. A complex analytic function has the well-known property that it is locally given by a power series, implying that an infinitesimal conformal transformation in $d = 2$ takes the form

$$\epsilon(z) = \sum_{-\infty}^{\infty} \epsilon_n z^{n+1}, \tag{2.41}$$

where ϵ_n are infinitesimal constants and where we have chosen $n+1$ in the exponent for later convenience.

We can now use eq. (2.21) to get the generators in the same way as we did for the translation, dilation, rotation and SCT in eqs. (2.22) - (2.25). Now however we have an infinite number of generators

$$l_n = -z^{n+1}\partial_z, \quad \bar{l}_n = -\bar{z}^{n+1}\partial_{\bar{z}}, \tag{2.42}$$

where the subscript on the differential operator indicates with respect to which coordinate we make the differentiation, $\partial_z = \frac{\partial}{\partial z}$ [31].

By a straightforward computation, using eq. (2.42), we find the following commutator relations

$$\begin{aligned} [l_n, l_m] &= (n-m)l_{n+m}, \\ [\bar{l}_n, \bar{l}_m] &= (n-m)\bar{l}_{n+m}, \\ [l_n, \bar{l}_m] &= 0. \end{aligned} \tag{2.43}$$

That is, we have the conformal algebra to be the direct product of two isomorphic algebras. For reference, sometimes eq. (2.43) is called the Witt algebra. In order to obtain a finite conformal transformation we use exponentiation as given in eq. (2.33). For the conformal map $\omega \to z$, $\bar{\omega} \to \bar{z}$ we have

$$\omega \to z(\omega) = e^{\sum_{-\infty}^{\infty} \xi_n l_n}\omega, \quad \bar{\omega} \to \bar{z}(\bar{\omega}) = e^{\sum_{-\infty}^{\infty} \bar{\xi}_n \bar{l}_n}\bar{\omega}, \tag{2.44}$$

where ξ_n, $\bar{\xi}_n$ are complex constants.

We conclude this section by writing out the transformation rule for a primary operator, i.e. an operator defined by satisfying this very rule. First we need to define the holomorphic conformal dimension h and its antiholomorphic counterpart $\bar{h}$ as

$$h = \frac{1}{2}(\Delta + s), \quad \bar{h} = \frac{1}{2}(\Delta - s), \tag{2.45}$$

where Δ is the scaling dimension of the considered field and s is its spin. Then, under a conformal map $z \to \omega(z)$, $\bar{z} \to \bar{\omega}$, a primary operator transforms as

$$\phi'(\omega, \bar{\omega}) = \left(\frac{\partial \omega}{\partial z}\right)^h \left(\frac{\partial \bar{\omega}}{\partial \bar{z}}\right)^{\bar{h}} \phi(z, \bar{z}). \tag{2.46}$$

Note that this is a generalization of the transformation rule, eq. (2.34), for a spinless field.

This is actually all we need to understand about how operators transform in a two-dimensional CFT, since the transformation rule in eq. (2.46) is valid for an arbitrary conformal transformation and any operator can be derived from the primary operators in the theory [31].

2.4 Stress-energy tensor

The stress-energy tensor is one of the most useful objects in field theory, especially since, as in this project, analysing the energy distribution in a system is often of interest. The starting point in identifying a precise and unambiguous definition for the stress-energy tensor is the Noether current associated with Lorentz transformations. In this section we will focus on the general characteristics of the stress-energy tensor, especially those associated with conformal coordinate changes. We will also extract some key concepts for the stress-energy tensor, following the first six chapters in the main source for this theory section, the "Yellow Book" [31].

Noether's theorem for a Lorentz-invariant theory with Lagrangian density $\mathcal{L}$ implies for the stress-energy tensor T:

$$T^{\mu\nu} = -\eta^{\mu\nu}\mathcal{L} + \frac{\partial \mathcal{L}}{\partial \partial_\mu \Phi}\partial^\nu \Phi, \tag{2.47}$$

with

$$\partial_\mu T^{\mu\nu} = 0. \tag{2.48}$$

Here Φ is the collection of fields included in the theory and the second equation is the conservation law [31]. Integrating both sides in the conservation law over the spatial coordinates yields the conserved charge, in this case the four-momentum whose time component $P^0(t)$ is exactly the energy, giving

$$P^0(t) = \int \mathrm{d}^{d-1}\vec{x}\, T^{00}(t, \vec{x}) = \int \mathrm{d}^{d-1}\vec{x} \left(\frac{\partial \mathcal{L}(t, \vec{x})}{\partial \dot{\Phi}(t, \vec{x})}\dot{\Phi}(t, \vec{x}) - \mathcal{L}(t, \vec{x})\right). \tag{2.49}$$

We here identify the last integrand in eq. (2.49) as the Hamiltonian density, as it is the Legendre transformation from $\mathcal{L}$ to $\mathcal{H}$. Moreover, we know that $\int \mathrm{d}^{d-1}\vec{x}\, \mathcal{H}(t, \vec{x}) = H(t) = P^0(t)$, both symbols for the energy in the system.

The stress-energy tensor as defined might not be symmetric but we can always add a tensor, $B^{\rho\mu\nu}$, which is antisymmetric in its first two indices such that the new

stress-energy tensor becomes symmetric, $T^{\mu\nu}_{\text{new}} = T^{\mu\nu} + \partial_\rho B^{\rho\mu\nu}$, without changing the equation of motion [31]. So throughout this thesis we will work under the assumption of a symmetric stress-energy tensor, just denoted $T^{\mu\nu}$.

In classical theories conformal invariance implies that the stress-energy tensor is traceless. This follows from making a scale transformation and demanding that the action is invariant. In quantum theories however this must not be true, but for two-dimensional theories it can again be shown that conformal invariance implies a traceless stress-energy tensor. Now this is true within an expectation value; in fact it is true in any correlation function except if another field takes its value in the same space-time point as the trace of the stress-energy tensor [31],

$$\langle T^{\mu}{}_{\mu}(x)\Phi(y)\rangle = 0, \quad x \neq y. \tag{2.50}$$

One of the key concepts in this thesis is that of how an operator, especially the stress-energy tensor, transforms under conformal transformations. We will here derive just this relation. We will from now on work in two dimensions with Euclidean metric, that is, with imaginary time.

In two dimensions we can write a conformal transformation of a field in a more convenient way by means of the stress-energy tensor (instead of using an infinite number of generators which we would have to find similarly to how we found the generators for dilation and SCTs in section 2.2). This rewritten form is called the conformal Ward identity, with "Ward identity" being the name of how we can express the effect that continuous symmetries have on correlation functions. The conformal Ward identity is then a combination of the three Ward identities associated with translation, rotation and scale invariance, since from section 2.2 we know that a special conformal transformation doesn't affect the transformation of an operator. Written out explicitly,

$$\delta_{\epsilon,\bar{\epsilon}}\langle X\rangle = -\frac{1}{2\pi i}\oint_{\mathrm{C}} \mathrm{d}z\, \epsilon(z)\langle T(z)X\rangle + \frac{1}{2\pi i}\oint_{\mathrm{C}} \mathrm{d}\bar{z}\, \bar{\epsilon}(\bar{z})\langle \bar{T}(\bar{z})X\rangle, \tag{2.51}$$

where X is a product of fields, C is a path containing all arguments $(\omega_i, \bar{\omega}_i)$ of the fields appearing in X, and ϵ is the infinitesimal conformal coordinate transformation [31].

From eq. (2.51) we can make an infinitesimal conformal transformation, $z \to \omega = z + \epsilon$, of the stress-energy tensor, omitting the expectation value symbols but remembering that the resulting expression is true only within a correlation function,

$$\delta_\epsilon T(\omega) = \frac{1}{2\pi i}\oint_{\mathrm{C}} \mathrm{d}z\, \epsilon(z)T(z)T(w). \tag{2.52}$$

This can be evaluated by using the Operator Product Expansion (OPE), a representation of the product between two operators in which the divergence of the product of two operators approaching the same point is made explicit. An OPE is written as a sum where each term in the sum is constituted of two parts that are multiplied together; one operator part, that is well behaved as the two points come close,

and a c-number part, that possibly diverges. The OPE for the stress-energy tensor multiplied with itself is given by

$$T(z)T(\omega) \sim \frac{c/2}{(z-\omega)^4} + \frac{T(\omega)}{(z-\omega)^2} + \frac{\partial T(\omega)}{(z-\omega)}, \tag{2.53}$$

where c is the central charge and $\partial T(\omega) = \frac{\partial T(\omega)}{\partial \omega}$ [31]. We here use the symbol $\sim$, as in any OPE expression, to indicate that the equality is modulo expressions regular (non-singular) when $z \to \omega$, of which there exists an infinite number [31].

We can now use the OPE eq. (2.53) in the conformal transformation of T in eq. (2.52) to get

$$\delta_\epsilon T(\omega) = -\frac{1}{12} c \partial_\omega^3 \epsilon(\omega) - 2T(\omega)\partial\epsilon(\omega) - \epsilon(\omega)\partial_\omega T(\omega), \tag{2.54}$$

where we simply have used residue calculus to calculate the integral. Note that it is only the $1/(z-\omega)^n$ parts which contributes to the integral in each term. By "exponentiating" this action of infinitesimal conformal transformation, eq. (2.54), on T we get the expression for a finite conformal transformation associated with the finite transformation, $z \to \omega$,

$$T'(\omega) = \left(\frac{\partial \omega}{\partial z}\right)^{-2} \left(T(z) - \frac{c}{12}\{\omega, z\}_{Sc}\right). \tag{2.55}$$

We have here introduced the Schwarzian derivative $\{\omega, z\}_{\mathrm{Sc}}$,

$$\{\omega, z\}_{\mathrm{Sc}} = \frac{\mathrm{d}^3\omega/\mathrm{d}z^3}{\mathrm{d}\omega/\mathrm{d}z} - \frac{3}{2}\left(\frac{\mathrm{d}^2\omega/\mathrm{d}z^2}{\mathrm{d}\omega/\mathrm{d}z}\right)^2. \tag{2.56}$$

That eq. (2.54) implies eq. (2.55) is far from obvious. However, one finds that the finite form, eq. (2.55), coincides with the infinitesimal form, eq. (2.54), when expanding the finite form to first order in ϵ assuming the infinitesimal transformation $z \to \omega = z + \epsilon$ [31].

2.5 Virasoro generators

In the section above, section 2.4, we discussed how correlation functions change under conformal transformations in CFTs. The general transformation rule, at infinitesimal level, is given by the conformal Ward identity in eq. (2.51). We can however find more structure from this expression, specifically an algebra named the Virasoro algebra related to the transformation. To begin with, we saw in eq. (2.13) that ϵ_μ, the functions which parameterize a conformal transformation (here considered in any dimension $d \geq 3$) are at most second order polynomials. (We will here, as we discussed in section 2.3, indicate the two space-time directions with ϵ and $\bar{\epsilon}$ and thus we have dropped the space-time index μ.) But now when we work in a two-dimensional space-time we know from eq. (2.41) that ϵ, and we note that everything is analogous for $\bar{\epsilon}$, can be given by an unrestricted power series, of the form

$$\epsilon(z) = \sum_{-\infty}^{\infty} \epsilon_n z^{n+1}, \tag{2.57}$$

where ϵ_n are infinitesimal constants and we choose $n+1$ in the exponent for z for later convenience.

Any individual term in the sum in eq. (2.57) implies a conformal transformation and we would then want to look at each of them individually. Furthermore, in eq. (2.51) where the correlation function is transformed by two individual terms, one for the holomorphic part and one for the antiholomorphic part, we can look at each of them separately. Introducing two operators to build the conformal Ward identity, eq. (2.51), we write

$$L_n = \frac{1}{2\pi i}\oint \mathrm{d}z\, z^{n+1}T(z), \tag{2.58}$$

$$\bar{L}_n = \frac{1}{2\pi i}\oint \mathrm{d}\bar{z}\, \bar{z}^{n+1}\bar{T}(\bar{z}). \tag{2.59}$$

Then the conformal Ward identity, eq. (2.51), can be written as

$$\delta_{\epsilon,\bar{\epsilon}}X = \sum_{-\infty}^{\infty}\left(-\epsilon_n L_n X + \bar{\epsilon}_n \bar{L}_n X\right). \tag{2.60}$$

The operators L_n and $\bar{L}_n$ are called Virasoro generators and form the Virasoro algebra.

To find this algebra we simply compute the commutators $[L_n, L_m]$, written on integral form as

$$[L_n, L_m] = \frac{1}{(2\pi i)^2}\oint_0 \mathrm{d}\omega\, \omega^{m+1}\oint_\omega \mathrm{d}z\, z^{n+1}T(z)T(\omega), \tag{2.61}$$

where the subscripts on the integral signs indicate that we integrate over circles centered around the origin and ω respectively. That this integral form, eq. (2.61), corresponds to the commutator can be seen from the expression

$$\oint_\omega \mathrm{d}z\, a(z)b(\omega) = \oint_{\mathrm{C}_1} \mathrm{d}z\, a(z)b(\omega) - \oint_{\mathrm{C}_2} \mathrm{d}z\, b(\omega)a(z) = [A, b(\omega)], \tag{2.62}$$

where $A = \oint \mathrm{d}z\, a(z)$ and where we have two arbitrary holomorphic fields a and b and two circles, C_1 and C_2, centred around the origin. To verify this expression, eq. (2.62), we use complex analysis to deform C_1 and C_2 to a circle around ω as shown in fig. 2.1. We know that we can only have a divergence at ω when thinking of the product inside the integrals as OPEs. Furthermore, we can connect the two circles by two infinitesimally close lines, thus canceling each other.

Now, in the Virasoro commutator we can think of L_m as the integral over $\omega^{m+1}T(\omega)$ and simply take out the integral and ω^{m+1} from the commutator since ω is not an operator:

$$[L_n, L_m] = \frac{1}{2\pi i}\oint_0 \mathrm{d}\omega\, \omega^{m+1}[L_n, T(\omega)]. \tag{2.63}$$

By inspection of the general expression for a commutator, eq. (2.62), and the rewritten form of the Virasoro commutator, eq. (2.63), one easily verifies the integral form of the Virasoro commutator in eq. (2.61).

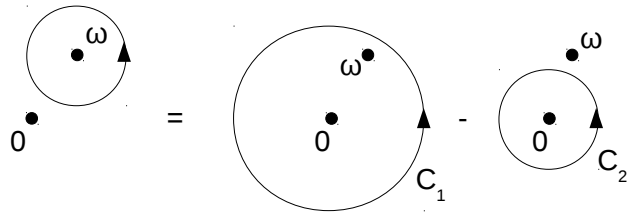

Figure 2.1: Integration paths, eq. (2.62).

When we now have motivated the integral form of the Virasoro commutator, eq. (2.61), we can use the OPE of the stress-energy tensor in eq. (2.53) to evaluate the integrals over C_1 and C_2. We get

$$\begin{aligned}
[L_n, L_m] &= \frac{1}{(2\pi i)^2} \oint_0 \mathrm{d}\omega\, \omega^{m+1} \oint_\omega \mathrm{d}z\, z^{n+1} \left(\frac{c/2}{(z-\omega)^4} + \frac{T(\omega)}{(z-\omega)^2} \right. \\
&\qquad \left. + \frac{\partial T(\omega)}{(z-\omega)} + \text{reg.} \right) \\
&= \frac{1}{2\pi i} \oint_0 \mathrm{d}\omega\, \omega^{m+1} \left(\frac{c}{12}(n+1)n(n-1)\omega^{n-2} \right. \\
&\qquad \left. + 2(n+1)\omega^n T(\omega) + \omega^{n+1}\partial T(\omega) \right) \\
&= \frac{c}{12}(n+1)n(n-1)\delta_{m+n,0} + (2(n+1)L_{m+n} \\
&\qquad - \frac{1}{2\pi i} \oint_0 \mathrm{d}\omega\, (n+m+2))\omega^{n+m+1} T(\omega) \Big) \\
&= \frac{c}{12} n(n^2-1)\delta_{m+n,0} + (n-m)L_{n+m}.
\end{aligned} \tag{2.64}$$

First, when evaluating the z-integral we use residue calculus, the only thing being relevant is $1/(z-\omega)^n$ since the regular terms integrate to zero by not having any poles. Evaluating the first term in the ω-integral follows by residue calculus as well, the second term is an identification of the Virasoro generator, eq. (2.58), and on the third term we used integration by parts. In the last line we only identified the Virasoro generator, eq. (2.58), and did some cleaning in the coefficients. The same calculation is carried out for $[\bar{L}_n, \bar{L}_m]$ and since we have the OPE $T(z)\bar{T}(\bar{\omega}) \sim 0$, we finally obtain the Virasoro algebra:

$$[L_n, L_m] = (n-m)L_{n+m} + \frac{c}{12} n(n^2-1)\delta_{n+m}, \tag{2.65}$$

$$[L_n, \bar{L}_m] = 0, \tag{2.66}$$

$$[\bar{L}_n, \bar{L}_m] = (n-m)\bar{L}_{n+m} + \frac{c}{12} n(n^2-1)\delta_{n+m}. \tag{2.67}$$

From these expressions, eqs. (2.65) - (2.67), we see that the Virasoro algebra constitutes a direct sum of two isomorphic algebras.

We will now connect the conformal transformation of operators with the coordinate transformation. We have that Virasoro generators generate infinitesimal conformal

transformations and by exponentiation we obtain finite transformations, as seen in eq. (2.33). Furthermore, a finite transformation of an operator is given by a similarity transformation (in the language of representation theory), and hence we have to sandwich the operator in between the exponential and its conjugate,

$$e^{\sum_{-\infty}^{\infty} -(\xi^n L_n + \bar{\xi}^n \bar{L}_n)} \phi(z,\bar{z}) e^{\sum_{-\infty}^{\infty} (\xi^n L_n + \bar{\xi}^n \bar{L}_n)} = \left(\frac{\partial \omega}{\partial z}\right)^h \left(\frac{\partial \bar{\omega}}{\partial \bar{z}}\right)^{\bar{h}} \phi(z,\bar{z}). \tag{2.68}$$

This equality comes from assuming ϕ to be a primary operator and then using the knowledge of how such an operator transforms, eq. (2.46). The question is now how to identify the conformal coordinate change which corresponds to the conformal transformation of the field. We know that the transformation of the field is a representation so what we need is nothing else but the corresponding transformation of the coordinates; as long as the representation is faithful we have a one-to-one correspondence and no ambiguities. That is, the corresponding coordinate change $\omega \to z$, $\bar{\omega} \to \bar{z}$ in eq. (2.68) is simply given by eq. (2.44), here written out again:

$$\omega \to z(\omega) = e^{\sum_{-\infty}^{\infty} \xi_n l_n} \omega, \quad \bar{\omega} \to \bar{z}(\bar{\omega}) = e^{\sum_{-\infty}^{\infty} \bar{\xi}_n \bar{l}_n} \bar{\omega}. \tag{2.69}$$

It is here important to note that ξ_n, $\bar{\xi}_n$ are the same as in eq. (2.68).

2.6 Möbius theory

Successive applications of the same Möbius transformation will be of great importance in chapters 3 and 4, where we apply CFT to Floquet theory. In this section we will investigate just this. More precisely, we will derive the transformation that corresponds to applying a Möbius transformation n times. The derivation is self-contained, based on ref. [34], with some additional facts about Möbius transformations that can be found in any standard book on complex analysis, for instance [33].

First, a Möbius transformation, T, is of the form

$$T(z) = \frac{az+b}{cz+d}, \quad ad - bc \neq 0, \tag{2.70}$$

that is a bijective map from $\mathbb{C}$ onto itself. Secondly, all Möbius transformations form a group, implying that successively applied Möbius transformations is a Möbius transformation. The group property further implies that all Möbius transformations have an inverse which is a Möbius transformation, that there exist an identity transformation $T(z) = z$, and that associativity is also fulfilled [33].

The inverse of a Möbius transformation can be written on a generic form which we can find from solving

$$T(T^{-1}(z)) = \frac{aT^{-1}(z)+b}{cT^{-1}(z)+d} = z, \tag{2.71}$$

thus obtaining

$$T^{-1} = \frac{dz-b}{-cz+a}. \tag{2.72}$$

One more important feature of Möbius transformations is that of fixed points. We denote a fixed point by γ, defined by

$$T(\gamma) = \frac{a\gamma + b}{c\gamma + d} = \gamma. \tag{2.73}$$

This equation for fixed points, eq. (2.73), is a second-order equation so we can either have two distinct fixed points or one with double multiplicity. The explicit expression for the fixed points is trivial to obtain from eq. (2.73), and one finds

$$\gamma_{1,2} = \frac{a - d \mp \sqrt{(a-d)^2 + 4bc}}{2c}. \tag{2.74}$$

We are now ready for the derivation of the expression, T^n, which corresponds to applying one and the same Möbius transformation, T, n times

$$T^n(z) = T(T(...T(z)...)). \tag{2.75}$$

First we note that T^n is also a Möbius transformation, which follows by the second fact that we stated about all Möbius transformations form a group. The derivation of T^n will use the knowledge and simple structure of the Möbius transformation which has 0 and ∞ as its fixed points. We will introduce another Möbius transformation S, which sends T's fixed points to 0 and ∞, that together with its inverse and T will have 0 and ∞ as fixed points. S is given by

$$S = \frac{z - \gamma_1}{z - \gamma_2}. \tag{2.76}$$

By the definition in eq. (2.70), S is a Möbius transformation if $\gamma_2 - \gamma_1 \neq 0$. We can see that it is important that we have a Möbius transformation, T, with two distinct fixed points; the other case with only one fixed point will be discussed later. The inverse to S found from the general expression in eq. (2.72): has the expression

$$S^{-1} = \frac{-\gamma_2 z + \gamma_1}{-z + 1}. \tag{2.77}$$

Let us now write down where some important points are mapped:

$$S^{-1}(0) = \frac{-\gamma_2 0 + \gamma_1}{-0 + 1} = \gamma_1, \qquad S^{-1}(\infty) = \frac{-\gamma_2 \infty + \gamma_1}{-\infty + 1} = \gamma_2, \tag{2.78}$$

$$T(\gamma_1) = \gamma_1, \qquad T(\gamma_2) = \gamma_2, \tag{2.79}$$

$$S(\gamma_1) = \frac{\gamma_1 - \gamma_1}{\gamma_1 - \gamma_2} = 0, \qquad S(\gamma_2) = \frac{\gamma_2 - \gamma_1}{\gamma_2 - \gamma_2} = \infty. \tag{2.80}$$

In $S^{-1}(\infty)$ and $S(\gamma_2)$ we of course really mean that we take the limit, $z \to \infty$ and $z \to \gamma_2$ respectively, but since these are rather trivial limits we can justify writing them in this faster notation. (We will have some similar cases later on.) Given the mappings T, S and S^{-1}, we can define a Möbius transformation U as

$$U = S \circ T \circ S^{-1}. \tag{2.81}$$

From eqs. (2.78) - (2.80) we see that $U(0) = S(T(S^{-1}(0))) = 0$ and $U(\infty) = S(T(S^{-1}(\infty))) = \infty$. It follows that U is a particular simple Möbius transformation, being in fact only a multiplication with a complex number

$$U(z) = \eta z, \quad \eta \in \mathbb{C}. \tag{2.82}$$

We prove this form of U, eq. (2.82), by inserting the fixed points in the generic Möbius expression for U:

$$U(0) = \frac{a0+b}{c0+d} = \frac{b}{d} = 0 \qquad \Rightarrow \; b = 0, \tag{2.83}$$

$$U(\infty) = \frac{a\infty+b}{c\infty+d} = \frac{a}{c} = \infty \quad \Rightarrow \; c = 0, \tag{2.84}$$

$$\Rightarrow \; U(z) = \frac{az}{d} = \eta z. \tag{2.85}$$

Now it is possible to write down an expression for successive transformations by a general Möbius transformation, $T^n(z) = T(T(...T(z)...)$. From eq. (2.81) we can write $T = S^{-1} \circ U \circ S$ which then becomes a neat expression for T^n:

$$\begin{aligned} T^n &= (S^{-1} \circ U \circ S)^n = S^{-1} \circ U \circ S \circ S^{-1} ... \circ U \circ ... S \circ S^{-1} \circ U \circ S \\ &= S^{-1} \circ U^n \circ S. \end{aligned} \tag{2.86}$$

We can rewrite, eq. (2.86), as $S \circ T^n = U^n \circ S$, which is called normal form. Then using how S and U is defined in eqs. (2.76) and (2.85) we get the expression for n successively applied Möbius transformations, T^n, when it has two distinct fixed points,

$$\frac{T^n(z) - \gamma_1}{T^n(z) - \gamma_2} = \eta^n \frac{z - \gamma_1}{z - \gamma_2}. \tag{2.87}$$

Not all Möbius transformations have two distinct fixed points, but instead one with double multiplicity for which the above expression is not valid. The latter point is easy to see from the derivation where the definition of S in eq. (2.76) would not be a Möbius transformation in that case. So let us now assume that our Möbius transformation T has only one fixed point, that is instead of eq. (2.74) we have

$$\gamma = \frac{a-d}{2c} \quad \text{and} \quad (a-d)^2 + 4bc = 0. \tag{2.88}$$

We can now define a new S such that T's fixed point is sent to ∞,

$$S(z) = \frac{1}{z - \gamma}. \tag{2.89}$$

By comparison with eq. (2.70) one immediately verifies that S is a Möbius transformation. The inverse to S is in accordance with the general inverse formula, eq. (2.72), is given by

$$S^{-1}(z) = \frac{-\gamma z - 1}{-z}. \tag{2.90}$$

We can now define U exactly as before by $U = S \circ T \circ S^{-1}$ which has ∞ as fixed point:

$$S^{-1}(\infty) = \frac{-\gamma\infty - 1}{-\infty} = \gamma, \tag{2.91}$$

$$T(\gamma) = \gamma, \tag{2.92}$$

$$S(\gamma) = \frac{1}{\gamma - \gamma} = \infty, \tag{2.93}$$

$$\Rightarrow \quad U(\infty) = S(T(S^{-1}(\infty))) = S(T(\gamma)) = S(\gamma) = \infty. \tag{2.94}$$

We now have the task of finding an explicit expression for a Möbius transformation with only one fixed point at ∞. We know that U can have only one fixed point since T has only one and is sandwiched between a Möbius transformation and its inverse. We can now find the expression for U by using the two equations given by the fixed point, eq. (2.88):

$$U(\infty) = \frac{a\infty + b}{c\infty + d} = \frac{a}{c} = \infty \qquad \Rightarrow \; c = 0, \tag{2.95}$$

$$(a-d)^2 + 4bc = (a-d)^2 = 0 \qquad \Rightarrow \; a = d, \tag{2.96}$$

$$\Rightarrow \; U(z) = \frac{az + b}{a} = z + b/a = z + \beta. \tag{2.97}$$

In the same way as before we can now do repeated transformations of the Möbius transformation T, just as in eq. (2.86), but with a different S and U. We thus get the normal form for a Möbius transformation T with a single fixed point, from $S \circ T^n = U^n \circ S$, with the expression

$$\frac{1}{T^n(z) - \gamma} = \frac{1}{z - \gamma} + n\beta. \tag{2.98}$$

3

Sine-square deformation

This chapter contains a thorough review of the recent work by Fan et al. in Ref. [2], building on some previous work by Wen and Wu in Ref. [1, 3]. In addition, we will fill out some missing steps in the analysis by Fan et al. In the next chapter we then build on this when investigating a generalization.

The work by Fan et al. aims at understanding how the energy distribution in a one-dimensional system behaves when subject to a square wave driving. The two settings for which the chosen system experiences a periodic drive is an arbitrary CFT and a sine-squared deformation of the same CFT.

The sine-squared deformation of a Hamiltonian has received considerable interest in the last decade. The reason is the special behavior of its ground state, which, imposing periodic boundary conditions, is the same as for the non-deformed Hamiltonian. This property can be used when performing numerical calculations of lattice models. This however is not why Fan et al. use a sine-square deformation. Rather, from these earlier works insights and techniques can be drawn which are useful for understanding the present problem of a periodic drive. A key insight is that the description of a sine-squared deformation of a CFT makes it possible to relate time evolution to a Möbius transformation and thus enabling an analytically calculable problem. Here we will follow Katsura [12] when discussing general sine-squared CFT deformations, building on the seminal article by Gendair et al. [13].

Before we start with the rather technical discussion, it may be good to have an overview to fall back on. We will start with describing the system and emphasize the two main features of its description within the CFT formalism. First, the time evolution of the system is governed by two different Hamiltonians which are turned on and off repeatedly ("square wave drive"). Secondly, to exploit the full machinery of CFT and study the Möbius transformation we need to map the problem onto the complex plane. However, before we can utilize the form of the Hamiltonians in the complex plane we need to overcome a branch cut problem coming from the finite size of the system. Then can we find the explicit Möbius transformation, referred to above, by more or less straightforward calculations. Lastly, we can then calculate the energy of the system by calculating the expectation value of the stress-energy tensor. We finish the chapter with an analysis of how to relate the energy density to the Möbius transformation which emulates the time evolution, here taken to be stroboscopic (i.e. monitored at periodic time intervals).

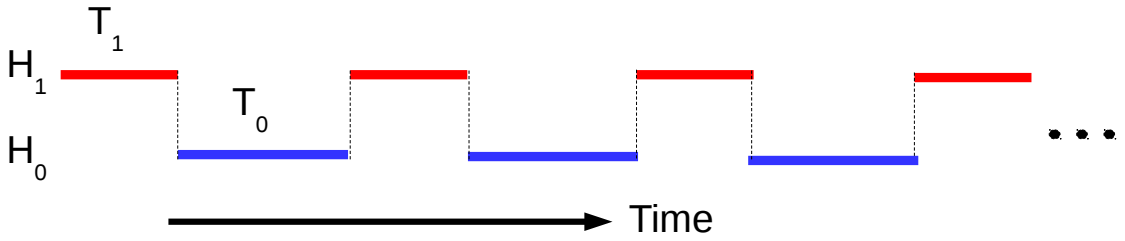

Figure 3.1: The driving scheme for the system. Quantum quenches are performed from an arbitrary CFT, described by H_0, to the sine-squared deformation of the same CFT, described by H_1, and then back to H_0 and so on. There are two independent driving parameters, T_0 and T_1, describing for how long the system is in the non-deformed and the deformed CFT respectively, with one period $T = T_0 + T_1$.

3.1 Our setup

We start with an arbitrary conformal field theory (CFT) in (1+1)D, one space plus one time dimension, with finite spatial size, L. We describe this theory with a Hamiltonian H_0 given by

$$H_0 = \int_0^L \mathrm{d}x\, T_{tt}(x), \tag{3.1}$$

with T_{tt} the time-time component of the corresponding stress-energy tensor. By a quantum quench we then set the system to be governed by the Hamiltonian H_1 which is a deformation of H_0 given by

$$H_1 = 2\int_0^L \mathrm{d}x \sin^2\left(\frac{\pi x}{L}\right) T_{tt}(x). \tag{3.2}$$

The system is then driven, made to go back and forth between these two Hamiltonian's as seen schematically in fig. 3.1. Thus, the full time-dependent Hamiltonian governing the time evolution is defined by

$$H(t) = \begin{cases} H_1, & 0 < t \bmod T < T_1 \\ H_0, & T_1 < t \bmod T < T_1 + T_0 \end{cases}. \tag{3.3}$$

It follows that one period T of the drive is given by $T = T_1 + T_0$. The expressions for the Hamiltonians in eqs. (3.1) and (3.2) are given in Minkowski space. It is important to keep this in mind, as we later will perform transformations to Euclidean and Euclidean light-cone coordinates.

Before the driving starts, at time $t = 0$, we prepare the system in the ground state to H_0, call it $|G_{H_0}\rangle$. We denote it with G instead of the usual 0 to distinguish this state from the vacuum. The reason why we need this distinction is that excitations in the driven system is not built up by creation operators acting on this ground state, $|G_{H_0}\rangle$, as they would be if we had no drive, i.e. with only H_0 (or H_1) as governing Hamiltonian.

The last ingredient for specifying the system are the boundary conditions. We will choose open boundary conditions. This is known to be a conformal boundary condition, i.e. going without saying that the conditions do not change under conformal transformations. Furthermore it is defined by that we have no energy flow over the edges, defined by $(0, t)$ and (L, t), and that the stress-energy tensor is set to a constant at the boundaries [31]. In an equation this is written as

$$T_{tx}(0) = T_{tx}(L) = 0. \tag{3.4}$$

In order to formally implement the boundary conditions it is preferable to write the stress-energy tensor in two parts, one for holomorphic fields and one for anti-holomorphic fields; for further discussion of holomorphic and anti-holomorphic fields see section 2.3. We will now make use of the usual trick of analytic continuation to go from two real and independent coordinates, (x, t), to the larger space of two complex and independent coordinates, $(\omega, \bar{\omega})$. In this $\mathbb{C}^2$ space we use the tools of CFT and then remember that the physics is played out on the two-dimensional surface where the two coordinates are each others complex conjugate, that is $\bar{\omega} = \omega^*$. Let us do this analysis carefully for the stress-energy tensor.

The quantum field theories that we have started with, both being CFTs in a Hamiltonian formulation, are expressed in Minkowski space with coordinates (t, x) and metric $\eta_{\mu\nu} = \text{diag}(-1, 1)$. Since the CFTs are 2D it is preferable to use complex coordinates, where all conformal coordinate changes are given by analytic functions. The first step is to go to imaginary time, $\tau = it$, so that we have coordinates (τ, x) and the geometry becomes Euclidean by the standard coordinate change $\eta'_{\alpha\beta} = \frac{\partial x^\mu}{\partial x'^\alpha}\frac{\partial x^\nu}{\partial x'^\beta}\eta_{\mu\nu}$, i.e. the new metric becomes $\text{diag}(1, 1)$. In the second step we are going to light-cone coordinates, which in Minkowski geometry is given by the usual $t = \pm x$ but now in Euclidean space implying that $\tau = \pm ix$. We can then make the coordinate change to

$$\omega = \tau + ix \quad \text{and} \quad \overline{\omega} = \tau - ix. \tag{3.5}$$

For now ω and $\bar{\omega}$ are dependent, with τ and x being independent variables. However, by an analytic continuation ω and $\bar{\omega}$ will bee taken as two independent complex variables. This is a standard trick in CFT, to be discussed further in section 2.3. With these coordinate changes and recalling that the stress-energy tensor is a tensor with transformation rule,

$$T'_{\alpha\beta}(x') = \frac{\partial x^\mu}{\partial x'^\alpha}\frac{\partial x^\nu}{\partial x'^\beta}T_{\mu\nu}(x), \tag{3.6}$$

we can write down how the components of the stress-energy tensor are related in the different coordinate systems. The first transformation is $(t, x) \mapsto (\tau = it, x)$ and the second is $(\tau, x) \mapsto (\omega = \tau + ix, \bar{\omega} = \tau - ix)$, where we need the inverse map to perform the transformation in eq. (3.6). We should remark that the last equality is an equality only as long as $\bar{\omega} = \omega^*$, that is the before analytic continuation. We

thus obtain

$$\underbrace{\begin{bmatrix} T_{tt} & T_{tx} \\ T_{tx} & T_{xx} \end{bmatrix}}_{\text{Minkowski}} = \underbrace{\begin{bmatrix} \overbrace{-T_{tt}}^{T_{\tau\tau}} & \overbrace{-iT_{tx}}^{T_{\tau x}} \\ \underbrace{-iT_{tx}}_{T_{\tau x}} & \underbrace{T_{xx}}_{T_{xx}} \end{bmatrix}}_{\text{Euclidian}} = \underbrace{\frac{1}{4}\begin{bmatrix} \overbrace{-T_{tt}-2T_{tx}-T_{xx}}^{4T_{\omega\omega}} & \overbrace{-T_{tt}+T_{xx}}^{4T_{\omega\bar{\omega}}} \\ \underbrace{-T_{tt}+T_{xx}}_{4T_{\bar{\omega}\omega}} & \underbrace{-T_{tt}+2T_{tx}-T_{xx}}_{4T_{\bar{\omega}\bar{\omega}}} \end{bmatrix}}_{\text{Euclidian light-cone}}. \tag{3.7}$$

Note that the stress-energy tensor is symmetric, which is why no distinction is done between T_{tx} and T_{xt}. Furthermore, since we work with a CFT theory we also know that the tensor is traceless, $g^{\mu\nu}T_{\mu\nu} = 0$, with the metric $g_{\mu\nu}$ defined in the different geometries.

So now to the most important part and that is how to write the time-time component of the stress energy tensor in complex coordinates. We already know that $T_{\bar{\omega}\omega} = T_{\omega\bar{\omega}} = 0$ given that $g^{\mu\nu}T_{\mu\nu} = -T_{tt} + T_{xx} = 0$, implying that

$$\begin{aligned} T_{\omega\omega} + T_{\bar{\omega}\bar{\omega}} &= \frac{1}{4}(-T_{tt} - 2T_{tx} - T_{xx} - T_{tt} + 2T_{tx} - T_{xx} + 2\underbrace{(-T_{tt} + T_{xx})}_{T^{\mu}{}_{\mu}=0}) \\ &= -T_{tt}. \end{aligned} \tag{3.8}$$

Now we will investigate the arguments of the components of the stress-energy tensor in the different coordinate systems, which we so far have been hiding. First, we could play with the assumption of T as just a two-tensor (we really know that we have time invariance for the stress-energy tensor) then we would write eq. (3.8) as

$$T_{tt}(x,t) = -(T_{\omega\omega}(\omega,\bar{\omega}) + T_{\bar{\omega}\bar{\omega}}(\omega,\bar{\omega})). \tag{3.9}$$

But from the equations of motion, eq. (2.48), it follows that $T_{\omega\omega}$ and $T_{\bar{\omega}\bar{\omega}}$ are holomorphic and anti-holomorphic respectively, i.e. we have $T_{\omega\omega} = T_{\omega\omega}(\omega)$ and $T_{\bar{\omega}\bar{\omega}} = T_{\bar{\omega}\bar{\omega}}(\bar{\omega})$ [35]. Furthermore, as said the stress-energy tensor is time invariant and we have time dependence in ω and $\bar{\omega}$, seen by $\omega = \tau + ix$ and $\bar{\omega} = \tau - ix$ where $\tau = it$. Using these two facts we then know that eq. (3.9) really is:

$$T_{tt}(x) = -(T_{\omega\omega}(ix) + T_{\bar{\omega}\bar{\omega}}(-ix)). \tag{3.10}$$

Before we can write the Hamiltonians in eqs. (3.1) and (3.2) in complex variables we must see what happens with the sine-squared function in eq. (3.2) under these coordinate changes. This is easiest done by writing the sine function in terms of exponentials:

$$2\sin^2\left(\frac{\pi x}{L}\right) = 2\left(\frac{e^{i\frac{\pi x}{L}} - e^{-i\frac{\pi x}{L}}}{2i}\right)^2 = 1 - \frac{1}{2}\left(e^{\frac{i2\pi x}{L}} + e^{\frac{-i2\pi x}{L}}\right). \tag{3.11}$$

We can easily combine this with the stress energy components in eq. (3.10) giving

$$\begin{aligned} 2\sin^2(\frac{\pi x}{L})T_{tt}(x) &= T_{\omega\omega}(ix) - \frac{1}{2}\left(e^{\frac{2\pi ix}{L}} + e^{-\frac{2\pi ix}{L}}\right)T_{\omega\omega}(ix) \\ &\quad + T_{\bar{\omega}\bar{\omega}}(-ix) - \frac{1}{2}\left(e^{\frac{2\pi ix}{L}} + e^{-\frac{2\pi ix}{L}}\right)T_{\bar{\omega}\bar{\omega}}(-ix) \\ &= T_{\omega\omega}(\omega) - \frac{1}{2}\left(e^{\frac{2\pi\omega}{L}} + e^{-\frac{2\pi\omega}{L}}\right)T_{\omega\omega}(\omega) \\ &\quad + T_{\bar{\omega}\bar{\omega}}(\bar{\omega}) - \frac{1}{2}\left(e^{\frac{2\pi\bar{\omega}}{L}} + e^{-\frac{2\pi\bar{\omega}}{L}}\right)T_{\bar{\omega}\bar{\omega}}(\bar{\omega}), \end{aligned} \tag{3.12}$$

where we by abuse of notation have made the definition $\omega = ix$ and $\bar{\omega} = -ix$. We could have used any other character but we use ω and $\bar{\omega}$ to remember that we work in the coordinate system given by the same variable name. We can now easily perform one standard CFT technique on eq. (3.12) which is that of analytic continuation, for further discussion see section 2.3. That is, now we make ω and $\bar{\omega}$ two independent complex variables, up to now they have been each other complex conjugates.

We will from now on only do conformal transformations which by definition only scales the metric so there will be no more mixing of entries in the stress-energy tensor. To lighten up the notation we make the definitions

$$T_{\omega\omega}(\omega) := -\frac{1}{2\pi}T(\omega) \quad \text{and} \quad T_{\bar{\omega}\bar{\omega}}(\bar{\omega}) := -\frac{1}{2\pi}\bar{T}(\bar{\omega}). \tag{3.13}$$

We should note that the minus sign and factor of 2π differ in the literature, and we have here used the same convention as in the standard text by Di Francesco et al. [31]. For future convenience we should note that using the notation where we do not write out indices on the stress-energy tensor T only is conventional when we work with coordinate systems described by two complex directions. Thus when we go back to describe the energy density in Minkowski space we again will use the convention of writing out the indices.

We can now write down the Hamiltonians H_0 and H_1 in the complex strip geometry, we have $\mathrm{d}\omega = i\,\mathrm{d}x$ and $\mathrm{d}\bar{\omega} = -i\,\mathrm{d}x$ from before the analytic continuation when we had $\omega = \tau + ix$ and $\bar{\omega} = \tau - ix$. By abuse of notation we will write out starting and endpoints of the integration instead of defining a curve in the complex plane, since we know that it practically is a one dimensional integral (T only being position dependent). From the definitions of the Hamiltonians H_0 and H_1 in eqs. (3.1) and (3.2) respectively and using eq. (3.12) for H_1 and remembering the definition in eq. (3.13) we obtain

$$H_0 = \int_0^L \frac{\mathrm{d}\omega}{2\pi i}T(\omega) - \int_0^{-L} \frac{\mathrm{d}\bar{\omega}}{2\pi i}\overline{T}(\overline{\omega}), \tag{3.14}$$

and

$$H_1 = H_0 - \frac{1}{2}\left(H_+ + H_-\right), \tag{3.15}$$

with

$$H_\pm = \int_0^L \frac{\mathrm{d}x}{2\pi i}e^{\pm\frac{2\pi}{L}\omega}\,T(\omega) - \int_0^{-L} \frac{\mathrm{d}\bar{\omega}}{2\pi i}e^{\mp\frac{2\pi}{L}\bar{\omega}}\,\bar{T}(\bar{\omega}). \tag{3.16}$$

The last ingredient to understand the setup is how to time-evolve the system. For this, we solve the time-dependent Schrödinger equation

$$H(t)\left|\psi(t)\right\rangle = i\partial_t\left|\psi(t)\right\rangle, \quad H(t) = \begin{cases} H_1 & 0 < t \bmod T < T_1 \\ H_0 & T_1 < t \bmod T < T_0 + T_1 \end{cases}. \tag{3.17}$$

Since the Hamiltonian is time dependent we need to be careful when writing down a solution, and use time ordering operator, TOO:

$$\left|\psi(t)\right\rangle = TOOe^{-i\int_0^t H(t')\mathrm{d}t'}\left|\psi(0)\right\rangle, \tag{3.18}$$

where $|\psi(0)\rangle = |G_{H_0}\rangle$, since this is the state that we prepared the system in. The unitary time-evolution operator can be written in a much simpler way if we only consider stroboscopic time evolution. Let us first consider only one period. Writing out the first terms in the formal expansion of the exponential and then using the time-ordering operator, we obtain

$$\begin{aligned} TOOe^{-i\int_0^T H(t')\mathrm{d}t'} &= TOOe^{-iH_1T_1-iH_0T_0} \\ &= TOO\left(1+(-iH_1T_1-iH_0T_0)+\frac{1}{2!}(-iH_1T_1-iH_0T_0)^2+...\right) \\ &= 1+-iH_1T_1-iH_0T_0 \\ &+\frac{1}{2!}(-i)^2\left((H_1T_1)^2+2T_0T_1H_0H_1+(H_0T_0)^2\right)+... \\ &= \left(1-iH_0T_0+\frac{(-i)^2}{2!}(H_0T_0)^2+...\right) \\ &\times\left(1-iH_1T_1+\frac{(-i)^2}{2!}(H_1T_1)^2+...\right) \\ &= e^{-iH_0T_0}e^{-iH_1T_1}. \end{aligned} \tag{3.19}$$

Here we have used that $TOO(H_0H_1+H_1H_0) = 2H_0H_1$ since when time ordering the product we know that H_1 is the Hamiltonian in the interval $0 < t < T_1$ and H_0 in the interval $T_1 < t < T_1 + T_0$, which is also the reason for the order of the two exponentials. If we would do this for several periods, the same procedure gives

$$\begin{aligned} TOO\exp\left\{-i\int_0^{nT}H(t')\,\mathrm{d}t'\right\} &= e^{-iH_0T_0}e^{-iH_1T_1}e^{-iH_0T_0}e^{-iH_1T_1}...e^{-iH_0T_0}e^{-iH_1T_1} \\ &= \left(e^{-iH_0T_0}e^{-iH_1T_1}\right)^n. \end{aligned} \tag{3.20}$$

When we work with the complex coordinate, ω, we have made a Wick rotation to imaginary time $\tau = it$. In this coordinate the stroboscopic time evolution operator after $n\mathcal{T}$ is

$$\left(e^{-H_0\tau_0}e^{-H_1\tau_1}\right)^n, \tag{3.21}$$

where we have the imaginary time intervals $\tau_0 = iT_0$ and $\tau_1 = iT_1$, and n is the number of periods, and $\mathcal{T} = iT$. Furthermore the Hamiltonians H_0 and H_1 are given by eqs. (3.14) and (3.15) respectively in the strip geometry, denoted with $(\omega, \bar{\omega})$ coordinates.

3.2 Stroboscopic time evolution as a Möbius transformation

The task in this section is for us to understand how we can calculate the stroboscopic time evolution of the expectation value for any operator $\mathcal{O}(\omega, \overline{\omega})$ after n periods of the drive, that is,

$$\langle\psi(n\mathcal{T})|O(\omega,\bar{\omega})|\psi(n\mathcal{T})\rangle = \langle G_{H_0}|\left(e^{H_1\tau_1}e^{H_0\tau_0}\right)^n O(\omega,\bar{\omega})\left(e^{-H_0\tau_1}e^{-H_0\tau_1}\right)^n|G_{H_0}\rangle\,, \tag{3.22}$$

where $\psi(n\mathcal{T})$ is the time-evolved ground state $|G_{H_0}\rangle$ after n periods of $\mathcal{T} = \tau_1 + \tau_0$ imaginary time. We will carry out this analysis in Heisenberg picture as indicated by sandwiching the operator by the time evolution operator instead of having the time dependence in the state. The derivation in this section will show that the time evolution of an operator can be described as a conformal transformation, more precisely a Möbius transformation.

We will show this in essentially three steps. First how the Hamiltonians H_0 and H_1 for the chosen CFT and its deformation, eqs. (3.14) and (3.15), are written in the complex plane geometry, with coordinate z, instead of the strip geometry, with coordinate ω. Second, we will show how the stroboscopic time evolution can be represented by a contour integration in the complex plane within an arbitrary close neighborhood to the operator. Third and last we will show how the Hamiltonians are nothing else than Virasoro generators, which are generators of conformal transformations. Given this we will also be able to identify the explicit Möbius transformation.

3.2.1 The Hamiltonians in complex plane coordinates

The starting point here is the Hamiltonians given by eq. (3.14) and eq. (3.15) for the chosen (arbitrary) CFT and its deformation respectively, given in the strip geometry where we already have imaginary time, that is, complex coordinates ω and $\bar{\omega}$. Now we want to do the transformation to the whole complex plane,

$$\omega \mapsto z = e^{\frac{2\pi}{L}\omega}, \quad \overline{\omega} \mapsto \overline{z} = e^{\frac{2\pi}{L}\overline{\omega}}. \tag{3.23}$$

This is illustrated in fig. 3.2 where we note that equal time points are represented by horizontal lines in the strip geometry and by circles in the complex plane. We should here remember that $\mathcal{T} = \tau_0 + \tau_1$ defines the period of the drive.

The transformation of the Hamiltonians exploits standard techniques, including a Jacobian and a change of integration path, that is, the integration along a horizontal line in the strip geometry becomes an integration around a circle in the complex plane. In addition, we must judiciously carry out the transformation of the stress-energy tensor. The transformation $\omega \mapsto z$ in eq. (3.23) is a conformal transformation as follows from the fact that it is analytical. This is obvious since the exponent function has a Taylor series expansion in a neighborhood of each point where it is defined, in fact the neighborhood may be taken to be the whole complex plane. All analytic functions are holomorphic, and since we have no $\overline{\omega}$ dependence in the transformation $z \to \omega$ it is conformal. We can then use our knowledge of how the stress-energy tensor transforms under conformal transformations (cf. our discussion in section 2.4)

$$\begin{aligned} T(\omega) &= (z')^2 T(z) + \frac{c}{12}\{z, \omega\}_{Sc} \\ &= (z')^2 T(z) + \frac{c}{12}\left(\frac{z'''}{z'} - \frac{3}{2}\left(\frac{z''}{z'}\right)^2\right) \\ &= \left(\frac{2\pi}{L}\right)^2 z^2 T(z) - \frac{1}{2}\left(\frac{2\pi}{L}\right)^2 \frac{c}{12}, \end{aligned} \tag{3.24}$$

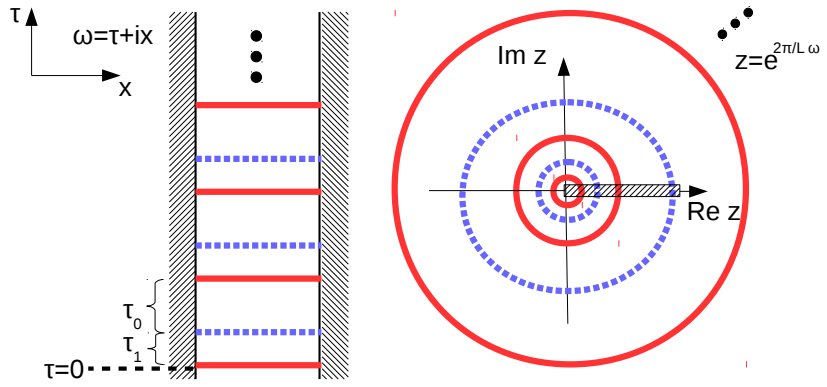

Figure 3.2: Schematic plot of how to go from the strip geometry to the complex-plane with a branch cut, using the mapping $\omega \mapsto z = e^{\frac{2\pi}{L}\omega}$. The branch cut originates from the two boundaries at $x = 0$ and $x = L$ being mapped onto the real positive axis. We start the driving at time $\tau = 0$ by switching on H_1 at the red bottom solid line (innermost red circle) until $\tau = \tau_1$ at the dotted blue line (innermost blue dotted circle) where the Hamiltonian $H(t)$ is switched to H_0. $H(t)$ is then switched back to H_1 after a time τ_0 with this process being repeated periodically.

with $z' = \frac{\partial z}{\partial \omega}$. Here the Schwarzian derivative, $\{z, \omega\}_{Sc} = \frac{z'''}{z'} - \frac{3}{2}\left(\frac{z''}{z'}\right)^2$ reduces to $\left(\frac{2\pi}{L}\right)^2$ using that $z' = \frac{2\pi}{L} z$. The anti-holomorphic part gives the analogous expression

$$\overline{T}(\overline{\omega}) = \left(\frac{2\pi}{L}\right)^2 \overline{z}^2 T(\overline{z}) - \frac{1}{2}\left(\frac{2\pi}{L}\right)^2 \frac{c}{12}. \tag{3.25}$$

Now when we know what happens to the stress-energy tensor we need only two small standard ingredients, the Jacobian and change in integration path, to be able to perform the coordinate transformation of the integral formulations of the Hamiltonians, H_0 and H_1 given in eqs. (3.14) and (3.15) respectively. First, we write down the Jacobian, seen directly from eq. (3.23):

$$\mathrm{d}\omega = \frac{L}{2\pi}\frac{1}{z}\,\mathrm{d}z\,, \quad \mathrm{d}\bar{\omega} = \frac{L}{2\pi}\frac{1}{\bar{z}}\,\mathrm{d}\bar{z}\,. \tag{3.26}$$

Moreover, we can also easily read of the path for z and $\overline{z}$ from the two lines from 0 to L and 0 to $-L$ in the strip geometry, thus obtaining two circles, C_z and $C_{\overline{z}}$, with different radii, when taking z and $\bar{z}$ to be independent. However, on the physical plane where $\bar{z} = z^*$, the radii are the same, but still with C_z oriented counterclockwise while $C_{\bar{z}}$ runs clockwise; cf. fig. 3.3.

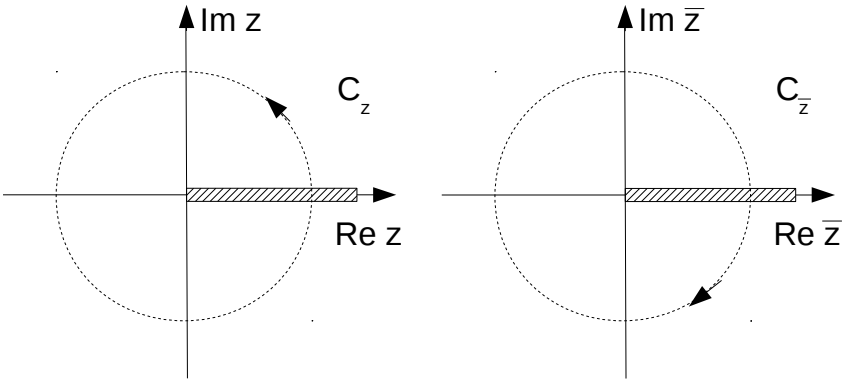

Figure 3.3: Integration paths in the complex plane after the change of coordinate system from the strip geometry to the complex-plane. Note that the integration direction is opposite for z and $\overline{z}$. The two radii are the same when considering the physical plane where $\bar{z} = z^*$ but may otherwise be different.

Now we are ready to write down H_0 in the complex plane,

$$\begin{aligned} H_0 &= \int_{C_z^{\circlearrowleft}} \frac{\mathrm{d}z}{2\pi i} \frac{L}{2\pi} \frac{1}{z} \left(\frac{2\pi}{L}\right)^2 \left(z^2 T(z) - \frac{1}{2}\frac{c}{12}\right) - (z \to \overline{z}) \\ &= \frac{2\pi}{L} \int_{C_z^{\circlearrowleft}} \frac{\mathrm{d}z}{2\pi i} z T(z) - (z \to \overline{z}) - \frac{2\pi}{L}\frac{c}{12}. \end{aligned} \tag{3.27}$$

To obtain the second line in eq. (3.27) we performed the contour integral over $1/z$ and $1/\overline{z}$ by going back to do the integration over x instead, in this way avoiding the problem with the branch cut in the complex plane. Then we have $\mathrm{d}z = \frac{2\pi i}{L} \exp\left\{\frac{2\pi}{L}(\tau + ix)\right\} \mathrm{d}x$ and $\mathrm{d}\overline{z} = -\frac{2\pi i}{L} \exp\left\{\frac{2\pi}{L}(\tau - ix)\right\} \mathrm{d}x$ as implied by eqs. (3.5) and (3.26). It follows that

$$\int_{\mathrm{C}_z^{\circlearrowleft}} \frac{\mathrm{d}z}{2\pi i} \frac{1}{z} = \int_0^L \frac{\mathrm{d}x}{L} = 1, \tag{3.28}$$

and

$$\int_{\mathrm{C}_{\overline{z}}^{\circlearrowleft}} \frac{\mathrm{d}\overline{z}}{2\pi i} \frac{1}{\overline{z}} = -\int_0^L \frac{\mathrm{d}x}{L} = -1. \tag{3.29}$$

The last thing we need for a full description of both Hamiltonians in the complex plane are expressions for $H_\pm$ (cf. eq. (3.15)). In fact we essentially know everything since $e^{\pm\frac{2\pi}{L}\omega} = z^{\pm 1}$ (and $e^{\mp\frac{2\pi}{L}\overline{\omega}} = \overline{z}^{\mp 1}$) and the rest of the analysis is the same as for H_0. Thus,

$$\begin{aligned} H_\pm &= \int_0^L \frac{\mathrm{d}\omega}{2\pi} e^{\pm\frac{2\pi}{L}\omega}\, T(\omega) - (\omega \to \bar{\omega}) \\ &= \frac{2\pi}{L} \int_{\mathrm{C}_z^{\circlearrowleft}} \frac{\mathrm{d}z}{2\pi i} \left(z^{1\pm 1} T(z) - z^{1\pm 1}\frac{1}{2}\frac{c}{12}\right) - (z \to \overline{z}) \\ &= \frac{2\pi}{L} \int_{\mathrm{C}_z^{\circlearrowleft}} \frac{\mathrm{d}z}{2\pi i} z^{1\pm 1} T(z) - (z \to \overline{z}). \end{aligned} \tag{3.30}$$

In the last line we perform the integrals over z^0 ($\bar{z}^0$) and z^2 ($\bar{z}^2$) all of which give zero contribution. Again we have to deal with the branch cut. We again do this by going back to the x-integral via eqs. (3.5) and (3.26),

$$\int_{\mathrm{C}_z^{\circlearrowleft}} \frac{\mathrm{d}z}{2\pi i} = \frac{e^{\frac{2\pi}{L}\tau}}{L} \int_0^L \mathrm{d}x\, e^{\frac{2\pi}{L} ix} = 0, \tag{3.31}$$

$$\int_{\mathrm{C}_z^{\circlearrowleft}} \frac{\mathrm{d}z}{2\pi i} \frac{1}{z^2} = \frac{e^{-\frac{2\pi}{L}\tau}}{L} \int_0^L \mathrm{d}x\, e^{-\frac{2\pi}{L} ix} = 0. \tag{3.32}$$

The only difference doing this for the $\bar{z}^2$ integral is that we pick up an overall minus sign from the Jacobian, as in the calculation for H_0 in eq. (3.29), thus making the corresponding integrals vanish. With this, we can now write down H_1, using the formula in eq. (3.15),

$$\begin{aligned} H_1 &= H_0 - \frac{1}{2}\left(H_+ + H_-\right) \\ &= \frac{2\pi}{L} \int_{\mathrm{C}_z^{\circlearrowleft}} \frac{\mathrm{d}z}{2\pi i} \frac{1}{2} \left(-1 + 2z - z^2\right) T(z) - (z \to \bar{z}) - \frac{2\pi}{L} \frac{c}{12}. \end{aligned} \tag{3.33}$$

3.2.2 Time evolution as a contour integral in a neighborhood of the field

In this section we shall explain why – within the region of stroboscopic time evolution of an operator – it does not matter that we have a branch cut in the complex plane. This will be done by expanding the time-evolved expression using the Campbell-Baker-Hausdorff formula and showing that each commutator effectively acts as a contour integral in a neighborhood of the operator.

We have the stroboscopic time evolution of an operator

$$\left(e^{H_1\tau_1} e^{H_0\tau_0}\right)^n \mathcal{O}(z,\bar{z}) \left(e^{-H_0\tau_0} e^{-H_1\tau_1}\right)^n, \tag{3.34}$$

which we expand by using the Campbell-Baker-Hausdorff formula

$$e^A B e^{-A} = B + [A,B] + \frac{1}{2!}[A,[A,B]] + \frac{1}{3!}[A,[A,[A,B]]] + ..., \tag{3.35}$$

where A and B are two arbitrary operators. We can apply this identity twice, with the time evolution operator acting on an operator, $\mathcal{O}$, as follows (here writing out the expression explicitly for one period),

$$\begin{aligned} & e^{H_1\tau_1} e^{H_0\tau_0} \mathcal{O}(z,\bar{z}) e^{-H_0\tau_0} e^{-H_1\tau_1} \\ &\qquad = e^{H_1\tau_1} \left(\mathcal{O} + \tau_0[H_0,\mathcal{O}] + \frac{\tau_0^2}{2!}[H_0,[H_0,\mathcal{O}]] + ... \right) e^{-H_1\tau_1} \\ &\qquad = \mathcal{O} + \tau_1[H_1,\mathcal{O}] + \frac{\tau_1^2}{2!}[H_1,[H_1,\mathcal{O}]] + ... \\ &\qquad + \quad \tau_0[H_0,\mathcal{O}] + \tau_1\tau_0[H_1,[H_0,\mathcal{O}]] + ... \\ &\qquad + \quad \frac{\tau_0^2}{2!}[H_0,[H_0,\mathcal{O}]] + ... \\ &\qquad + ... \end{aligned} \tag{3.36}$$

What we should take with us from eq. (3.36) is that all commutator terms contain a commutator between a position-dependent operator, $\mathcal{O}(z,\overline{z})$, and a position independent operator, H_0 or H_1. Then, for higher-order terms, this commutator, which itself is a position-dependent operator, is commuted with H_0 or H_1, and so on. From this we can understand that we need only to show that $[H_0,\mathcal{O}]$ and $[H_1,\mathcal{O}]$ are independent of the branch cut: all higher-order terms then follow by the same logic since we then have a new operator say $\mathcal{O}'(z,\bar{z}) = [H_0,\mathcal{O}(z,\bar{z})]$ (or $[H_1,\mathcal{O}(z,\bar{z})]$ depending on which commutator we have). It is obvious that this is true for any number of periods since the only thing that happens is that we have more mixtures between H_0 and H_1 in the higher-order commutators.

Let us focus on the easiest case, $[H_0,\mathcal{O}]$. To prepare for the analysis, we first rewrite H_0 as

$$\begin{aligned} H_0 &= \int_{C_z^{\circlearrowleft}} \frac{\mathrm{d}z}{2\pi} z T(z) - \int_{C_{\bar{z}}^{\circlearrowleft}} \frac{\mathrm{d}\bar{z}}{2\pi} \bar{z}\bar{T}(\bar{z}) = \int_{C_z^{\circlearrowleft}} \frac{\mathrm{d}z}{2\pi} z T(z) + \int_{C_{\bar{z}}^{\circlearrowleft}} \frac{\mathrm{d}\bar{z}}{2\pi} \bar{z}\bar{T}(\bar{z}) \\ &\overset{!}{=} \int_{C_z^{\circlearrowleft}} \frac{\mathrm{d}z}{2\pi} z \left(T(z) + \overline{T}(z)\right). \end{aligned} \tag{3.37}$$

The second equality simply embodies a change of sign when changing integration direction, $\circlearrowleft \to \circlearrowleft$. What we should notice is the last equality, embellished with an exclamation mark because this equality is true only if we consider the physical two-dimensional surface, $\overline{z} = z^*$, in the four dimensional space $(z,\overline{z}) \in \mathbb{C}^2$. When $\overline{z} = z^*$ we instantly know that the two integration paths are the same: circles with the same radii $r = |z| = |z^*|$. We can also see the exclamation mark as a reminder that it is unconventional to have an expression like $\overline{T}(z)$ and in fact not even true outside of this context: On the physical plane we would have $\overline{T}(z^*)$, a remark only to stress the crucial fact that we are here dealing with an integration path. The rewriting of H_0 as in eq. (3.37) (and, analogously, of H_1) will be necessary at a later stage when we need to add integrals with integrands of the form $(T+\overline{T})$; we have done it already so as to make the calculations easier to follow notation-wise.

We can now go ahead with the analysis of the commutator $[H_0,\mathcal{O}]$, with $\mathcal{O}$ an arbitrary operator. First, as usual they are equal-time commutators, which means we are at the same distance from the origin in the complex plane. In order to evaluate this commutator we will instead of having an integration which intersects the point where the operator is defined, $\mathcal{O}(z,\overline{z})$, have circles with radii infinitesimally displaced from $(z,\bar{z})$, as seen in fig. 3.4a. The operator is at a distance $r = |z| = |z^*| = |\overline{z}|$ since we are working with the physical plane $\overline{z} = z^*$. Hence, the circles corresponding to the two shifted integration paths are infinitesimally close, with radii $r_\pm = r \pm \epsilon$. From time ordering, which now is radial ordering, the path outside of r have the order $T\mathcal{O}$ (with T the stress-energy tensor), and vice versa for the smaller circle.

We thus obtain

$$\begin{aligned}[H_0, \mathcal{O}(z,\overline{z})] &= \left[\int_{C_r^{\circlearrowleft}} \frac{\mathrm{d}z'}{2\pi} z' \left(T(z') + \overline{T}(z')\right), \mathcal{O}\right] \\ &= \int_{C_{r_+}^{\circlearrowleft}} \frac{\mathrm{d}z'}{2\pi} z' \left(T(z') + \overline{T}(z')\right) \mathcal{O} - \int_{C_{r_-}^{\circlearrowleft}} \frac{\mathrm{d}z'}{2\pi} z' \mathcal{O} \left(T(z') + \overline{T}(z')\right) \\ &= \int_{C_{r_+}^{\circlearrowleft}} \frac{\mathrm{d}z'}{2\pi} z' \left(T(z') + \overline{T}(z')\right) \mathcal{O} + \int_{C_{r_-}^{\circlearrowleft}} \frac{\mathrm{d}z}{2\pi} z' \mathcal{O} \left(T(z') + \overline{T}(z')\right).\end{aligned} \tag{3.38}$$

The last equality can be visualised as in fig. 3.4a where it is also evident that the integration paths are not closed. This is why in fig. 3.4b we have added horizontal lines just above and below the real axis to get a closed integration path.

Before we write down the expression that confirms that we can add the two "horizontal" path integrals we need to introduce the radial ordering operator, that is time ordering which is radial in the complex plane coordinates. Let z and z' be two different points in the complex plane. Then the radial ordering operator, $\mathcal{R}$, is defined by

$$\mathcal{R}\mathcal{O}_1(z)\mathcal{O}_2(w) = \begin{cases} \mathcal{O}_1(z)\mathcal{O}_2(w) & \text{if} \quad |z| > |w| \\ \mathcal{O}_2(w)\mathcal{O}_1(z) & \text{if} \quad |z| < |w| \end{cases} . \tag{3.39}$$

We will now show that we can add the two horizontal lines as done in fig. 3.4b to no cost, since the integrals along these two lines cancel each other. We write

$$\begin{aligned}&\int_{r_-+i\delta}^{r_++i\delta} \frac{\mathrm{d}z'}{2\pi} z' \mathcal{R}\left(T(z') + \overline{T}(z')\right) \mathcal{O} + \int_{r_+-i\delta}^{r_--i\delta} \frac{\mathrm{d}z'}{2\pi} z' \mathcal{R}\mathcal{O} \left(T(z') + \overline{T}(z')\right) \\ &\qquad = \underbrace{\int_{r_-+i\delta}^{r_++i\delta} \frac{\mathrm{d}z'}{2\pi} z' \mathcal{R} T(z')\, \mathcal{O} + \int_{r_+-i\delta}^{r_--i\delta} \frac{\mathrm{d}z'}{2\pi} z' \mathcal{R}\mathcal{O}\, \overline{T}(z')}_{=0} \\ &\qquad + \underbrace{\int_{r_-+i\delta}^{r_++i\delta} \frac{\mathrm{d}z'}{2\pi} z' \mathcal{R} \overline{T}(z')\, \mathcal{O} + \int_{r_+-i\delta}^{r_--i\delta} \frac{\mathrm{d}z'}{2\pi} z' \mathcal{R}\mathcal{O}\, T(z')}_{=0} .\end{aligned} \tag{3.40}$$

In the second and third lines we have taken one "T" and one "$\overline{T}$" term from each integral in the first line and paired them together. These pairs of integrals cancel each other, since from the open boundary condition in the strip geometry $T(z) = \overline{T}(\overline{z})$ just above and below the real axis. Thus, the integrands are identical but with the integrations carried out in opposite directions.

Now there is only one more thing to do before we can conclude that $[H_0, \mathcal{O}]$ is unaffected by the branch cut and that is to perform a standard complex-analysis deformation of the integration curve, which is allowed as long as the integral is closed and we don't move past any poles (cf. fig. 3.4c). One remark that we would like to do is that the integrands may have the energy-tensor and the operator $\mathcal{O}$ in different orders, but implicitly there are always a radial operator that fixes the order also when the integration path is not a circle centered at the origin.

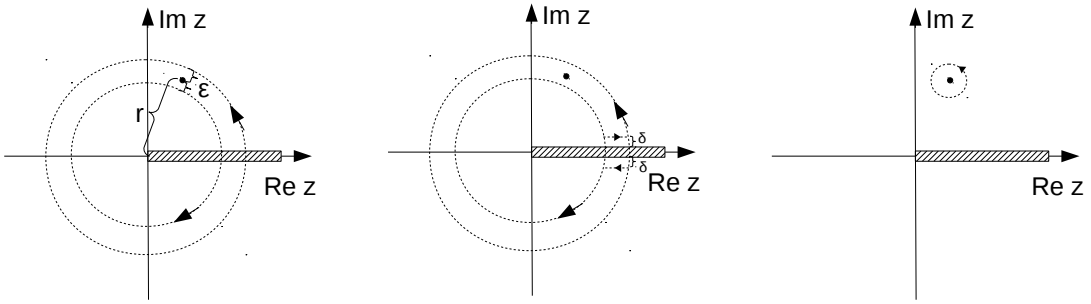

(a) **(b)** **(c)**

Figure 3.4: Sequence of figures which shows the steps in the argument that the commutators $[H_0, \mathcal{O}]$ and $[H_1, \mathcal{O}]$ are nothing but contour integrals of H_0 and H_1 integrands around the operator $\mathcal{O}$. Figure (a) depicts how the commutator is calculated, where we formally let $\epsilon \to 0$. In figure (b) we have added two integrals along the horizontal lines above and below the branch cut who cancel each other. In the last figure (c) we used that the absence of poles inside the enclosed area of the integration path allows us to deform the path. Thus we arrive at an integral in the neighborhood of the operator $\mathcal{O}$.

3.2.3 Hamiltonians as Virasoro generators

In this section we will use the fact that the time evolution is independent of the branch cut, which is what will let us rewrite the Hamiltonians in terms of generators of the Virasoro algebra. Then can we use all the knowledge and theory of the Virasoro algebra to write down a closed expression for the conformal transformation that emulate the time evolution.

What we gained from the previous discussion of how the stroboscopic time evolution is unaffected by the branch cut may technically seem rather small but the implications are quite powerful. As follows from the previous discussion, the Hamiltonians restricted to be part of the time evolution of an operator, $\mathcal{O}(z, \bar{z})$, may be written as

$$H_0 = \frac{2\pi}{L} \oint_z \frac{\mathrm{d}z'}{2\pi i} z' T(z') + (z' \to \bar{z}') - \frac{c\pi}{6L}, \tag{3.41}$$

$$H_1 = \frac{2\pi}{L} \oint_z \frac{\mathrm{d}z'}{2\pi i} \frac{1}{2}(-\frac{1}{2} + z' - \frac{z'^2}{2}) T(z') + (z' \to \bar{z}') - \frac{c\pi}{6L}. \tag{3.42}$$

The important difference from eqs. (3.27) and (3.33) is that we now have a closed integration path around the point z ($\bar{z}$) for the holomorphic (anti-holomorphic) part. This is what makes it possible to use the theory in section 2.4 where eqs. (2.58) and (3.42) shows how the generators of the Virasoro algebra are connected to the stress-energy tensor. Combining eqs. (2.58), (3.41) and (3.42), we can write the Hamiltonians as:

$$H_0 = \frac{2\pi}{L} \left(L_0 + \bar{L}_0 \right), \tag{3.43}$$

$$H_1 = \frac{2\pi}{L} \left(L_0 - \frac{1}{2} \left(L_{-1} + L_1 \right) + \bar{L}_0 - \frac{1}{2} \left(\bar{L}_{-1} + \bar{L}_1 \right) \right). \tag{3.44}$$

It follows that stroboscopic time evolution is the same as acting with exponentiated Virasoro generators, with the CBH commutator expansion (eq. (3.36)) as a basis when making the action of the generators explicit. Since we now know that the stroboscopic time evolution of a field is a conformal transformation of the field, we know that what we seek is a conformal coordinate change, $z \to z_1$ (with z_1 the new coordinate after one time period). For example, if we time-evolve a primary operator one period we get

$$e^{\tau_1 H_1} e^{\tau_0 H_0} \mathcal{O}(z,\overline{z}) e^{-\tau_0 H_0} e^{-\tau_1 H_1} = \left(\frac{\partial z_1}{\partial z}\right)^h \left(\frac{\partial \overline{z}}{\partial \overline{z}}\right)^{\overline{h}} \mathcal{O}(z_1,\overline{z}_1). \tag{3.45}$$

For any other operator such as the quasi-primary stress-energy tensor we would get a similar but slightly more messy expression. On the left hand side of eq. (3.45) is the expression for a conformal transformation on the operator, i.e. the Virasoro generators L_n and $\bar{L}_n$ which acts on the complex Hilbert space where the operators live. However, eq. (3.45) also shows how this transformation on the Hilbert space relate to a conformal coordinate transformation $z \to z_1, \bar{z} \to \bar{z}_1$, i.e. a transformation generated by Witt generators l_n and $\bar{l}_n$ which acts on the coordinate space described by $\mathbb{C}$. The relation between the Virasoro generators on the left-hand side in eq. (3.45), hidden in the Hamiltonians H_0 and H_1, and the Witt generators giving the coordinate change on the right-hand side is simple: We have $L_n \to l_n$ and $\bar{L}_n \to \bar{l}_n$, discussed further in section 2.5. This allows for a simple representation of the Witt generators,

$$l_n = -z^{n+1}\partial_z. \tag{3.46}$$

In particular, l_0 acts as dilation,

$$e^{-al_0} z = \left(\sum_{n=0}^{\infty} \frac{(az\partial_z)^n}{n!}\right) z = e^a z, \tag{3.47}$$

which is seen directly if one writes out the first terms in the sum and letting the derivatives act and then factorizes out z and identifies the Taylor expansion of e^a. This is what we will use, together with a trick of going to a coordinate system in which H_1 is described entirely in terms of l_0.

The coordinate transformation associated with one period of the drive is given by

$$e^{-\frac{2\pi\tau_0}{L} l_0} e^{-\frac{2\pi\tau_1}{L}\left(l_0 - \frac{1}{2}(l_{-1}+l_1)\right)} z. \tag{3.48}$$

We will now apply the trick to write z as a function of another coordinate χ in which the Hamiltonian H_1 is described only by the L_0 Virasoro generator and possibly constant terms. Taking off from the holomorphic part of eq. (3.42) and imposing a conformal transformation $z \to \xi$, whose explicit expression is to be found, we obtain

$$H_1 = \frac{2\pi}{L} \oint \frac{\mathrm{d}\chi}{2\pi i} \left(\frac{\partial \chi}{\partial z}\right)^{-1} \left(-\frac{1}{2} + z - \frac{z^2}{2}\right) \left(\left(\frac{\partial \chi}{\partial z}\right)^2 T(\chi) + \frac{c}{12}\{\chi, z\}_{Sc}\right) - \frac{c\pi}{6L}. \tag{3.49}$$

The two terms without the stress-energy tensor T will have no effect on the transformation since they are c-numbers. (Formally, we can see this from the CBH-expansion, eq. (3.36), that these terms commute with $\mathcal{O}$, thus giving zero contribution.) The equation that results from eq. (3.49), with H_1 a dilation, is immediately identified as

$$\chi = \left(\frac{\partial\chi}{\partial z}\right)^{-1} \underbrace{\left(-\frac{1}{2}+z-\frac{z^2}{2}\right)}_{-\frac{1}{2}(z-1)^2} \left(\frac{\partial\chi}{\partial z}\right)^2. \tag{3.50}$$

Equation (3.50) is easily rewritten as an integral equation,

$$\int \frac{\mathrm{d}\chi}{\chi} = -2\int \frac{\mathrm{d}z}{(z-1)^2}, \tag{3.51}$$

giving

$$\frac{1}{2}\ln\chi = \frac{1}{z-1} + \text{constant}. \tag{3.52}$$

Let us now verify that eq. (3.52) defines a conformal transformation. Rewriting it as

$$z \mapsto \chi(z) = e^{\frac{2}{z-1}+\text{constant}}, \tag{3.53}$$

we see that it is holomorphic (and by that also conformal; cf. our discussion after eq. (3.23)) on the punctured complex plane with $z = 1$ removed (corresponding to Euclidean time $\tau = 0$), where eq. (3.53) has a Taylor expansion. Thus, except at the origin (corresponding to $z = 1$) we have H_1 explicitly in χ-coordinates as

$$H_1 = \frac{2\pi}{L}\oint \frac{\mathrm{d}\chi}{2\pi i}\chi T(\chi) + (\chi \to \overline{\chi}) - \frac{c\pi}{6L}. \tag{3.54}$$

The important thing to note is that we indeed have H_1 expressed as an L_0 operator, seen by the equation for Virasoro generators given in eq. (2.58), plus a c-number.

We are now ready to find the full coordinate transformation $z \mapsto z_1$, implemented by Witt generators l_0^z (representing H_0) and l_0^χ (representing H_1), where the super-index z and χ indicate on which coordinate system they act as dilations. That is, the time evolution $e^{\tau_1 H_1} e^{\tau_0 H_0}\mathcal{O}e^{-\tau_0 H_0}e^{-\tau_1 H_1}$ of the operator $\mathcal{O}$ corresponds to the transformation of $\mathcal{O}$ under the conformal coordinate transformation $e^{-\frac{2\pi\tau_0}{L}l_0^z}e^{-\frac{2\pi\tau_1}{L}l_0^\chi}z$. For clarity, let us perform the transformation in painstaking detail, accounting for each single step:

$$\begin{aligned}
e^{-\frac{2\pi\tau_0}{L}l_0^z}e^{-\frac{2\pi\tau_1}{L}l_0^\chi}z &\overset{(3.52)}{=} e^{-\frac{2\pi\tau_0}{L}l_0^z}e^{-\frac{2\pi\tau_1}{L}l_0^\chi}\left(1+\frac{1}{\frac{1}{2}\ln\chi}\right) = e^{-\frac{2\pi\tau_0}{L}l_0^z}\left(1+\frac{1}{\frac{1}{2}\ln e^{-\frac{2\pi\tau_1}{L}l_0^\chi}\chi}\right) \\
&\overset{(3.47)}{=} e^{-\frac{2\pi\tau_0}{L}l_0^z}\left(1+\frac{1}{\frac{\pi\tau_1}{L}+\frac{1}{2}\ln\chi}\right) \overset{(3.52)}{=} e^{-\frac{2\pi\tau_0}{L}l_0^z}\left(1+\frac{1}{\frac{\pi\tau_1}{L}+\frac{1}{z-1}}\right) \\
&= e^{-\frac{2\pi\tau_0}{L}l_0^z}\left(\frac{\left(1+\frac{\pi\tau_1}{L}\right)z-\frac{\pi\tau_1}{L}}{\frac{\pi\tau_1}{L}z+\left(1-\frac{\pi\tau_1}{L}\right)}\right) = \frac{\left(1+\frac{\pi\tau_1}{L}\right)e^{-\frac{2\pi\tau_0}{L}l_0^z}z-\frac{\pi\tau_1}{L}}{\frac{\pi\tau_1}{L}e^{-\frac{2\pi\tau_0}{L}l_0^z}z+\left(1-\frac{\pi\tau_1}{L}\right)} \\
&\overset{(3.47)}{=} \frac{\left(1+\frac{\pi\tau_1}{L}\right)e^{\frac{2\pi\tau_0}{L}}z-\frac{\pi\tau_1}{L}}{\frac{\pi\tau_1}{L}e^{\frac{2\pi\tau_0}{L}}z+\left(1-\frac{\pi\tau_1}{L}\right)} = \frac{(1+\frac{\pi\tau_1}{L})e^{\frac{\pi\tau_0}{L}}-\frac{\pi\tau_1}{L}e^{-\frac{\pi\tau_0}{L}}}{\frac{\pi\tau_1}{L}e^{\frac{\pi\tau_0}{L}}z+(1-\frac{\pi\tau_1}{L})e^{-\frac{\pi\tau_0}{L}}}.
\end{aligned} \tag{3.55}$$

The last expression in eq. (3.55) manifest the Möbius form of the transformation (cf. the definition given in eq. (2.70)) as it must, since any transformation generated by $\{l_{-1}, l_0, l_1\}$ on the complex plane is a Möbius transformation. We also know that all Möbius transformations form a group, SL(2,$\mathbb{C}$), and from this information we know that by acting many times with the above transformation, corresponding to a stroboscopic time evolution over several periods the resulting transformation is also a new Möbius transformation but with other coefficients.

In the process of finding the Möbius transformation for many periods we will need to "hide" some of the information in the coefficients in order to make it less messy. If we define f and its coefficients a, b, c and d by

$$z_1 = f(z) = \frac{az+b}{cz+d} = \frac{(1+\frac{\pi\tau_1}{L})e^{\frac{\pi\tau_0}{L}} - \frac{\pi\tau_1}{L}e^{-\frac{\pi\tau_0}{L}}}{\frac{\pi\tau_1}{L}e^{\frac{\pi\tau_0}{L}}z + (1-\frac{\pi\tau_1}{L})e^{-\frac{\pi\tau_0}{L}}}, \tag{3.56}$$

and write the coordinates after several periods as

$$z_n = f^n(z) = f(f(...f(z)...)) = \frac{Az+B}{Cz+D}, \tag{3.57}$$

then the task is to find the coefficients A, B, C and D in terms of a, b, c, d and n, with n the number of periods. We know from the general Möbius theory, section 2.6, that any Möbius transformation $T(z)$ with two distinct fixed points, repeated n times $T(T(...T(z))) = T^n(z)$, can be written as

$$\frac{T^n(z)-\gamma_1}{T^n(z)-\gamma_2} = \eta\frac{z-\gamma_1}{z-\gamma_2}, \tag{3.58}$$

where $\gamma_{1,2}$ are the fixed points and $\eta \in \mathbb{C}$ a scaling and rotation. In the case of only one fixed point we instead have the equation

$$\frac{1}{T^n(z)-\gamma} = \frac{1}{z-\gamma} + n\beta, \tag{3.59}$$

where γ is the fixed point, with multiplicity two, and β is a complex number. The two expressions eqs. (3.58) and (3.59) are derived above in section 2.6.

Now it is easy to get equations for z_n, simply by replacing $T(z)$ with z_n in eq. (3.59) and eq. (3.58) for one (two) fixed point(s) respectively:

$$\frac{1}{z_n-\gamma} = \frac{1}{z-\gamma} + n\beta, \tag{3.60}$$

$$\frac{z_n-\gamma_1}{z_n-\gamma_2} = \eta^n\frac{z-\gamma_1}{z-\gamma_2}. \tag{3.61}$$

We can see that both these expressions, eqs. (3.60) and (3.61), are first order in z_n and thus will give an expression for z_n which can be written on the usual Möbius form since it is built out of a number of successive Möbius transformations. From some tedious but straightforward algebra we can write a formula for z_n from only

algebraic manipulations of eqs. (3.60) and (3.61) to get closed expressions for z_n, for one fixed point

$$z_n = \frac{(1+n\beta\gamma)z - n\beta\gamma^2}{n\beta z + (1-n\beta\gamma)} = \frac{Az+B}{Cz+D}, \tag{3.62}$$

and for two fixed points

$$z_n = \frac{(\gamma_1 - \eta^n\gamma_2)z - (1-\eta^n)\gamma_1\gamma_2}{(1-\eta^n)z - (\gamma_2 - \eta^n\gamma_1)} = \frac{Az+B}{Cz+D}. \tag{3.63}$$

To obtain A, B, C and D in terms of the coefficients a, b, c and d for a single period we need the relation between a Möbius transformation and its fixed points, $\gamma_{1,2}$ (two fixed points), γ (one fixed point), and the scaling and rotation η. We get the fixed points by solving

$$f(\gamma) = \frac{a\gamma + b}{c\gamma + d} = \gamma, \tag{3.64}$$

which is a second-order equation with either one or two distinct solutions. In the case of two distinct fixed points we need to use eq. (3.58) and we find η by solving

$$\frac{f(z) - \gamma_1}{f(z) - \gamma_2} = \eta\frac{z - \gamma_1}{z - \gamma_2}. \tag{3.65}$$

Similarly, if we have only one fixed point we need to find β, that is, solving

$$\frac{1}{f(z) - \gamma} = \frac{1}{z - \gamma} + \beta. \tag{3.66}$$

Solving these three equations, eqs. (3.64) - (3.66), yields

$$\gamma_{1,2} = \frac{a - d \mp \sqrt{(a-d)^2 + 4bc}}{2c}, \tag{3.67}$$

$$\eta = \frac{c\gamma_2 + d}{c\gamma_1 + d}, \tag{3.68}$$

$$\gamma = \frac{a-d}{2c}, \tag{3.69}$$

$$\beta = \frac{a+d}{2c}, \tag{3.70}$$

where a, b, c and d are given by eq. (3.56). As for the expressions for η and β we can use $ad - bc = 1$ and the expressions for the fixed points to rewrite them, if desired (where, in the case of only one fixed point, we can also use $(a-d)^2 + 4bc = 0$).[1]

[1] β differ from the work by Fan et al. in Ref. [2] where they write $\beta = c$. However this does not effect any qualitatively statements, only a minor change in the energy density plot, see fig. 3.5.

3.3 Energy distribution

Calculating the energy in the system amounts to calculating the expectation value of the time-time component of the stress-energy tensor. After some rather technical calculations in section 3.2, necessary to obtain a closed form for the Möbius transformation which corresponds to stroboscopic time evolution over several periods, we can now take on this task.

The expectation value to be calculated is given by

$$\langle\psi(nT)|\, T_{tt}(x)\, |\psi(nT)\rangle = \langle G_{H_0}|\, e^{iH_1T_1}e^{iH_0T_0}T_{tt}(x)e^{-iH_0T_0}e^{-iH_1T_1}\, |G_{H_0}\rangle\,. \tag{3.71}$$

We will start from this expression of the energy density written in Minkowski space. This expression of the energy density, eq. (3.71), will be transformed in subsection 3.3.2 by the transformations discussed in sections 3.1 and 3.2 all the way to the final Möbius transformation, which emulates the stroboscopic time evolution.

The section is divided into three subsections. In the first we will calculate the expectation value of the stress-energy tensor in the complex-plane coordinates. We will need the result of this calculation in the second subsection where we give the expression for the energy density at stroboscopic snapshots and plot it against the real space position. Finally, in the third subsection we discuss how we can understand the energy behaviour in terms of the Möbius transformation that governs the stroboscopic time evolution.

3.3.1 Expectation value for stress-energy tensor

The starting point here is the expectation value of the stress-energy tensor in complex coordinates after n periods, as before having prepared the system in the ground state of H_0:

$$\langle G_{H_0}|\, T(z_n)\, |G_{H_0}\rangle\,. \tag{3.72}$$

In section 3.1 we carried out a transformation from ω (strip geometry) to z (complex plane), and then, in section 3.2, we followed up on this by a Möbius transformation from z to z_n, associated with the stroboscopic time evolution. In the next subsection we shall study how these transformations play out for the expectation value in eq. (3.71). But for now, and to prepare for this we need to go to the upper half plane in order to take advantage of known results from CFT. We thus make the transformation

$$z_n \to \xi = \sqrt{z_n}. \tag{3.73}$$

This is a conformal transformation, as can be seen from

$$\begin{aligned}\sqrt{z} &= \sqrt{|z|e^{i\arg(z)}} \\ &= (x^2+y^2)^{1/4}\left(\cos\frac{1}{2}\arctan\frac{y}{x} + i\sin\frac{1}{2}\arctan\frac{y}{x}\right) = u(x,y)+iv(x,y),\end{aligned} \tag{3.74}$$

where $u(x,y)$ and $v(x,y)$ fulfill the Cauchy-Riemann equations. Using that $z_n \to \xi$ is conformal, the expectation value, eq. (3.72), in the ξ-coordinate takes the form

$$\langle G_{H_0}|\, T(z_n)\, |G_{H_0}\rangle = \langle G_{H_0}|\left(\frac{\partial\xi}{\partial z_n}\right)^2 T(\xi) + \frac{c}{12}\{\xi, z_n\}_{\mathrm{Sc}}\, |G_{H_0}\rangle\,. \tag{3.75}$$

Let us first investigate $\langle G_{H_0}| T(\xi) |G_{H_0}\rangle$ (the multiplicative factor of $\frac{\partial \xi}{\partial z_n}$ is easy to calculate but unimportant). First we should note that this expectation value is "horizontally" translation invariant due to no boundary, that is no boundary condition, along the real axis. This means that the expectation value can only depend on the distance from the real axis. Explicitly, if we let $\xi = a + ib$ and using c as a horizontal translation, setting $c = -a$, a, b and $c \in \mathbb{R}$:

$$\begin{aligned} &\langle G_{H_0}| T(a+ib) |G_{H_0}\rangle = \langle G_{H_0}| T(a+c+ib) |G_{H_0}\rangle , \\ \Rightarrow\ &\langle G_{H_0}| T(a+ib) |G_{H_0}\rangle = \langle G_{H_0}| T(ib) |G_{H_0}\rangle . \end{aligned} \tag{3.76}$$

We also know how $T(\xi)$ behaves under a scale transformations (a special case of a Möbius transformation with zero Schwarzian derivative $\{\lambda z, z\} = 0$). It follows that

$$T(\lambda\xi) = \frac{1}{\lambda^2} T(\xi), \quad \lambda \in \mathbb{C}, \tag{3.77}$$

with $\lambda\xi$ in the upper half plane. In particular, we can choose $\lambda = 1 - ia/b$ with $\lambda ib = a + ib$ and use the "horizontal" translation invariance in eq. (3.76) together with the scaling property in eq. (3.77) to obtain

$$\begin{aligned} \langle G_{H_0}| T(ib) |G_{H_0}\rangle &\overset{(3.76)}{=} \langle G_{H_0}| T(a+ib) |G_{H_0}\rangle = \langle G_{H_0}| T(i\lambda b) |G_{H_0}\rangle \\ &\overset{(3.77)}{=} \frac{1}{\lambda^2} \langle G_{H_0}| T(ib) |G_{H_0}\rangle , \end{aligned} \tag{3.78}$$

which is true only if $\langle G_{H_0}| T(ib) |G_{H_0}\rangle = 0$. Since this is true for any b, that is any point along the imaginary axis, and we have translation invariance horizontally, we get $\langle G_{H_0}| T(\xi) |G_{H_0}\rangle = 0$ for all ξ in the upper half plane.

We have now shown that the expectation value, $\langle G_{H_0}| T(z_n) |G_{H_0}\rangle$, only depends on the Schwarzian derivative of the transformation $z_n \mapsto \xi = \sqrt{(z_n)}$ to the upper half plane. Written out, the Schwarzian derivative in this case is given by

$$\begin{aligned} \{\xi, z_n\}_{\mathrm{Sc}} &= \frac{\xi'''}{\xi'} - \frac{3}{2}\left(\frac{\xi''}{\xi'}\right)^2 \\ &= \frac{3}{8}\frac{1}{z_n^2}. \end{aligned} \tag{3.79}$$

3.3.2 Energy in the system

Now are we ready to calculate the energy in the system after n-periods of time, $nT = n(T_1 + T_0)$. We started in our setup with some CFT described by the Hamiltonian H_0, eq. (3.1), obtained from the time-time component T_{tt} of the stress-energy tensor which describes the energy density of the system. We have $T_{tt} = \frac{1}{2\pi}(T(\omega) + \bar{T}(\bar{\omega}))$, where we only discuss $T(\omega)$ since everything is analogous for $\bar{T}(\bar{\omega})$. When going from ω (the strip geometry) to z (the whole complex plane geometry) we picked up a constant term which we just throw away since as usual we are only interested in energy differences. We thus write for the expectation value after n periods:

$$\langle \psi(nT)| T(\omega) |\psi(nT)\rangle = \left(\frac{\partial z}{\partial \omega}\right)^2 \langle \psi(nT)| T(z) |\psi(nT)\rangle + \cancel{\left(\frac{L}{2\pi}\right)^2 \frac{c}{12}}. \tag{3.80}$$

Using that a stroboscopic time evolution can be represented by a Möbius transformation, we can go to Heisenberg picture and write

$$\left(\frac{\partial z}{\partial \omega}\right)^2 \langle \psi(nT)| \, T(z) \, |\psi(nT)\rangle = \left(\frac{\partial z}{\partial \omega}\right)^2 \left(\frac{\partial z_n}{\partial z}\right)^2 \langle G_{H_0}| \, T(z_n) \, |G_{H_0}\rangle \, . \tag{3.81}$$

Here $|G_{H_0}\rangle$ is the initial state. Note that there is no contribution from the Schwarzian derivative when doing a Möbius transformation.

The expectation value of $\langle G_{H_0}| \, T(z_n) \, |G_{H_0}\rangle$ was calculated in the previous subsection by going to the upper half plane by the transformation $z_n \mapsto \xi = \sqrt{z_n}$. Here we noticed that the expectation value in the ξ coordinate vanished, leaving us only with the Schwarzian derivative $\{\xi, z_n\}_{\mathrm{Sc}}$. This gives us

$$\left(\frac{\partial z}{\partial \omega}\right)^2 \left(\frac{\partial z_n}{\partial z}\right)^2 \langle G_{H_0}| \, T(z_n) \, |G_{H_0}\rangle = \left(\frac{\partial z}{\partial \omega}\right)^2 \left(\frac{\partial z_n}{\partial z}\right)^2 \frac{c}{12} \{\xi, z_n\}_{\mathrm{Sc}}. \tag{3.82}$$

By using eqs. (3.23), (3.57) and (3.79) together with the expression for z_n in terms of z given in eq. (3.57) finally gives us the explicit formula for the energy density

$$\begin{aligned} \langle \psi(nT)| \, T_{tt}(x) \, |\psi(nT)\rangle &= \frac{1}{2\pi} \left(\frac{2\pi}{L} z\right)^2 \left(\frac{(AD-BC)}{(Cz+D)^2}\right)^2 \frac{c}{32} \frac{(Cz+D)^2}{(Az+B)^2} + (z \to \bar{z}) \\ &= \frac{\pi c}{16 L^2} \frac{z^2 (AD-BC)^2}{(Cz+D)^2 (Az+B)^2} + (z \to \bar{z}). \end{aligned} \tag{3.83}$$

Here A, B, C and D are the coefficients in the Möbius transformation $z \mapsto z_n$ given in eq. (3.62) (eq. (3.63)) for one (two) fixed point(s).[2] The number of fixed points is dependent on the two driving parameters T_1 and T_0 who are also hidden in the coefficients A, B, C and D together with the number of periods n, a relation that we shall study in subsection 3.3.3.

The last step we need to do before we can analyse and plot the energy as a function of the position in the one-dimensional system is to go back to the physical plane, restricting the coordinates to satisfy $\bar{z} = z^*$ and then going back to Minkowski space, letting $\tau_{0,1} \mapsto iT_{0,1}$. That is in, all coefficients A, B, C and D we will simply change $\tau_{0,1}$ to $iT_{0,1}$ implying that the coordinates will be given by

$$z = e^{\frac{2\pi i}{L}((T_0+T_1)+x)}, \quad \bar{z} = e^{\frac{2\pi i}{L}((T_0+T_1)-x)}. \tag{3.84}$$

Computing the expression for the energy density, eq. (3.83), putting in z ($\bar{z}$) from above eq. (3.84) and $iT_{0,1}$ instead of $\tau_{0,1}$, we need to choose different expressions for the coefficients in the Möbius transformation depending on whether we have one fixed point or two. As a result, we obtain the three different plots shown in fig. 3.5. The non-heating phase and the heating phase corresponding to when we

[2]Note a difference of the multiplicative factor $\frac{1}{2\pi}$ compared to the corresponding expression in the work by Fan et al. [2], originating from our choice of convention in going from $T_{\omega\omega}$ to $T(\omega)$.

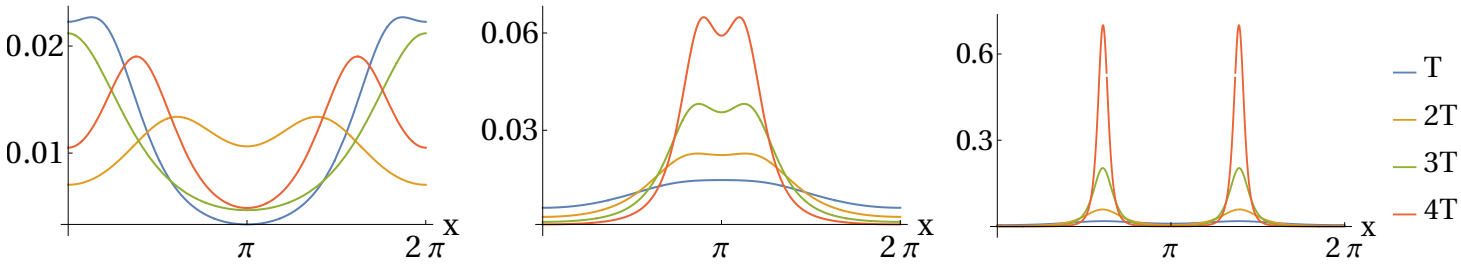

(a) Non-Heating **(b)** Critical **(c)** Heating

Figure 3.5: The different colors are the energy distribution in the system after 1, 2, 3 and 4 periods, $T = T_1 + T_0$. The length of the system was chosen to be $L = 2\pi$ and the central charge $c = 1$. (a) For the non-heating phase we have used $T_0 = 0.5L$ and $T_1 = 0.1L$. We here notice a spatially oscillating behavior for the energy. (b) For the critical phase we have chosen $T_0 = 0.9L$ and $T_1 \approx 0.06$ but the exact value used is given by solving eq. (3.96) with the given value for T_0. We note a slow (polynomial) growth with peaks that move toward x for increasing n such that $z(x)$ ($\bar{z}(x)$) corresponds to γ (γ^*).[3] (c) The heating phase here comes from using $T_0 = 0.9L$ and $T_1 = 0.1L$. We can see a more rapidly growing, exponential growth, with peaks at x for which $z(x)$ ($\bar{z}(x)$) corresponds to the stable fixed point, γ_2 (γ_2^*).

have two fixed points in the Möbius transformation which emulates time evolution and the critical phase when the same has only one fixed point. Furthermore, both the heating and critical phase are seen to gain energy in the system with time, that is, absorbing energy in corresponds to the general belief of Floquet systems where the drive is giving the system energy as discussed in section 1.1 but interestingly in the non-heating phase we have no absorption of energy. The characteristics of the plots depend only on the driving parameters T_0 and T_1. In the subsection 3.3.3 we will discuss how the Möbius transformation relates to the energy plots in fig. 3.5 and we will see explicitly how to mathematically discriminate between the three phases.

3.3.3 Möbius transformation related to the energy spectrum

In this subsection we will analyse the energy distribution given in eq. (3.83) to understand how the Möbius transformation related to the stroboscopic time evolution can describe the three different phases seen in fig. 3.5. First we will write down the energy density once more, but now in terms of z_n and z only, and focus on the part containing z_n since that is the only time-dependent part. Evaluating $\{\xi, z_n\} = \frac{3}{8}\frac{c}{z_n^2}$ in eq. (3.82) we obtain

$$\langle\psi(nT)|\, T_{tt}(x)\, |\psi(nT)\rangle = \frac{1}{2\pi}\frac{c}{32}\left(\frac{\partial z}{\partial \omega}\right)\left(\frac{\partial z_n}{\partial z}\right)^2 \frac{1}{z_n^2} + (z \to \bar{z}), \tag{3.85}$$

[3]The only difference compared to the corresponding figure in Fan et al. [2] is that the peaks start to grow at different places before they move towards γ.

where again we will only investigate the holomorphic term since the anti-holomorphic term follows in the same way. That is, we will investigate how z_n and $\frac{\partial z_n}{\partial z}$ depend on n, or more precisely how or if their absolute values grow with n.

First we will show that $|z_n| = 1$, implying that all contributions to the different energy absorption phases are given by the $\frac{\partial z_n}{\partial z}$ on the right hand side of eq. (3.85). First recall that

$$z_n(z) = f^n(z) = f(f(...f(z)...)), \quad f(z) = \frac{az+b}{cz+d}. \tag{3.86}$$

That is, if we can show that $|f(z)| = 1$ then it follows that $|z_n| = 1$ since $|f^n(z)| = |f(z)|^n$. The coefficients in the $f(z)$ function are given in eq. (3.56), and reading off, performing the analytic continuation which changes $\tau_{0,1}$ to $iT_{0,1}$, we obtain

$$f(z) = \frac{(1+i\frac{\pi T_1}{L})e^{i\frac{\pi T_0}{L}}z - i\frac{\pi T_1}{L}e^{-i\frac{\pi T_0}{L}}}{i\frac{\pi T_1}{L}e^{i\frac{\pi T_0}{L}}z + (1-i\frac{\pi T_1}{L})e^{-i\frac{\pi T_0}{L}}} = \frac{az+b}{b^*z+a^*}, \tag{3.87}$$

where the second equality is a simple but crucial result. Now we will make a straightforward calculation of the absolute value of this expression:

$$\begin{aligned} |f(z)|^2 &= \left|\frac{az+b}{b^*z+a^*}\right|^2 \\ &= \frac{|a|^2|z|^2 + |b|^2 + ab^*z + a^*bz^*}{|b|^2|z|^2 + |a|^2 + ab^*z + a^*bz^*} \\ &= \frac{|a|^2 + |b|^2 + ab^*z + a^*bz^*}{|a|^2 + |b|^2 + ab^*z + a^*bz^*} = 1. \end{aligned} \tag{3.88}$$

Note that in order to get to the last row we have used that $|z| = 1$, as seen from $z = \exp\Big\{i\frac{2\pi}{L}(T_0 + T_1 + x)\Big\}$, again after analytic continuation.

Next we will investigate the derivative $\frac{\partial z_n}{\partial z}$ of the Möbius transformation which governs the different energy absorption behaviours seen in fig. 3.5, as we discussed in section 1.1 the general belief is that the drive makes the system absorb energy while as we could see in the figure we have two phases where this is true but we could also, interestingly, drive the system in such a way that it does not absorb any energy but just oschilate. But we already know that z_n as a function of z has two different expressions, depending on whether there are one or two fixed points, which in turn depends on the values of the driving parameters T_0 and T_1. Let us first assume two fixed points. Using eq. (3.63) we then have

$$\begin{aligned} \frac{\partial z_n}{\partial z} &= \frac{\partial}{\partial z}\frac{Az+B}{Cz+D} \\ &= \frac{(\gamma_1-\gamma_2)^2\eta^n}{\big((z-\gamma_2)+(\gamma_1-z)\eta^n\big)^2} = \begin{cases} \eta^n, & z=\gamma_1 \\ \eta^{-n}, & z=\gamma_2 \end{cases}. \end{aligned} \tag{3.89}$$

From this expression we can see that if $|\eta| < 1$ ($|\eta| > 1$) then the expression in eq. (3.89) grows exponentially, $\sim \eta^n$, when x is such that $z(x)$ is near γ_2 (γ_1).

Differently, for x such that $z(x)$ is near γ_1 (γ_2), the expression decreases. The discrimination of the driving parameter space, T_0 and T_1, that gives the two cases seen in eq. (3.89) is visualized in fig. 3.6b.

This leads us to investigate how the parameter η depends on the driving parameters, T_0 and T_1. We know that after analytic continuation we have $d = a^*$ and $c = b^*$, that is $a + d = 2\,\mathrm{Re}\{a\}$, $a - d = 2i\,\mathrm{Im}\{a\}$ and $bc = |b|^2$. Hence

$$\begin{aligned}\eta &= \frac{c\gamma_2 + d}{c\gamma_1 + d} \\ &= \frac{\frac{a-d}{2} + \sqrt{(a-d)^2 + 4bc}/2 + d}{\frac{a-d}{2} - \sqrt{(a-d)^2 + 4bc}/2 + d} \\ &= \frac{\mathrm{Re}\{a\} + \sqrt{|b|^2 - \mathrm{Im}\{a\}^2}}{\mathrm{Re}\{a\} - \sqrt{|b|^2 - \mathrm{Im}\{a\}^2}}.\end{aligned} \tag{3.90}$$

Equation (3.90) reveals that there are three different cases for η depending on $|b|^2 - \mathrm{Im}\{a\}^2$ being positive, zero or negative. In the positive case we can directly see that η is a real function with $|\eta| > 1$ if $\mathrm{Re}\{a\}$ is positive and $|\eta| < 1$ if $\mathrm{Re}\{a\}$ is negative. In either case we have an exponential growth as discussed after eq. (3.89). Noticing that

$$\mathrm{Re}\{a\} = \cos\frac{\pi T_0}{L} - \frac{\pi T_1}{L}\sin\frac{\pi T_0}{L}, \tag{3.91}$$

we see that there are two different cases for the four quadrants that the arguments of the cosine and sine functions sweep through. In the first two $\mathrm{Re}\{a\}$ will bee negative in the heating phase, while in quadrant three and four $\mathrm{Re}\{a\}$ will bee positive in the heating phase, as given in fig. 3.6b. This can be seen from the following relations, coming from eq. (3.91):

$$\cos\frac{\pi T_0}{L} > 0 \quad \text{and} \quad \sin\frac{\pi T_0}{L} > 0 \quad \text{and} \quad T_1/L > \frac{\cos \pi T_0/L}{\pi \sin \pi T_0/L}, \quad \mathrm{Re}\{a\} < 0, \tag{3.92}$$

$$\cos\frac{\pi T_0}{L} < 0 \quad \text{and} \quad \sin\frac{\pi T_0}{L} > 0, \qquad\qquad\qquad\qquad\quad \mathrm{Re}\{a\} < 0, \tag{3.93}$$

$$\cos\frac{\pi T_0}{L} < 0 \quad \text{and} \quad \sin\frac{\pi T_0}{L} < 0 \quad \text{and} \quad T_1/L > \frac{\cos \pi T_0/L}{\pi \sin \pi T_0/L}, \quad \mathrm{Re}\{a\} > 0, \tag{3.94}$$

$$\cos\frac{\pi T_0}{L} > 0 \quad \text{and} \quad \sin\frac{\pi T_0}{L} < 0, \qquad\qquad\qquad\qquad\quad \mathrm{Re}\{a\} > 0. \tag{3.95}$$

When $|b|^2 - \mathrm{Im}\{a\}^2$ is negative then η is complex but with absolute value = 1. That is, we have no general growth with n in eq. (3.89) but a complex number that changes with n, thus an oscillating behaviour.

When $|b|^2 - \mathrm{Im}\{a\}^2 = 0$ then $\eta = 1$, and we have

$$-\mathrm{Im}\{a\}^2 + |b|^2 = (a-d)^2 + 4bc = 0 \quad \Rightarrow \quad \gamma_1 = \gamma_2, \tag{3.96}$$

that is, we have only one fixed point and need to use the other form of the Möbius transformation, eq. (3.62), to describe the time evolution. We now also understand

that by just looking at η we can infer which type of phase is produced by the driving. For η real and different from unity we get exponential growth, while for η complex (giving $|\eta| = 1$) we have an oscillating behaviour. The case $\eta = 1$ corresponds to the critical case. Note that eq. (3.96) for the driving parameters defines the border between the heating and non-heating phase.

By analysing the derivative, $\frac{\partial z_n}{\partial z}$, for the Möbius transformation with one fixed point, given in eq. (3.62), we can understand where the peaks move and by which rate they grow. Differentiating eq. (3.62), we have that

$$\frac{\partial z_n}{\partial z} = \frac{AD - BC}{(Cz + D)^2} = \frac{1}{n^2\beta^2(z - (\gamma - \frac{1}{n\beta}))^2}, \tag{3.97}$$

revealing a peak around x for $z(x) = \gamma - 1/n\beta$, making the peak move towards γ. The previous statement relies on the two facts that $z(x)$ and γ are bound to the unit circle after analytic continuation. Which gives that $\gamma - 1/n\beta$ moves towards the unit circle where we find $z(x)$. These two statements, that $|z(x)| = |\gamma| = 1$ after analytic continuation, are seen from

$$z = e^{i\frac{2\pi}{L}(T_0+T_1+x)}, \tag{3.98}$$

and

$$|\gamma| = \left|\frac{a-d}{2c}\right| \overset{(3.96)}{=} \frac{|\sqrt{-4bc}|}{|2c|} = \frac{2|b|}{2|b|} = 1. \tag{3.99}$$

In the last step we use that $c = b^*$ which we saw in eq. (3.87) after analytic continuation. Furthermore, we can make the qualitative statement that the peak grows with a polynomial rate. This statement is seen from that in the denominator of eq. (3.97) we have $z - (\gamma - 1/n\beta)$ where $\gamma - 1/n\beta$ goes towards γ, that is, the unit circle where z is confined in a polynomial rate in n.

Now when we know where the different energy absorption properties seen in fig. 3.5 are coming from we will investigate for which parameter values we get the different phases. Recall that by inspection of eq. (3.96) we could discriminate between the three phases. Now by simply rewriting that equation in terms of the driving parameters T_0 and T_1 we can visualize the parameter space for the different phases. The result is presented in fig. 3.6a, with T_0 and T_1 scaled by L, the length of the one-dimensional system. Furthermore, in eq. (3.89) we could see that depending on whether or not the absolute value of η is bigger than one we would have peaks at x such that $z(x) = \gamma_1$ ($z(x)^* = \gamma_1^*$) or $z(x) = \gamma_2$ ($z(x)^* = \gamma_2^*$). We found in eq. (3.90) that the sign of $\mathrm{Re}\{a\}$ determines if $|\eta|$ is bigger or smaller than unity, where here the sign of $\mathrm{Re}\{a\}$ is given in eqs. (3.92) - (3.95) and visualized in fig. 3.6b.

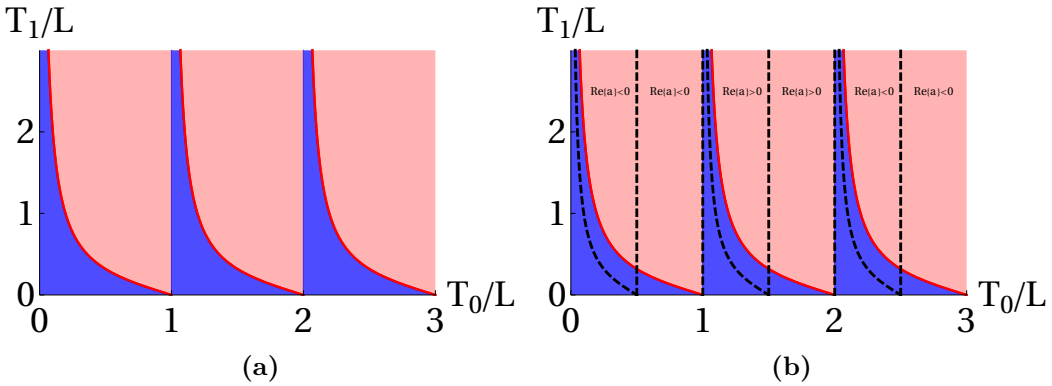

Figure 3.6: In panel (a) we can we see the parameter values corresponding to the three different phases of energy absorption (cf. fig. 3.5). The heating phases are marked by light red color, while blue color indicate non-heating phases. The border between the two, marked by dark red, corresponds to the critical phase. Panel (b) shows which sign $\mathrm{Re}\{a\}$ has in the various heating phases. This gives us knowledge about how the peaks in the corresponding heating phases are related to γ_2 ($\mathrm{Re}\{a\} < 0$) or γ_1 ($\mathrm{Re}\{a\} > 0$).

4

Sine-k-square deformation

In this chapter we will generalize the sine-squared deformation of the CFT studied in the previous chapter to higher harmonics. To be precis, as before we will start with an arbitrary CFT described by H_0 and use the same square wave driving protocol as before, seen in fig. 3.1. However, now we will use a different deformation, call it H_k. In formulas:

$$H_0 = \int_0^L \mathrm{d}x \ T_{tt}(x), \tag{4.1}$$

$$H_k = 2\int_0^L \mathrm{d}x \ \sin^2\left(\frac{k\pi x}{L}\right) \ T_{tt}(x), \tag{4.2}$$

$$H(t) = \begin{cases} H_k, & 0 < t \bmod T < T_k \\ H_0, & T_k < t \bmod T < T_k + T_0 \end{cases} . \tag{4.3}$$

Note that $k = 1$ gives the same deformation as before so here we will focus on $k = 2, 3, ...$ We will follow the same scheme as above in chapter 3, when we had H_1 as deformation, and see that many results follow by the same calculation. Thus we provide the necessary arguments without the need to reproduce all calculations. However, whenever before we used Möbius theory we will need to be more careful: As we shall see, the stroboscopic time evolution can still be evaluated as a conformal transformation, but not a Möbius transformation. This means that we loose the group properties that we took advantage of in chapter 3 when emulating the time evolution of several periods as a Möbius transformation.

4.1 Stroboscopic time evolution as a conformal transformation

In this section we will explain how to describe stroboscopic time evolution by a conformal transformation generated by Virasoro generators. We will find similar expressions for the Hamiltonians H_0 and H_k as those given for H_0 and H_1 in eq. (3.43) and 3.44 respectively. We follow the same scheme as in chapter 3 and shall argue that we can use most results from sections 3.1 and 3.2 and deduce the effect from replacing H_1 by H_k.

We start with a discussion how to get from the model in Minkowski space to Euclidean space, and with analytic continuation to the two-dimensional complex Euclidean space, $\mathbb{C}^2$. Both the metric and the stress-energy tensor will follow the exact same transformation rules as before, since they are unaffected by which particular deformation we use. That is, we still have

$$T_{tt} = -(T_{\omega\omega} + T_{\bar{\omega}\bar{\omega}}), \tag{4.4}$$

as in eq. (3.8). It follows that H_0 is exactly the same as in chapter 3 (remembering the definition $T_{\omega\omega} := -\frac{1}{2\pi}T(\omega)$):

$$H_0 = \int_0^L \frac{\mathrm{d}\omega}{2\pi i} T(\omega) - \int_0^{-L} \frac{\mathrm{d}\bar{\omega}}{2\pi i} \bar{T}(\bar{\omega}). \tag{4.5}$$

Turning to H_k, we have

$$2\sin^2\left(\frac{k\pi x}{L}\right) = 1 - \frac{1}{2}\left(e^{i\frac{2\pi k x}{L}} + e^{-i\frac{2\pi k x}{L}}\right), \tag{4.6}$$

where the only difference to the corresponding expression for H_1 in eq. (3.11) is that $k = 1$ is replaced by an arbitrary positive integer, $k = 1, 2, ...$ All arguments after eq. (3.11) on how to perform the analytic continuation are still valid for arbitrary k. We have H_k as

$$H_k = H_0 - \frac{1}{2}(H_{+k} + H_{-k}), \tag{4.7}$$

where

$$H_{\pm k} = \int_0^L \frac{\mathrm{d}\omega}{2\pi i} e^{\pm\frac{2\pi k}{L}\omega} T(\omega) - \int_0^L \frac{\mathrm{d}\bar{\omega}}{2\pi i} e^{\mp\frac{2\pi k}{L}\bar{\omega}} \bar{T}(\bar{\omega}). \tag{4.8}$$

The unitary operator describing the stroboscopic time evolution that we found in chapter 3 could be written as a compact time-ordered expression, eq. (3.19), independent of the form of the two Hamiltonians. We thus conclude that the n-period time-evolution operator is the same as that in eq. (3.21) but now with H_k replacing H_1. Thus we write for the time-evolution operator:

$$(e^{-H_0\tau_0} e^{-H_k\tau_k})^n. \tag{4.9}$$

Here τ_0 and τ_k are the imaginary time intervals for which the system is governed by H_0 and H_k respectively.

Next we perform a transformation from the strip geometry, with ω coordinate, to the complex plane with a branch cut, with z coordinate. The conformal map is the same as before, given by eq. (3.23), rewritten here for clarity:

$$\omega \mapsto z = e^{\frac{2\pi}{L}\omega}, \quad \overline{\omega} \mapsto \overline{z} = e^{\frac{2\pi}{L}\overline{\omega}}. \tag{4.10}$$

Here recall fig. 3.2, illustrating how this map takes horizontal equal-time lines in the strip geometry to circles in the complex plane.

The discussion about how the stress-energy tensor transforms is of course unaffected by the choice of the Hamiltonians, and therefore still given by eq. (3.24). The

Jacobian and change in path is of course also unaffected of the deformation, and thus still given by eq. (3.26) with the discussion of integral paths that follows. The only difference appears when writing down H_k, or more precisely the new $H_{\pm k}$ parts, in complex plane coordinate z where we pick up another polynomial in front of the stress-energy tensor. In accordance with the expression for the Jacobian, eq. (3.26), and with $e^{\pm\frac{2\pi k}{L}\omega} = z^{\pm k}$, we have that

$$\begin{aligned} H_{\pm k} &= \frac{2\pi}{L}\int_{C_z^{\circlearrowleft}} \frac{\mathrm{d}z}{2\pi i}\left(z^{1\pm k}T(z) - z^{1\pm k}\frac{1}{2}\frac{c}{12}\right) - (z\to\overline{z}) \\ &= \frac{2\pi}{L}\int_{C_z^{\circlearrowleft}} \frac{\mathrm{d}z}{2\pi i} z^{1\pm k}T(z) - (z\to\overline{z}). \end{aligned} \tag{4.11}$$

In the second line we have used

$$\int_{C_z^{\circlearrowleft}} \frac{\mathrm{d}z}{2\pi i} z^{1\pm x} = \frac{e^{\frac{2\pi}{L}\tau}}{L}\int_0^L \mathrm{d}x\, e^{-\frac{2\pi(2\pm k)}{L}ix} = \begin{cases} 0, & k\neq 2 \\ e^{\frac{2\pi}{L}\tau}, & k=2 \end{cases}. \tag{4.12}$$

We should remark that we have here thrown away the constant term that appears when $k = 2$. We justify this by looking at how the exponentiated Hamiltonian acts on an operator via the CBH-formula, as seen in eq. (3.36), where we note that any c-number part of the Hamiltonian will commute with the operator and thus give no contribution to the action.

We write the Hamiltonians H_0 and H_k in the complex plane in analogy to eqs. (3.27) and (3.33), with the only difference that $z^{1\pm k}$ with arbitrary k replaces 1 and z^2 (corresponding to the case with $k = 1$):

$$H_0 = \frac{2\pi}{L}\int_{C_z^{\circlearrowleft}} \frac{\mathrm{d}z}{2\pi i} zT(z) - (z\to\overline{z}) - \frac{2\pi}{L}\frac{c}{12}, \tag{4.13}$$

$$\begin{aligned} H_k &= H_0 - \frac{1}{2}\left(H_{+k} + H_{-k}\right) \\ &= \frac{2\pi}{L}\int_{C_z^{\circlearrowleft}} \frac{\mathrm{d}z}{2\pi i}\frac{1}{2}\left(-z^{1-k} + 2z - z^{1+k}\right)T(z) - (z\to\overline{z}) - \frac{2\pi}{L}\frac{c}{12}. \end{aligned} \tag{4.14}$$

The last step before we can go on to the more technical part of finding an explicit conformal transformation that emulates the time evolution for our new system is to write the Hamiltonians in terms of Virasoro generators. That is, we need to show that the time evolution of an operator is a contour integral in a neighborhood of that operator, in analogy to what we did in subsection 3.2.2. We start by noticing that all arguments in that section (up to the paragraph after eq. (3.36) where we find that we only need to investigate the two commutators $[H_0, \mathcal{O}(z,\bar{z})]$ and $[H_1, \mathcal{O}(z,\bar{z})]$) are independent of the choice of H_0 and H_1. It follows that we only need to investigate $[H_k, \mathcal{O}]$. The only difference from H_1 in subsection 3.2.2 is that H_k comes with powers of z of degree $1 \pm k$ in front of the stress-energy tensor, implying that this time we have the possibility of a pole. But this pole is located at the origin which is outside the integration path and we will never be close since we start at time $t = 0$ which corresponds to $|z| = 1$ while the origin corresponds to time $t = -\infty$. That

is, the whole argument in subsection 3.2.2 holds without modifications. We write the Hamiltonians H_0 and H_k by identifying the corresponding Virasoro generators, given by eq. (2.58), in the expressions for the Hamiltonians in eqs. (4.13) and (4.14). In this way we obtain:

$$H_0 = \frac{2\pi}{L}\left(L_0 + \bar{L}_0\right) - \frac{c\pi}{6L}, \tag{4.15}$$

$$H_k = \frac{2\pi}{L}\left(L_0 - \frac{1}{2}\left(L_{-k} + L_k\right) + \bar{L}_0 - \frac{1}{2}\left(\bar{L}_{-k} + \bar{L}_k\right)\right) - \frac{c\pi}{6L}. \tag{4.16}$$

4.2 Stroboscopic time evolution as a generalized Möbius transformation

From the previous section we now know that the stroboscopic time evolution of an operator is a conformal transformation also in the more general case of a sine-k deformation. Guided by our approach for the simpler sine-squared deformation in subsection 3.2.3, we therefore set off to search for the appropriate conformal coordinate change. We again exemplify how a conformal transformation, such as one period of time evolution, of an operator can be described by a conformal coordinate change

$$e^{\tau_k H_k} e^{\tau_0 H_0} \mathcal{O}(z,\bar{z}) e^{-\tau_0 H_0} e^{-\tau_k H_k} = \left(\frac{\partial z_1}{\partial z}\right)^h \left(\frac{\partial \bar{z}_1}{\partial \bar{z}}\right)^{\bar{h}} \mathcal{O}(z_1,\bar{z}_1). \tag{4.17}$$

As before the coordinate transformation is given by the corresponding Witt generators to the Virasoro generators who transform the operator on the Hilbert space, hidden in the expressions for H_0 and H_k in the left hand side of eq. (4.17). That is, we seek the coordinate transformation $z \mapsto z_1$, or more generally after n time periods, the coordinate transformation $z \mapsto z_n$, given by

$$z \mapsto z_n = \left(e^{-\frac{2\pi}{L}\tau_0 l_0} e^{-\frac{2\pi}{L}\tau_k\left(l_0 - \frac{1}{2}(l_{-k}+l_k)\right)}\right)^n z, \quad l_m = -z^{m+1}\partial_z. \tag{4.18}$$

We will now make a coordinate change as in eq. (3.49) to rewrite H_k to act as a dilation, that is, being described solely by L_0. In other words, we apply the coordinate change $z \mapsto \chi = \chi(z)$, that we impose to be conformal, in the integral representation of H_k,

$$H_k = \frac{2\pi}{L}\oint \frac{\mathrm{d}\chi}{2\pi i}\left(\frac{\partial\chi}{\partial z}\right)^{-1}\left(-\frac{z^{1-k}}{2} + z - \frac{z^{1+k}}{2}\right)\left(\left(\frac{\partial\chi}{\partial z}\right)^2 T(\chi) + \frac{c}{12}\{\chi, z\}_{Sc}\right) - \frac{c\pi}{6L}. \tag{4.19}$$

To get H_k to act as a dilation we need the coordinate change $z \mapsto \chi$ to give $H_k = \frac{2\pi}{L}\oint \frac{\mathrm{d}\chi}{2\pi i}\chi T(\chi) + c$-number. Comparing this with eq. (4.19) (where the Schwarzian $\{\chi, z\}$ and $c\pi/6L$ are included in the c-number) we get the following differential equation

$$\chi = \frac{\mathrm{d}\chi}{\mathrm{d}z}\left(-\frac{z^{1-k}}{2} + z - \frac{z^{1+k}}{2}\right). \tag{4.20}$$

Using the algebraic relation

$$\left(-\frac{z^{1-k}}{2}+z-\frac{z^{1+k}}{2}\right)=-\frac{1}{2}\frac{(z^k-1)^2}{z^{k-1}}, \tag{4.21}$$

we can rewrite eq. (4.20) as the integral equation

$$\int\frac{\mathrm{d}\chi}{\chi}=-2\int\mathrm{d}z\,\frac{z^{k-1}}{(z^k-1)^2}. \tag{4.22}$$

Calculating the integrals gives

$$\ln\chi=\frac{2}{k}\frac{1}{z^k-1}+\text{constant}, \tag{4.23}$$

which is the conformal coordinate change we seek in order to rewrite H_k as a pure dilation. That eq. (4.23) is a conformal coordinate change follows by the arguments of the corresponding coordinate change given by eq. (3.52). That is,

$$\chi=e^{\frac{2}{k}\frac{1}{z^k-1}+\text{constant}}, \tag{4.24}$$

is holomorphic on the punctured complex plane with $z=1$ removed (and by that also conformal; cf. our discussion after eq. (3.23)). Now we have H_k in χ-coordinates,

$$H_k=\frac{2\pi}{L}\oint\frac{\mathrm{d}\chi}{2\pi i}\chi T(\chi)+\text{c-number}, \tag{4.25}$$

by this verifying that we indeed have H_k acting as a dilation. (That is, we can identify eq. (4.25) as the L_0 Virasoro generator by using the relation between Virasoro generators and the stress-energy tensor given in eq. (2.58).)

We are now ready to derive the explicit formula for the coordinate change corresponding to one period of the Floquet drive. Evaluating eq. (4.18) for $n=1$, we follow the same scheme as before in eq. (3.55) but now with a generalized relation between z and χ giving:

$$\begin{aligned}
e^{-\frac{2\pi\tau_0}{L}l_0^z}e^{-\frac{2\pi\tau_k}{L}l_0^\chi}z &\overset{(4.23)}{=} e^{-\frac{2\pi\tau_0}{L}l_0^z}e^{-\frac{2\pi\tau_k}{L}l_0^\chi}\left(\frac{1}{\frac{k}{2}\ln\chi}+1\right)^{1/k}\\
&=e^{-\frac{2\pi\tau_0}{L}l_0^z}\left(\frac{1}{\frac{k}{2}\frac{2\pi\tau_k}{L}+\frac{k}{2}\ln\chi}+1\right)^{1/k}\overset{(4.23)}{=}e^{-\frac{2\pi\tau_0}{L}l_0^z}\left(\frac{1}{\frac{k}{2}\frac{2\pi\tau_k}{L}+\frac{1}{z^k-1}}+1\right)^{1/k}\\
&=\left(\frac{\left(1+\frac{\pi k\tau_k}{L}\right)e^{\frac{\pi k\tau_0}{L}}z^k-\frac{\pi k\tau_k}{L}e^{-\frac{\pi k\tau_0}{L}}}{\frac{\pi k\tau_k}{L}e^{\frac{\pi k\tau_0}{L}}z^k+\left(1-\frac{\pi k\tau_k}{L}\right)e^{-\frac{\pi k\tau_0}{L}}}\right)^{1/k}=\left(\frac{az^k+b}{cz^k+d}\right)^{1/k}.
\end{aligned} \tag{4.26}$$

The last equality is there to define the coefficients a, b, c and d which are very similar to the corresponding coefficients when $k=1$, cf. eq. (3.56); the only difference is a k in front of the time interval parameters τ_0 and τ_k. This transformation of z,

$$z\mapsto z_1=f(z)=\left(\frac{az^k+b}{cz^k+d}\right)^{1/k}, \tag{4.27}$$

clearly is not a Möbius transformation; compare with the definition given in eq. (2.70). By an abuse of language we shall still call this a generalized Möbius transformation since it has certain features which resembles a true Möbius transformation. Furthermore, even before we had the explicit formula in eq. (4.27), we started from an expression that is an exponentiation of $\{l_{-k}, l_0, l_k\}$, eq. (4.18). This is a subalgebra of the Witt algebra and with $k = 1$ the special case which generates true Möbius transformation. This also makes an argument for calling eq. (4.27) a generalized Möbius transformation. In fact, we shall see that we can use some features of Möbius theory to understand how to iterate this transformation so that we obtain a closed expression for f^n with f given by eq. (4.27).

We seek an expression for the transformation corresponding to n periods of driving, that is, we seek

$$z \mapsto z_n = f^n(z), \tag{4.28}$$

where f is given by eq. (4.27). We start by defining a Möbius transformation T,

$$T(z) = \frac{az + b}{cz + d}, \tag{4.29}$$

where a, b, c and d are the same as for f, given in eq. (4.26). Then we can write f in terms of this Möbius transformation T as

$$f(z) = \Big(T(z^k)\Big)^{1/k}. \tag{4.30}$$

Furthermore, n applications of f gives

$$f^n(z) = f(f(...f(f(z))...) = f(f(...f(\Big(T(z^k)\Big)^{1/k})...), \tag{4.31}$$

where

$$f\left(\Big(T(z^k)\Big)^{1/k}\right) = \left(T\left(\ \Big(\Big(T(z^k)\Big)^{1/k}\Big)^k\ \right)\right)^{1/k} = \Big(T\Big(T(z^k)\Big)\Big)^{1/k}. \tag{4.32}$$

Note that the exponent of T, $1/k$, is canceled by that f takes the k:th power of its argument, a pattern that repeats itself for the higher orders of f. We obtain

$$f^n(z) = \Big(T^n(z^k)\Big)^{1/k}, \tag{4.33}$$

where the important thing to note is that T is a true Möbius transformation, thus we know how to write down an expression for the n repetitions of the transformation, T^n. That is, for T^n we can now reuse the analysis from subsection 3.2.3, eqs. (3.58) and (3.59) and the derivation that follows, to find explicit expressions for the coefficients. We thus have the coordinate transformation

$$z \mapsto z_n(z) = f^n(z) = \left(\frac{Az^k + B}{Cz^k + D}\right)^{1/k}, \tag{4.34}$$

with A, B, C and D, we will now omit to write out the n dependence in favor for the appearance of equations to come, given by eqs. (3.62) and (3.63) for one (two) fixed point(s) respectively, given here again:

$$\begin{bmatrix} A & B \\ C & D \end{bmatrix} = \begin{bmatrix} 1+n\beta\gamma & -n\beta\gamma^2 \\ n\beta & 1-n\beta\gamma \end{bmatrix}, \tag{4.35}$$

and

$$\begin{bmatrix} A & B \\ C & D \end{bmatrix} = \begin{bmatrix} \gamma_1 - \eta^n\gamma_2 & -(1-\eta^n)\gamma_1\gamma_2 \\ 1-\eta^n & -(\gamma_2 - \eta^n\gamma_1) \end{bmatrix}. \tag{4.36}$$

The coefficients γ, $\gamma_{1,2}$, η and β are given by eqs. (3.67) - (3.70), which we also reproduce here:

$$\gamma_{(1,2)} = \frac{a-d}{2c}\left(\pm\frac{\sqrt{(a-d)^2+4bc}}{2c}\right), \quad \eta = \frac{c\gamma_2+d}{c\gamma_1+d}, \quad \beta = \frac{a+d}{2c}, \tag{4.37}$$

where now a, b, c and d, we omit to write out the k dependence in favor for the appearance of future equations, are given by eq. (4.26), that is

$$\begin{bmatrix} a & b \\ c & d \end{bmatrix} = \begin{bmatrix} (1+\frac{\pi k\tau_k}{L})e^{\frac{\pi k\tau_0}{L}} & -\frac{\pi k\tau_k}{L}e^{-\frac{\pi k\tau_0}{L}} \\ \frac{\pi k\tau_k}{L}e^{\frac{\pi k\tau_0}{L}} & (1-\frac{\pi k\tau_k}{L})e^{-\frac{\pi k\tau_0}{L}} \end{bmatrix}. \tag{4.38}$$

Now when we have made explicit the transformation $z \mapsto z_n$ in eqs. (4.34) - (4.38) we are ready to derive an expression for the energy density, following the same recipe as in subsection 3.3.2.

4.3 Energy density

In this section we will derive the explicit formula for the energy density after n periods. Recalling the analysis in section 3.3, one realizes that the only thinkable change when replacing the Möbius transformation by another conformal transformation (such that the "generalized" Möbius transformation in eq. (4.34)) is in the argument why a Schwarzian derivative is not to be added when considering the transformation related to time evolution, $z \mapsto z_n$. Needless to say, one must also carefully modify calculational details considering the fact that $z_n(z)$ is a different function now. The procedure of finding the expectation value is the same as before as none of the arguments rely on the specific form of the deformation.

To substantiate this, let us consider the relevant expectation value

$$\langle\psi(nT)|\,|T(\omega)\,|\psi(nT)\rangle\,, \tag{4.39}$$

defined in the strip geometry with ω as coordinate. Let us then carry out the following successive transformations: (i) a mapping to the full complex plane with z as coordinate, (ii) a time evolution emulated by the map $z \to z_n$, and, finally (iii) a transformation to the upper half plane $z_n \mapsto \xi(z_n) = \sqrt{z_n}$. (Where the third and final map to the upper half plane is motivated by that we can use standard

CFT techniques for the calculation of the expectation value for the stress-energy tensor there.) All transformations are conformal so we know that the stress-energy tensor transforms according to eq. (2.55). We also have that $T_{tt} = \frac{1}{2\pi}(T(\omega + \bar{T}\bar{\omega})$ and it is therefore sufficient to calculate the expectation value of $T(\omega)$ ($\bar{T}(\bar{\omega})$ follows analogously). Putting it all together:

$$\begin{aligned}
\langle\psi(nT)|\, T(\omega)\, |\psi(nT)\rangle &= \left(\frac{\partial z}{\partial \omega}\right)^2 \langle\psi(nT|\, T(z)\, |\psi(nT)\rangle + \cancel{\left(\frac{L}{2\pi}\right)^2 \frac{c}{12}} \\
&= \left(\frac{\partial z}{\partial \omega}\right)^2 \left(\frac{\partial z_n}{\partial z}\right)^2 \langle G_{H_0}|\, T(z_n)\, |G_{H_0}\rangle \\
&+ \left(\frac{\partial z}{\partial \omega}\right)^2 \frac{c}{12}\{z_n, z\}_{\mathrm{Sc}} \\
&= \left(\frac{\partial z}{\partial \omega}\right)^2 \left(\frac{\partial z_n}{\partial z}\right)^2 \left(\frac{\partial \xi}{\partial z_n}\right)^2 \cancel{\langle G_{H_0}|\, T(\xi)\, |G_{H_0}\rangle}^{\,0} \\
&+ \left(\frac{\partial z}{\partial \omega}\right)^2 \left(\frac{\partial z_n}{\partial z}\right)^2 \{\xi, z_n\}_{\mathrm{Sc}} \frac{c}{12} + \left(\frac{\partial z}{\partial \omega}\right)^2 \{z_n, z\}_{\mathrm{Sc}} \frac{c}{12}.
\end{aligned} \tag{4.40}$$

All arguments, but one, for each equality are the same as the ones given in subsection 3.3.2. The new argument is for the second equality where we now need to keep the Schwarzian derivative, $\{z_n, z\}$, since the map $z \to z_n$ is not a Möbius transformation (which is the only transformation giving a vanishing Schwarzian derivative [31]). By comparing eq. (4.40) with its analog, eq. (3.82), we see that the first nonzero part is the same except that $z_n(z)$ is a different function and we also have added a new term, $\{z_n, z\}$, to the expression.

Before we can write down the expression that explicitly gives the energy density after n periods we need to calculate all the different derivatives in eq. (4.40). First the two that we have already done: the derivative $\frac{\partial z}{\partial \omega}$ and the Schwarzian derivative $\{\xi, z_n\}$. Equation (4.10) tells us that

$$\frac{\partial z}{\partial \omega} = \frac{2\pi}{L} z. \tag{4.41}$$

Furthermore, the transformation to the upper half plane $z_n \to \xi$ given by eq. (3.73), also calculated in eq. (3.79), gives

$$\{\xi, z_n\} = \frac{3}{8}\frac{1}{z_n^2}. \tag{4.42}$$

The new ingredient is the new expression of $z_n(z)$ given in eq. (4.34). We need to take the three first derivatives of this expression in order to calculate the Schwarzian

derivative, $\{z_n, z\}$. In the process we get $\frac{\partial z_n}{\partial z}$ as well. The first derivative:

$$\begin{aligned}\frac{\partial z_n}{\partial z} &= \frac{1}{\partial z}\left(\frac{Az^k+B}{Cz^k+D}\right)^{1/k} \\ &= \frac{1}{k}\left(\frac{Az^k+B}{Cz^k+D}\right)^{1/k-1}\left(\frac{Akz^{k-1}}{Cz^k+D}-\frac{(Az^k+B)Ckz^{k-1}}{(Cz^k+D)^2}\right) \\ &= \left(\frac{Az^k+B}{Cz^k+D}\right)^{1/k-1}\frac{(AD-BC)z^{k-1}}{(Cz^k+D)^2}\ \frac{Az^k+B}{Az^k+B} \\ &= \frac{(AD-BC)z^{k-1}}{(Cz^k+D)(Az^k+B)}z_n \equiv (AD-BC)h(z)z_n \equiv \kappa h(z)z_n.\end{aligned} \tag{4.43}$$

We have here defined the function $h(z)$ and constant κ for convenience. We can then carry out the second and third derivative of $z_n(z)$ in terms of h:

$$\frac{\partial^2 z_n}{\partial z^2} = \kappa h(z)z_n'(z) + \kappa h'(z)z_n = \left(\kappa^2 h^2(z) + \kappa h'(z)\right)z_n, \tag{4.44}$$

$$\frac{\partial^3 z_n}{\partial z^3} = \left(\kappa^3 h^3(z) + 3\kappa^2 h(z)h'(z) + \kappa h''(z)\right)z_n. \tag{4.45}$$

We must now calculate the first two derivatives of h, that is

$$\begin{aligned}h'(z) &= \left(\frac{(k-1)z^{k-2}}{(Az^k+B)(Cz^k+D)} - \frac{kAz^{k-1}z^{k-1}}{(Az^k+B)^2(Cz^k+D)}\right. \\ &\qquad\left. - \frac{kCz^{k-1}z^{k-1}}{(Az^k+B)(Cz^k+D)^2}\right) \\ &= \frac{z^{2k-2}}{(Az^k+B)^2(Cz^k+D)^2}\Big((k-1)z^{-k}(Az^k+B)(Cz^k+D) \\ &\qquad - kA(Cz^k+D) - kC(Az^k+B)\Big) \\ &= h^2(z)\left((k-1)BDz^{-k} - (AD+BC) - (k+1)ACz^k\right) \equiv h^2(z)g(z),\end{aligned} \tag{4.46}$$

where we have defined a new function $g(z)$ for convenience. We can then express the second derivative of $h(z)$ in terms of h and g,

$$h''(z) = 2h(z)h'(z)g(z) + h^2(z)g'(z) = 2h^3(z)g^2(z) + h^2(z)g'(z). \tag{4.47}$$

Finally, we need the first derivative of g:

$$g'(z) = -k(k-1)BD\frac{1}{z^{k+1}} - (k+1)kACz^{k-1}. \tag{4.48}$$

We are now ready to write down an expression for the Schwarzian derivative. Remembering that we have explicit expressions for the functions h, g, and g' as well

as for the constant κ, we can write the Schwarzian derivative on the compact form

$$\begin{aligned}
\{z_n, z\}_{\mathrm{Sc}} &= \frac{z_n'''}{z_n'} - \frac{3}{2}\left(\frac{z_n''}{z_n'}\right)^2 \\
&= \kappa^2 h^2(z) + 3\kappa h'(z) + \frac{h''(z)}{h(z)} - \frac{3}{2}\left(\kappa h(z) + \frac{h'(z)}{h(z)}\right)^2 \\
&= -\frac{1}{2}\kappa^2 h^2(z) + \frac{h''(z)}{h(z)} - \frac{3}{2}\frac{h'(z)^2}{h^2(z)} \\
&= -\frac{1}{2}\kappa^2 h^2(z) + \frac{2h^3(z)g^2(z) + h^2(z)g'(z)}{h(z)} - \frac{3}{2}\frac{(h^2(z)g(z))^2}{h^2} \\
&= -\frac{1}{2}\kappa^2 h^2(z) + \frac{1}{2}h^2(z)g^2(z) + h(z)g'(z).
\end{aligned} \tag{4.49}$$

This explicit expression for $\{z_n, z\}_{\mathrm{Sc}}$ must be zero for $k = 1$ since that corresponds to when the transformation $z \to z_n$ is a Möbius transformation (which we remember is the only conformal transformation for which the Schwarzian derivative vanish [31]). To show that $\{z_n, z\}_{\mathrm{Sc}} = 0$ for $k = 1$ will be rather cumbersome but the philosophy is nothing else but expanding h, g and g', given in eqs. (4.43), (4.46) and (4.48) respectively, in the expression for $\{z_n, z\}$, given by eq. (4.49), and then order terms in powers of z. We obtain:

$$\begin{aligned}
\{z_n, z\}_{\mathrm{Sc}}\frac{1}{h^2(z)} =& -\frac{1}{2}\kappa^2 + \frac{1}{2}g^2(z) + \frac{g'(z)}{h(z)} \\
=& \left(\frac{1}{2}(k-1)^2 - k(k-1)\right)(BD)^2 z^{-2k} \\
&+ \left(-(k-1) - k(k-1)\right) BD(AD+BC)z^{-k} \\
&-\frac{1}{2}(AD-BC)^2 + \frac{1}{2}(AD+BC)^2 \\
&-\Big((k-1)(k+1) + k(k+1) + k(k-1)\Big)ABCD \\
&+ \left((k+1) - k(k+1)\right) AC(BC+AD)z^{k} \\
&+ \left(\frac{1}{2}(k+1)^2 - k(k+1)\right)(AC)^2 z^{2k} \\
=& -(k^2-1)\Bigg(\frac{1}{2}(BD)^2 z^{-2k} + BD(AD+BC)z^{-k} + 3ABCD \\
&\qquad + AC(AD+BC)z^{k} + \frac{1}{2}(AC)^2 z^{2k}\Bigg).
\end{aligned} \tag{4.50}$$

We can now explicitly see that the Schwarzian expression $\{z_n, z\}$ vanishes only when $k = 1$. As we have already mentioned, this is how it must be, because only when $k = 1$ are $z \mapsto z_n$ a Möbius transformation, the only type of conformal transformation with zero Schwarzian derivative [31].

Now we are ready to write down the expression for the energy density after n periods. First we remember that $T_{tt} = \frac{1}{2\pi}(T(\omega) + \bar{T}(\bar{\omega}))$. We also need the expectation value for $T(\omega)$ given by eq. (4.40) in which we have $\frac{\partial z}{\partial \omega}$, $\frac{\partial z_n}{\partial z}$ and $\{\xi, z_n\}$ given by

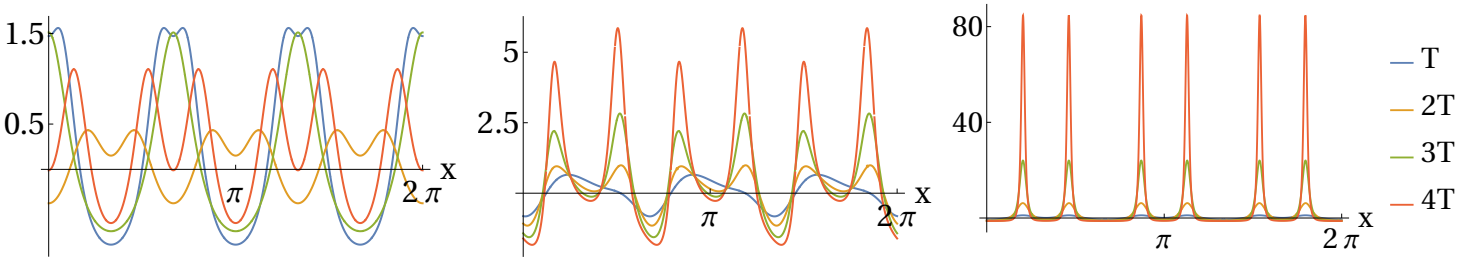

(a) Non-Heating **(b)** Critical **(c)** Heating

Figure 4.1: We have chosen to illustrate the generalized system with $k = 3$. The different colors are the energy distribution in the system after 1, 2, 3 and 4 periods, $T = T_1 + T_0$. The length of the system was chosen to be $L = 2\pi$ and the central charge $c = 1$. We have here consequently chosen the driving parameters T_0 and T_k such that the value of η is approximately the same as in the corresponding phases plotted in fig. 3.5 for better comparison. (a) Non-heating phase given by $T_0 = 0.166L$ and $T_k = 0.033L$. (b) Critical phase given by $T_0 = 0.3L$ and $T_k \approx 0.016L$ (where a more exact value can be obtained by solving eq. (4.59) with the given value for T_0). (c) Heating phase given by $T_0 = 0.3L$ and $T_k = 0.033L$.

eqs. (4.41), (4.43) and (4.42) respectively. Putting it all together, we obtain the energy density after n periods,

$$\begin{aligned}\langle\psi(nT)|\, T_{tt}(x)\, |\psi(nT)\rangle = \frac{\pi c}{16L^2}\frac{z^{2k}(AD-BC)^2}{(Az^k+B)^2(Cz^k+D)^2} \\ + \left(\frac{\partial z}{\partial \omega}\right)^2 \{z_n, z\}_{\mathrm{Sc}}\frac{c}{12} + (z \to \bar{z}).\end{aligned} \tag{4.51}$$

Note that by setting $k = 1$, which makes the Schwarzian derivative vanish identically, gives precisely the same expression as before the generalization, eq. (3.83). This serves as a check of our generalized approach. The last thing we need to do before plotting this expression is to write the expression for the energy density after the analytic continuation $\tau_{0,k} \mapsto iT_{0,k}$. We here use that the coordinates transform as

$$z(\tau) \mapsto z(T) = e^{\frac{2\pi}{L}i(T_0+T_k)+ix}, \quad \bar{z}(\tau) \mapsto \bar{z}(T) = e^{\frac{2\pi}{L}i(T_0+T_k)-ix}. \tag{4.52}$$

Then plotting the energy density, eq. (4.51), we observe the same characteristics as before, with a non-heating phase, a heating phase and a critical phase, compare fig. 4.1 to the corresponding figure for $k = 1$, fig. 3.5.

4.4 Energy distribution related to the generalized Möbius transformation

In this section we will try to understand the three phases in terms of the generalized Möbius transformation, eq. (4.34), and identify the parameter spaces of the driving parameters T_0 and T_k that correspond to the different phases.

We start with the expression for the energy density in terms of z and z_n only, focusing on the parts containing z_n as z_n is the only time-dependent variable. We have

$$\langle\psi(nT)|\, T_{tt}(x)\, |\psi(nT)\rangle = \frac{c}{32}\left(\frac{\partial z}{\partial \omega}\right)^2\left(\frac{\partial z_n}{\partial z}\right)^2\frac{1}{z_n^2} + \frac{c}{12}\frac{\partial z}{\partial \omega}\{z_n, z\}. \tag{4.53}$$

We thus have three expressions in need of investigation, z_n, $\frac{\partial z_n}{\partial z}$ and $\{z_n, z\}$. To understand the discrimination between the phases we need to investigate the absolute values of these expressions since they play important roles in the growth or non-growth of the energy density.

Before we investigate these three terms, z_n, $\frac{\partial z_n}{\partial z}$ and $\{z_n, z\}$, we should remind ourselves about that the generalized Möbius transformation, $z \to z_n$, has two fundamental different descriptions and which to be used is determined by the driving parameters T_0 and T_k. This is seen from the fact that the generalised Möbius transformation in eq. (4.33) is built up by a true Möbius transformation, eq. (4.29), which gives the coefficients after several periods A, B, C and D; how they build up the generalized Möbius transformation is seen in eq. (4.34). From our discussion in section 2.6 we could see that the expression after several successive applications of a true Möbius transformation is dependent of whether or not we have one or two fixed points. Furthermore, in subsection 3.3.3 we could conclude that the heating phase as well as the non-heating phase relates to the Möbius transformation with two fixed points while the critical phase relates to the Möbius transformation with one fixed point. Moreover, we could also understand how the number of fixed points relates to the driving parameters T_0 and T_1. We will see that the number of fixed points relates to the different phases in the same way now. In passing, in the analysis to follow we shall freely interchange between talking about the number of fixed points and which phase we are focusing on.

First, we note that $|z_n| = 1$ and thus not contributing to the discrimination of the phases. The argument is simple, similar to that in the corresponding discussion in subsection 3.3.3. We can see this from

$$z_n = f^n(z) = \left(T^n(z^k)\right)^{1/k}, \tag{4.54}$$

and given $|T(z^k)| = 1$, we verify that $|z_n| = |T(z^k)|^{n/k} = 1$, using that T is a Möbius transformation with coefficients a, b, c and d given by eq. (4.26). After analytic continuation, the relations $d = a^*$ and $c = b^*$ yield

$$\left|T(z^k)\right|^2 = \left|\frac{az^k + b}{b^*z^k + a^*}\right|^2 = \frac{|a|^2|z^k|^2 + |b|^2 + ab^*z^k + a^*bz^{k^*}}{|b|^2|z^k|^2 + |a|^2 + ab^*z^k + a^*bz^{k^*}} = 1, \tag{4.55}$$

where, to obtain the last equality, we need $|z^k| = |z|^k = 1$. This follows immediately after analytic continuation since then $z = \exp\left\{\frac{2\pi}{L}i(T_0 + T_k + x)\right\}$.

Second, we calculate $\frac{\partial z_n}{\partial z}$. Using eq. (4.43) we get

$$\left|\frac{\partial z_n}{\partial z}\right| = \left|\frac{(AD - BC)z^{k-1}}{(Cz^k + D)(Az^k + B)}z_n\right| = \left|\frac{(AD - BC)}{(Cz^k + D)(Az^k + B)}\right|, \tag{4.56}$$

where we used that $|z_n| = 1$ from eqs. (4.54) and (4.55), where we also noted that $|z| = 1$ which we have used also here. Assume that we have chosen driving parameters such that the Möbius transformation T, eq. (4.29) (that builds up the generalized Möbius transformation, eq. (4.31), and which emulates the time-evolution) has two fixed points. Then the parameters A, B, C and D are given by eq. (4.36). After a few algebraic manipulations we obtain:

$$\begin{aligned}\frac{(AD-BC)}{(Cz^k+D)(Az^k+B)} &= \frac{(\gamma_1-\gamma_2)^2\eta^n}{\gamma_2(\gamma_1-z^k)^2\eta^{2n}+\gamma_1(z^k-\gamma_2)^2+(\gamma_1+\gamma_2)(\gamma_1-z^k)(z^k-\gamma_2)} \\ &= \begin{cases}\eta^n/\gamma_1, & z^k=\gamma_1 \\ \eta^{-n}/\gamma_2, & z^k=\gamma_2\end{cases}.\end{aligned} \tag{4.57}$$

We can here see a clear resemblance with the corresponding expression, eq. (3.89), in the previous chapter. Analogous to the discussion after eq. (3.89), we have exponential growth, $\sim \eta^n$, for $|\eta| < 1$ ($|\eta| > 1$) at x such that $z(x)^k = \gamma_2$ ($z(x)^k = \gamma_1$). Note the exponent k of z in eq. (4.57), different from its analog, eq. (3.89), in chapter 3 where we have $k = 1$. It follows that we have $2k$ peaks in this generalized case (one k from the "z-part" and another k from the "$\bar{z}$-part"). To discriminate between the cases for having peaks at x such that $z^k(x) = \gamma_1$ or $z^k(x) = \gamma_2$ we need to analyse η just as we did in eq. (3.90). Since we don't use the explicit expressions for the coefficients a, b, c and d, so the same results holds here. That is, we discriminate by the sign of $\mathrm{Re}\{a\}$ such that: $\mathrm{Re}\{a\} < 0$ and $\mathrm{Re}\{a\} > 0$ gives peaks at $z^k(x) = \gamma_1$ and $z^k(x) = \gamma_2$ respectively. The explicit expression for $\mathrm{Re}\{a\}$ is given by,

$$\mathrm{Re}\{a\} = \cos\frac{k\pi T_0}{L} - \frac{k\pi T_k}{L}\sin\frac{k\pi T_0}{L}. \tag{4.58}$$

Again we get that in the two first quadrants that the cosine and sine functions sweep through gives $\mathrm{Re}\{a\} < 0$ and quadrant three and four gives $\mathrm{Re}\{a\} > 0$.

Furthermore, the analysis to discriminate the phases in chapter 3 focused on η, in particular whether or not it is real or complex, where in the complex case we have that $|\eta| = 1$ giving $\eta = 1$ to be critical. From eq. (4.37) we noted that η in terms of the Möbius parameters a, b, c and d is the same as in the previous chapter. The analysis then has only one difference which is how k appears in a, b, c and d. We thus have

$$|b|^2 - \mathrm{Im}\{a\}^2 = \left(\frac{k\pi T_k}{L}\right)^2 - \left(\sin\frac{k\pi T_0}{L} + \frac{k\pi T_k}{L}\cos\frac{k\pi T_0}{L}\right)^2 = 0, \tag{4.59}$$

defining the line for the critical phase that discriminates between the heating phase ($|b|^2 - \mathrm{Im}\{a\}^2 > 0$) and non-heating phase ($|b|^2 - \mathrm{Im}\{a\}^2 < 0$), as discussed after the expression for η in eq. (3.90).

Now to the new component in the expression for the energy density, eq. (4.51), (not present when $k = 1$): the Schwarzian derivative $\{z_n, z\}$. As we shall see, it does not make any major difference to the behavior of the energy density. First,

note that the only n-dependence in the expression for $\{z_n, z\}$, given in eq. (4.50), is in the coefficients A, B, C and D. From this observation we can directly tell that the parameter space of T_0 and T_k will be partitioned in the same way as before, depending on whether η is complex, real or exactly equal to unity. It follows that the parameter space will be divided according to eq. (4.59). Furthermore, in eq. (4.50) we have given the expression for $\{z_n, z\}/h^2$ in the fourth power of the coefficients A, B, C and D, with no assumptions on z. That is, we have

$$\{z_n, z\}/h^2 \propto \eta^4. \tag{4.60}$$

However, from the definition of h given in eq. (4.43) and the expressions for the coefficients A, B, C and D in eq. (4.36) we get

$$\begin{aligned} h^2 &= \left(\frac{z^{k-1}}{\gamma_2(\gamma_1 - z^k)^2\eta^{2n} + \gamma_1(z^k - \gamma_2)^2 + (\gamma_1+\gamma_2)(\gamma_1 - z^k)(z^k - \gamma_2)} \right)^2 \\ &\propto \begin{cases} 1, & z^k = \gamma_1 \\ \eta^{-4n}, & z^k = \gamma_2 \\ \eta^{-4n}, & z^k \neq \gamma_1 \text{ and } |\eta| > 1 \end{cases} . \end{aligned} \tag{4.61}$$

From these two equations, eqs. (4.60) and (4.61), one concludes that for $|\eta| < 1$ we have no growth with n for $\{z_n, z\}$. It follows from that in eq. (4.60) we see a decreasing behavior for all $z(x)$ and from eq. (4.61) we only have growth for $z^k = \gamma_2$ but at the same rate as for the falloff, implying that the multiplication (which corresponds to $\{z_n, z\}$) of the two gives at most a constant behaviour with time (growing n). The other case with $|\eta| > 1$ gives peaks around x such as $z(x)^k = \gamma_1$. It follows from that we in eq. (4.61) can see a decreasing behavior, $\sim \eta^{-4n}$, for all $z(x)$ except for $z^k(x) = \gamma_1$ where we instead have a constant behavior with growing n. Furthermore, from eq. (4.60) we have exponential growth, $\sim \eta^{4n}$, for all $z(x)$. It follows that the multiplication of the two expressions eqs. (4.60) and (4.61), which is $\{z_n, z\}$, then is constant for all $z(x)$ but $z^k(x) = \gamma_1$ where we have only growth. We conclude that for $|\eta| < 1$ the Schwarzian derivative $\{z_n, z\}$ gives no contribution to the energy density and for $|\eta| > 1$ it gives the same kind of contribution as that coming from $\frac{\partial z_n}{\partial z}$ implying that the peaks only get bigger. Thus, no qualitative difference from from what we would have obtained if we had neglected the Schwarzian derivative.

The last step to complete our understanding of how the generalized Möbius transformation, f^n given by eq. (4.27), relates to the energy density, eq. (4.53), is to investigate how both $\frac{\partial z_n}{\partial z}$ and $\{z_n, z\}$ behaves when $|b|^2 - \mathrm{Im}\{a\}^2 = 0$, that is at the critical phase given by values of the parameters T_0 and T_k that fulfill eq. (4.59). In this case the Möbius transformation, eq. (4.29), building up the generalized Möbius transformation, eq. (4.33), has only one fixed point. Let us first consider the derivative $\frac{\partial z_n}{\partial z}$, where we again can use $|z| = |z_n| = 1$ as we did in the corresponding expression where we had two fixed points, eq. (4.56). We can now calculate the absolute value of $\frac{\partial z_n}{\partial z}$ using the expressions for the coefficients A, B, C and D in eq. (4.35), describing the true Möbius transformation with one fixed point that builds up the generalized Möbius transformation. We obtain

$$\left| \frac{\partial z_n}{\partial z} \right| = \left| \frac{AD - BC}{(Cz^k + D)(Az^k + B)} \right| = \left| \frac{1/(n^2\beta^2)}{(z^k - (\gamma - 1/n\beta))\left((\gamma + 1/n\beta)z^k - \gamma^2\right)} \right|, \tag{4.62}$$

where we have only carried out some trivial algebra, and also used that $AD-BC=1$. We can see that we get peaks that move towards x such that $z^k=\gamma$, where the denominator goes towards zero, but everywhere else we have a decreasing factor of $1/n^2$. The growth can only be polynomial in n since the factors $\gamma-1/n\beta$ and $\gamma+1/n\beta$ approach γ polynomially.

Let us now continue our discussion of the critical phase by an analysis of the contribution from the Schwarzian derivative, $\{z_n,z\}$. Since it is a rather messy expression to analyse we again simply notice from eq. (4.50) that we have

$$\{z_n,z\}/h^2\propto\eta^{4n}, \tag{4.63}$$

(cf. the analogy to eq. (4.60)). Moreover, we have just discussed $\frac{\partial z_n}{\partial z}$ which now, for one fixed point with $AD-BC=1$, is exactly equal to $h(z)$. That is, from eq. (4.62) and the discussion which followed we have for h that

$$h^2\propto 1/\eta^{4n},\quad z^k(x)\not\approx\gamma, \tag{4.64}$$

with peaks growing at polynomial rate in n for $z^k(x)$ at a point near γ. In other words, the Schwarzian derivative $\{z_n,z\}$ gives essentially the same contribution as $\frac{\partial z_n}{\partial z}$ to the energy density but is also responsible for the irregularities between the peaks in fig. 4.1b.

We conclude this subsection by presenting the parameter spaces, in the T_0,T_k-plane, that correspond to the heating and non-heating phases, together with the border which defines the critical phase. Figure 4.2a is obtained from eq. (4.59) which defines the border between real and complex η. In fig. 4.2b we have added the borders for the quadrants that determine the sign of $\mathrm{Re}\{a\}$ in the heating phase: quadrant one and two giving $\mathrm{Re}\{a<0\}$ and quadrant three and four giving $\mathrm{Re}\{a\}>0$, as discussed after eq. (4.58). That discussion also revealed the similarities with the corresponding discussion in the previous chapter after eq. (3.90), giving that we know that for $\mathrm{Re}\{a\}<0$ we have peaks around $z^k=\gamma_2$ and $\bar{z}^k=\gamma_2^*$, while for $\mathrm{Re}\{a\}>0$ we have peaks around $z^k=\gamma_1$ and $\bar{z}^k=\gamma_1^*$. We should note that we have a factor of k in the arguments of the sine and cosine functions in eqs. (4.58) and (4.59) which in their corresponding expressions in eqs. (3.91) and (3.96) respectively are a simple 1, thus not explicit. This is the reason for why we have a more rapid repetition of the parameter interval along the T_0/L axis with larger k, as seen in fig. 4.2a with $k=3$ (having three times as many repetitions of the parameter interval compared to fig. 3.6a with $k=1$). Furthermore, the k dependence in eq. (4.59) also gives that the non-heating parameter space is suppressed towards the axes.

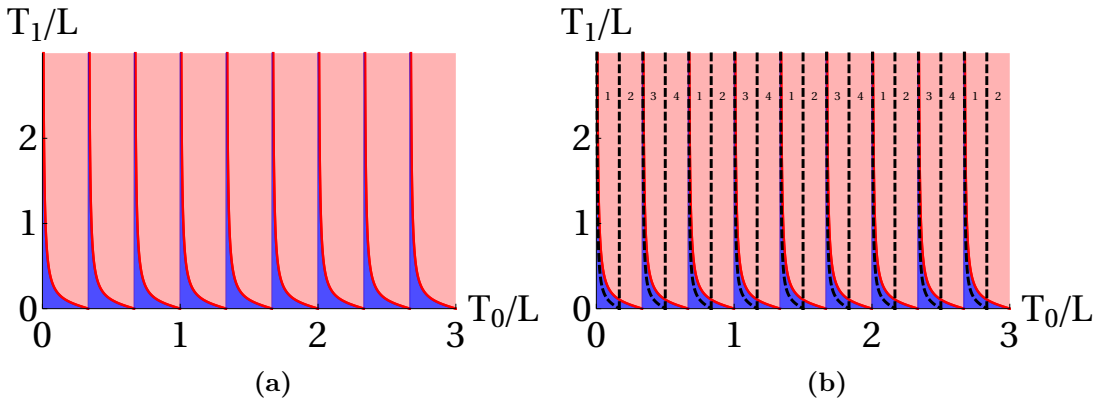

Figure 4.2: In panel (a) we can read off the parameter values corresponding to the three different phases of energy absorption (cf. fig. 4.1). The heating phases are marked by light red color, while blue color indicates non-heating phases. The border between the two, marked by dark red, corresponds to the critical phase. Panel (b) shows which sign $\mathrm{Re}\{a\}$ has in the various heating phases; we indicate this by labeling each region by the quadrant which the cosine and sine functions go through, as given in eq. (4.58). We know that the sign of $\mathrm{Re}\{a\}$ is negative in quadrant one and two, and positive in quadrant three and four. This gives us knowledge about how the peaks in the corresponding heating phases are related: to γ_2 ($\mathrm{Re}\{a\} < 0$) or to γ_1 ($\mathrm{Re}\{a\} > 0$).

5

Conclusion

This thesis has served as a review of the work on Floquet CFT by Fan et al. in Ref. [2], trying to make their analysis more transparent by adding details and additional arguments. Also, we have proposed a generalization of their work, by this revealing several interesting features of this class of Floquet systems which can be described by CFT. We have tried to present the technicalities in calculations and arguments in great detail so as no previous knowledge of CFT should be needed. The main conclusion from the work by Fan et al. [2] – that it is in principal possible for an interacting Floquet system not to heat up – is found to be still valid within our generalization. This holds promise for the use of specially designed Floquet systems as components in future quantum technologies.

The model that we have discussed is a square-wave drive where the Hamiltonian jumps back and forth between an arbitrary CFT and a deformation of the same CFT. Following Fan et al. [2], we first studied a sine-square deformation in chapter 3, which we then generalized to a sine-k-square deformation in chapter 4. By analysing the stress-energy tensor we could calculate and plot the energy density at stroboscopic snapshots given by eqs. (3.83) and (4.51) and visualized in figs. 3.5 and 4.1 for the sine-square deformation and for the sine-k-squared deformation (with $k = 3$) respectively. What we found in these plots were that in both cases we have three phases: One phase which does not absorb energy and two phases which absorbs energy. In the case were no energy is absorb this is manifested by that at stroboscopic snapshots the energy distribution has oscillating feature along the system's spatial direction. In the other two phases when energy is absorbed it is manifested by that energy peaks grow for each monitored period, in one of the phases the peaks grow polynomially while in the other there is exponential growth. Moreover, the number of peaks is two times k.

We have also investigated the parameter space of the driving parameters to see for which values we get the different phases; the results are shown in figs. 3.6 and 4.2 for the sine-square and sine-k-square deformation respectively. The parameter values which give the critical phase and hence also divide the spaces that corresponds to the non-heating phase and heating-phase are given by eq. (4.59). This equation is written for the more general case of a sine-k-squared deformation; by setting $k = 1$ we reproduce the sine-squared case studied by Fan et al. [2]. From this equation we can see that the connected area for the values giving the non-heating phase

shrinks with growing k as well as getting more repetitive. That is, we need a higher frequency of the drive to still get a non-heating phase for larger k.

To investigate and generalize this field further would require a deformation, call it $f(x)$, with an arbitrary Fourier series instead of the sine-k-square deformation. To find such a generalization would be an important step. Using conformal transformations to represent stroboscopic time evolution should still be possible, since the discussion in subsection 3.2.2 for arriving at that conclusion had little or nothing to do with the specifics about the deformation used. However, all terms in the Fourier expansion will have its owns Virasoro generators and with higher harmonics in the expansion we will have Virasoro generators $L_{\pm k}$ with larger k. To find out how this affects the energy density will be the hard part. We can with confidence say that finding the one-period time evolution is doable with the same trick as here in both chapters 3 and 4, that is, performing a coordinate change so as to be able to describe the deformed Hamiltonian's action as a dilation, see eqs. (3.53) and (4.24). In other words, we only need the coordinate change $\chi = \exp\left\{\int \frac{\mathrm{d}z}{z\tilde{f}(z)}\right\}$ where $\tilde{f}(z)$ is the deformation, $f(x)$, after an analytic continuation and coordinate change to the full complex plane. But to then get an expression for several time periods might be more difficult, we have been able to exploit Möbius theory which a priori is not evident that one can use when using an arbitrary Fourier expansion as deformation function. What we exploited in Möbius theory in order to get an expression for several applications of the same transformation is the fixed point structure and perhaps one could use this also for a more general deformation. However, this is a rather more difficult problem than in the Möbius case.

We have seen that Floquet systems really have the potential to not only show topological phases but also, on a theoretical level, being possible to engineer so that they do not heat up. To arrive at the goal of combining these two properties, and exploit them in future quantum technologies we need to push forward to gain knowledge under which general circumstances we can obtain Floquet systems which do not heat up. With all the activity in the area of topological matter as well as with Floquet systems maybe, optimistically, we will soon be able to realize this goal.

References

[1] X. Wen and J.-Q. Wu, "Quantum dynamics in sine-square deformed conformal field theory: quench from uniform to nonuniform conformal field theory", Physical Review B **97** (2018).

[2] R. Fan, Y. Gu, A. Vishwanath, and X. Wen, "Emergent spatial structure and entanglement localization in Floquet conformal field theory", Physical Review X **10** (2020).

[3] X. Wen and J.-Q. Wu, *Floquet conformal field theory*, (2018) `https://arxiv.org/abs/1805.00031`.

[4] M. S. Rudner and N. H. Lindner, "Band structure engineering and non-equilibrium dynamics in Floquet topological insulators", Nature Reviews Physics **2**, 229 (2020).

[5] L. D'Alessio and M. Rigol, "Long-time behavior of isolated periodically driven interacting lattice systems", Physical Review X **4** (2014).

[6] A. Lazarides, A. Das, and R. Moessner, "Equilibrium states of generic quantum systems subject to periodic driving", Physical Review E **90** (2014).

[7] G. Jotzu et al., "Experimental realization of the topological Haldane model with ultracold fermions", Nature **515**, 237 (2014).

[8] N. Flaschner et al., "Experimental reconstruction of the Berry curvature in a Floquet Bloch band", Science **352**, 1091 (2016).

[9] M. C. Rechtsman et al., "Photonic Floquet topological insulators", Nature **496**, 196 (2013).

[10] Y. H. Wang, H. Steinberg, P. Jarillo-Herrero, and N. Gedik, "Observation of Floquet-Bloch states on the surface of a topological insulator", Science **342**, 453 (2013).

[11] J. W. McIver et al., "Light-induced anomalous Hall effect in graphene", Nature Physics **16**, 38 (2019).

[12] H. Katsura, "Sine-square deformation of solvable spin chains and conformal field theories", Journal of Physics A: Mathematical and Theoretical **45**, 115003 (2012).

[13] A. Gendiar, R. Krcmar, and T. Nishino, "Spherical deformation for one-dimensional quantum systems", Progress of Theoretical Physics **122**, 953 (2009).

[14] T. Hikihara and T. Nishino, "Connecting distant ends of one-dimensional critical systems by a sine-square deformation", Physical Review B **83** (2011).

[15] A. Gendiar, M. Daniška, Y. Lee, and T. Nishino, "Suppression of finite-size effects in one-dimensional correlated systems", Physical Review A **83** (2011).

[16] N. Shibata and C. Hotta, "Boundary effects in the density-matrix renormalization group calculation", Physical Review B **84** (2011).
[17] C. Hotta and N. Shibata, "Grand canonical finite-size numerical approaches: a route to measuring bulk properties in an applied field", Physical Review B **86** (2012).
[18] C. Hotta, S. Nishimoto, and N. Shibata, "Grand canonical finite size numerical approaches in one and two dimensions: real space energy renormalization and edge state generation", Physical Review B **87** (2013).
[19] H. Katsura, "Exact ground state of the sine-square deformed xy spin chain", Journal of Physics A: Mathematical and Theoretical **44**, 252001 (2011).
[20] I. Maruyama, H. Katsura, and T. Hikihara, "Sine-square deformation of free fermion systems in one and higher dimensions", Physical Review B **84** (2011).
[21] T. Tada, "Sine-square deformation and its relevance to string theory", Modern Physics Letters A **30**, 1550092 (2015).
[22] K. Okunishi and H. Katsura, "Sine-square deformation and supersymmetric quantum mechanics", Journal of Physics A: Mathematical and Theoretical **48**, 445208 (2015).
[23] N. Ishibashi and T. Tada, "Infinite circumference limit of conformal field theory", Journal of Physics A: Mathematical and Theoretical **48**, 315402 (2015).
[24] N. Ishibashi and T. Tada, "Dipolar quantization and the infinite circumference limit of two-dimensional conformal field theories", International Journal of Modern Physics A **31**, 1650170 (2016).
[25] K. Okunishi, "Sine-square deformation and Möbius quantization of 2d conformal field theory", Progress of Theoretical and Experimental Physics **2016**, 063A02 (2016).
[26] X. Wen, S. Ryu, and A. W. W. Ludwig, "Evolution operators in conformal field theories and conformal mappings: entanglement hamiltonian, the sine-square deformation, and others", Physical Review B **93** (2016).
[27] S. Tamura and H. Katsura, "Zero-energy states in conformal field theory with sine-square deformation", Progress of Theoretical and Experimental Physics **2017** (2017).
[28] T. Tada, "Conformal quantum mechanics and sine-square deformation", Progress of Theoretical and Experimental Physics **2018** (2018).
[29] M. Bukov, L. D'Alessio, and A. Polkovnikov, "Universal high-frequency behavior of periodically driven systems: from dynamical stabilization to Floquet engineering", Advances in Physics **64**, 139 (2015).
[30] G. Floquet, "Sur les équations différentielles linéaires à coefficients périodiques", fr, Annales scientifiques de l'École Normale Supérieure **2e série, 12**, 47 (1883).
[31] P. M. D̃. S. Philippe Di Francesco, *Conformal field theory* (Springer, 1997).
[32] J. F. C̃. Schweigert, *Symmetries, lie algebras and representations* (Cambridge University Press, 1997).
[33] D. P. L̃. S. Matthias Beck Gerald Marchesi, *A first course in complex analysis* (Orthogonal Publishing, 2002).
[34] M. P. Hitchman, *Geometry with an introduction to cosmic topology*, `https://mphitchman.com/geometry/section3-5.html`.

[35] P. Ginsparg, *Applied conformal field theory*, (1989) https://arxiv.org/abs/hep-th/9108028.